

Agentic Planning with Reasoning for Image Styling via Offline RL

Subhojyoti Mukherjee¹ Stefano Petrangeli¹ Branislav Kveton¹ Trung Bui¹ Franck Deroncourt¹
Arko Mukherjee¹

Qualitative Results: Agentic Planning with Reasoning for Image Styling

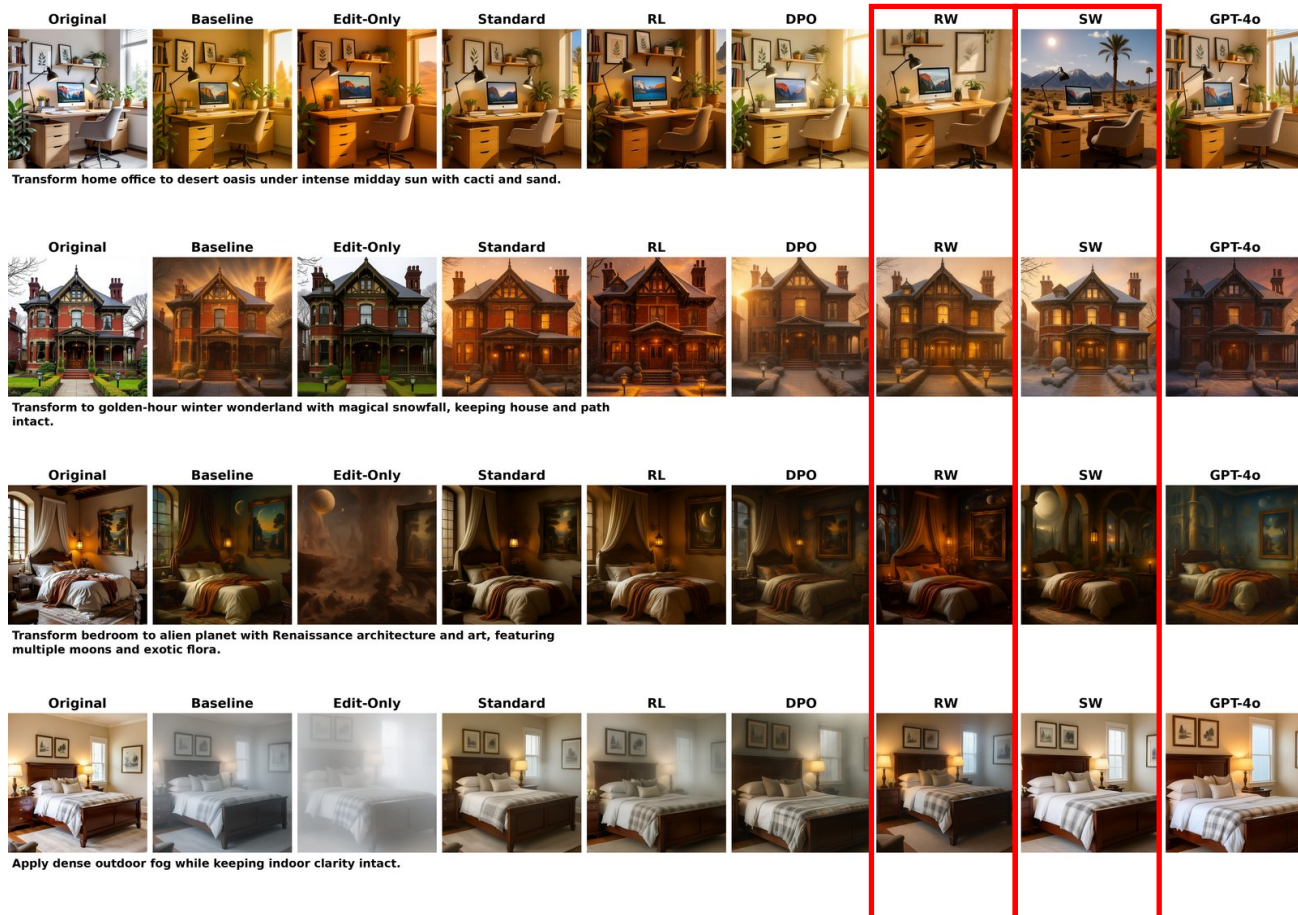


Figure 1: Agentic planning with reasoning for image styling via offline RL. We train a small vision-language planner (Qwen3-VL 4B/8B) that decomposes styling goals into sequences of tool calls (e.g., `time_of_day`, `artistic_medium`, `mood_lighting`) with explicit reasoning. Each row compares several types of planners: Baseline (B: pretrained only with planning), Edit-Only (E: direct editing without planning), Standard (S: supervised training on random planning trajectories), RL (R: reward-filtered training on high-quality planning trajectories), DPO (D: preference training on trajectory pairs), Reward-Weighted (RW: trains on trajectories weighted by their quality scores), Standardized Reward-Weighted (SW: trains on trajectories weighted by their quality scores and normalized by their standard deviation)—and GPT-4o Planner (large closed-source planner). **Row 1:** Desert oasis transformation with midday sun (Regular, Text-8B)—SW successfully transforms indoor office to outdoor desert scene with cacti and sand while maintaining compositional coherence. **Row 2:** Golden-hour winter wonderland with magical snowfall (Complex, Vision-4B)—SW excels at atmospheric lighting and snow effects while preserving architectural details. **Row 3:** Alien planet with Renaissance architecture (Simple, Text-8B)—SW achieves multi-element transformation with exotic flora and multiple moons. **Row 4:** Dense outdoor fog effect (Regular, Vision-4B)—SW successfully applies atmospheric fog while maintaining indoor clarity. Red boxes highlight RW and SW, our best reward-aware methods which consistently excel. Edit-Only demonstrates limitations of direct editing without structured planning. Our compact open-source planners outperform GPT-4o zero-shot baseline on image quality with orders of magnitude fewer parameters.

Abstract

Direct prompt-based editing often fails on complex transformations because vague and subjective prompts often require nuanced understanding of what should be changed in the image. Our core intuition is that leveraging compositional image editing tools rather than direct prompting profits from structured agent-level planning with explicit reasoning, leading to better results. This structured planning framework enables efficient offline RL post-training on quality-scored trajectories to improve performance. We present a tool-based agentic RL post-training framework that addresses this through structured planning with chain-of-thought reasoning. Our key contributions include: (1) A tool-based agentic planning methodology that combines a compositional library of orthogonal primitive transformations, structured context representation, and explicit per-step reasoning to decompose complex styling into interpretable tool sequences. (2) A synthetic data generation pipeline producing three large-scale datasets (each ~10K trajectories) with reasoning chains, plans, and quality scores—necessary because no existing datasets provide explicit tool-based styling supervision. Our datasets and code are publicly available at [this HuggingFace repository](#). (3) Offline RL training methods for learning planners with reasoning as our core algorithmic contributions, which consistently improve over the Edit-Only baseline in visual quality and instruction following. (4) Comprehensive evaluation across 4B and 8B parameter Qwen3-VL models showing that our methods outperform other baselines in the majority of the compositional tasks, backed up by human evaluations on both the synthetic data and final results. Our work demonstrates that structured planning with reward-aware training enables models to produce higher-quality images that better follow user instructions compared to direct editing approaches.

1. Introduction

The ability to transform images according to high-level aesthetic intents—changing a scene from day to night, summer to autumn, modern to Victorian, or photorealistic to painterly—is fundamental to creative workflows across industries including entertainment, advertising, and design. This problem has a rich history predating modern genera-

tive AI: classical image-to-image translation methods (Isola et al., 2017), neural style transfer (Gatys et al., 2016), and cycle-consistent adversarial networks (Zhu et al., 2017) pioneered techniques for cross-domain visual transformations. While these early approaches demonstrated the potential for automated image styling, they were often limited to specific transformations or required paired training data. Recent advances in vision-language foundation models such as DALL-E (Ramesh et al., 2021; 2022), Stable Diffusion (Rombach et al., 2022), and Qwen3-VL have democratized image editing through natural language prompts (Bai et al., 2025; 2023; Liu et al., 2023), enabling users to specify desired transformations in plain text without domain-specific expertise.

Current state-of-the-art image styling relies predominantly on direct prompt-based editing, where users provide natural language instructions to foundation models that generate or modify images. Any modern image editing model can perform styling tasks—commercial systems like Midjourney, and DALL-E 3 (Betker et al., 2023), as well as open-source alternatives like Stable Diffusion and its derivatives. Recent specialized methods have emerged for specific use cases: StyleBooth (Han et al., 2025) enables personalized style transfer from reference images, while Styleshot (Gao et al., 2024) focuses on few-shot style adaptation. These approaches share a common paradigm: direct mapping from natural language prompts to styled images, often in a single forward pass or iterative refinement of the same prompt.

However, direct prompt-based editing faces a fundamental limitation: prompts are often imprecise and fail on complex multi-dimensional transformations that require coordinating changes across multiple visual attributes. Consider the instruction "Transform to golden-hour winter wonderland with magical snowfall, preserving house and path." This seemingly simple request requires coordinating time-of-day lighting transitions (golden-hour warm tones), seasonal changes (winter aesthetics), weather effects (natural snowfall), atmospheric coherence (unified lighting and mood), and preservation constraints (maintaining architectural structure). As shown in Figure 1 Row 2, direct editing (Edit-Only baseline) produces inconsistent results with poor instruction adherence, misaligned colors, and structural artifacts. This failure stems from the ambiguity inherent in natural language: a single prompt does not explicitly specify which visual dimensions to modify, in what order, or how to balance competing requirements. The gap between user intent and model interpretation leads to results that often deviate from human preferences.

We address this challenge through tool-based agentic RL post-training with structured compositional planning and synthetic data generation. Our approach decomposes complex styling tasks into explicit intermediate representations,

¹Adobe Research, San Jose, CA, USA. Correspondence to: Subhojyoti Mukherjee <subhomuk@adobe.com>.

enabling more precise control and better alignment with human preferences. The framework comprises four synergistically connected components: (1) *Compositional Tool Library*: We design a library of orthogonal primitive tools where each tool accepts parameters, creating an infinite compositional space from finite primitives. Multi-step tool sequences (typically 2-5 tools) enable complex transformations through systematic composition. (2) *Structured Document Representation*: We extract explicit text-based encoding of the image’s current visual state across all tool dimensions, providing state awareness that grounds planning in concrete attributes rather than implicit visual understanding. (3) *Per-Step Chain-of-Thought Reasoning*: For each tool in a plan, the model generates explicit reasoning explaining *why* that tool is chosen. For example, Tool: `time_of_day(sunset)` accompanied by Reasoning: "Setting golden-hour lighting creates warm sunset tones that enhance the winter atmosphere while providing natural illumination." This improves planning coherence and interpretability. (4) *Reward-Aware R Training (Our Core Algorithmic Contribution)*: We propose *Reward-Weighted (RW)* and *Standardized Reward-Weighted (SW)* training methods that consistently improve over direct prompt-based pixel-level editing (Edit-Only baseline) in both visual quality and instruction following. RW weights each trajectory by its quality score—high-quality samples receive more influence than poor samples through true per-sample weighted loss. SW extends this by normalizing rewards before weighting for more stable training across datasets with different reward distributions. These methods demonstrate that structured planning with reward-aware training enables models to produce higher-quality images that better follow user instructions compared to direct prompt-to-image editing.

We adopt an offline RL approach (Lange et al., 2012; Levine et al., 2020) for four key advantages: (1) Human-validated data quality: Decoupling data generation from training enables thorough human validation of trajectories prior to learning; we validated 3,000 samples with a 77% pass rate (Appendix J). (2) One-time inference cost: Teacher inference is incurred once during data collection, after which multiple student models and training algorithms can be trained without additional inference. (3) Reproducibility and reuse: The fixed, validated dataset can be released, enabling replication and extension without regenerating data. (4) Fair algorithm comparison: Multiple training methods (S, R, RW, SW, DPO) can be evaluated on identical trajectories. While offline RL does not adapt trajectories to an improving policy, we find it highly effective in practice: our 4B/8B models outperform the much larger GPT-4o zero-shot baseline on image quality in 10 of 11 settings. A follow-up GPT-4o evaluation on 279 samples confirmed method rankings and showed moderate correlation with automated metrics. (Section 3.3, Appendix J.5). We train planners

in both text-only and vision-language modalities, with the image editor remaining frozen to focus on planning quality (see Appendix I.1 for details).

Our main contributions are:

(1) Tool-Based Agentic RL Framework for Image Styling: We introduce a complete pipeline with compositional tool libraries, structured document representations, per-step chain-of-thought reasoning, and systematic synthetic data generation, providing a blueprint for building planning agents in creative domains.

(2) Large-Scale Synthetic Datasets: We generate and will release three large-scale datasets for image styling research: Simple (10,000 trajectories with 1-2 step edits), Regular (10,000 trajectories with 3-5 step compositional edits across 10 interior design themes), and Complex (10,000 trajectories with 3-5 step compositional edits across 83 diverse themes). Each trajectory includes structured context, multi-step action plans with chain-of-thought reasoning, and quality scores, addressing the lack of existing datasets for action-based image styling. We publicly release all datasets to facilitate future research.¹

(3) Reward-Weighted (RW) and Standardized Reward-Weighted (SW) Training Methods: We demonstrate that per-sample quality weighting is crucial for learning compositional planning. Our reward-aware training methods consistently improve over direct prompt-based editing (Edit-Only baseline) across both visual quality and instruction following dimensions. RW weights each trajectory by its quality score, giving high-quality samples greater influence through *true* per-sample weighted loss computation. SW extends this by normalizing rewards before weighting for more stable training across trajectories with different rewards.

(4) Comprehensive Empirical Analysis: Through experiments on approximately $n = 10,000$ synthetic trajectories across three datasets with GPT-4o-based ground-truth-free evaluation (VLM-as-a-Judge), we provide insights into when different RL methods excel and how task complexity affects training dynamics. We demonstrate that method effectiveness varies by dataset characteristics, with reward-weighted approaches showing particular strength on complex compositional tasks.

The remainder of this paper is organized as follows. Section 2 describes our problem formulation, compositional tool library, and Section 2 presents our synthetic data generation pipeline. Section 4 presents our training algorithms including reward-filtered R (Andukuri et al., 2024), reward-weighted fine-tuning (RW and SW), and direct preference optimization (DPO) (Rafailov et al., 2023). Section 5 pro-

¹<https://huggingface.co/datasets/subhojyoti1990/image-agent-styling>

vides experimental results comparing methods across task complexity levels. Section 6 concludes with limitations and future directions. Due to space constraints, we defer a comprehensive review of related work in vision-language models, RLHF, and tool-based planning to Appendix B.

2. Problem Setup

We formulate image styling as a sequential decision-making problem where an agent learns to compose tools from a compositional tool library. Given an input image, a user’s natural language prompt, and a structured representation of the image’s current visual state, the agent must produce a sequence of tool calls that transform the image to match the desired aesthetic. We use structured representation to ground the planning process in explicit visual attributes, enabling the model to reason about specific dimensions (e.g., “current lighting is harsh midday, need warm golden-hour”) rather than relying solely on implicit visual understanding.

2.1. Four-Stage Structured Editing Pipeline

Classical image editing maps user’s editing goal e_i (natural language prompt) and base image I_i directly to edited image \hat{I}_i : $e_i, I_i \rightarrow \hat{I}_i$. However, vague prompts often produce poor results. For example, “[Transform this to a Renaissance oil painting](#)” fails because the prompt doesn’t specify which time period (1400s vs 1500s vs 1600s), color palette (warm earth tones?), artistic techniques (chiaroscuro lighting?), or which elements to preserve. Direct editing $e_i, I_i \rightarrow \hat{I}_i$ with vague prompts produces inconsistent results. Our goal is to replace vague e_i with precise \hat{e}_i that yields better \hat{I}_i . We address this through structured editing with four stages.

Stage 1 (Extract Structured Context): First, we extract a structured representation of the image’s visual state. Formally, $e_i, I_i \rightarrow c_i$ where c_i is plain text describing the image’s current visual state across 10 dimensions: location (urban city), architecture (modern glass), time period (contemporary 2020s), time of day (midday harsh lighting), season (summer), weather (clear), mood (neutral documentary), color grading (natural desaturated), artistic medium (realistic photograph), atmospheric effects (clear visibility).

Compositional Tool Library: Before detailing the planning stage, we describe our compositional tool library. Our tool library contains parameterized transformations across 10 orthogonal dimensions that is based on the visual state contexts discussed above: `location_setting`, `architecture_style`, `time_period`, `time_of_day`, `season`, `weather`, `mood_lighting`, `color_grading`, `artistic_medium`, `atmospheric_effects`. These dimensions were selected to cover the primary controllable visual attributes in modern text-to-image models while maintaining orthogonality (Li et al., 2019; Kazemi et al., 2019; Zhang et al., 2023b). Each dimension controls one visual aspect

with minimal interference—for example, `time_of_day` affects lighting but not architecture; `season` changes vegetation but not building styles. This orthogonality enables clean composition where effects combine predictably. Complex styling emerges from tool sequences: Figure 1’s “[golden-hour winter wonderland with snowfall](#)” decomposes into $\{time_of_day(golden-hour), season(winter), weather(snowfall)\}$. See Appendix C for complete tool specifications.

Stage 2 (Plan Actions with Reasoning): Second, we generate an action plan with step-by-step reasoning. Formally, $e_i, c_i \rightarrow \{z_{i,j}\}_{j=1}^{m_i}, \{a_{i,j}\}_{j=1}^{m_i}$ generates m_i actions (typically 2-5) where $z_{i,j}$ is the chain-of-thought reasoning and $a_{i,j}$ is action j in trajectory i (symbolic action with parameters). For Renaissance transformation, the model first reasons then acts:

$z_{i,1}$ = “Setting Renaissance era establishes historical context ...”
 $a_{i,1}$ = `time_period(1500s)`
 $z_{i,2}$ = “Oil painting introduces characteristic brush strokes ...”
 $a_{i,2}$ = `artistic_medium(oil-painting)`
 $z_{i,3}$ = “Warm earth palette matches period pigment chemistry”
 $a_{i,3}$ = `color_grading(warm-earth-tones)`
 $z_{i,4}$ = “Dramatic light-dark contrast follows Renaissance ...”
 $a_{i,4}$ = `mood_lighting(chiaroscuro)`

Stage 3 (Synthesize Precise Instruction): Third, we synthesize a precise editing instruction. Formally, $e_i, c_i, \{z_{i,j}\}, \{a_{i,j}\} \rightarrow \hat{e}_i$ produces the synthesized natural language instruction \hat{e}_i : “[Transform this urban photograph into an authentic Renaissance oil painting from the 1500s. Apply oil painting with visible brush strokes and layered texture characteristic of Leonardo and Raphael. Use warm earth-tone palette limited to period-appropriate pigments: ochres, umbers, siennas. Add dramatic chiaroscuro lighting with strong directional illumination. Preserve original composition while transforming surface qualities.](#)” This explicit instruction is improved \hat{e}_i from our goal statement above.

Stage 4 (Render Final Image): Finally, we render the edited image using a frozen black-box editor. Formally, $\hat{e}_i, I_i \rightarrow \hat{I}_i$ using frozen image editor (Qwen-Image-Edit). We keep the editor frozen to focus on planning quality, not editing capability. Each trajectory receives reward score $r_i \in [0, 5]$ assessing trajectory quality.

Our Contribution: Stages 1-3 Our core contribution spans Stages 1-3: building a pipeline to extract structured context, generate high-quality action plans with explicit reasoning, and synthesize precise editing instructions. Only Stage 4 (image rendering) uses a frozen black-box editor (Qwen-Image-Edit). This design separates the *planning*

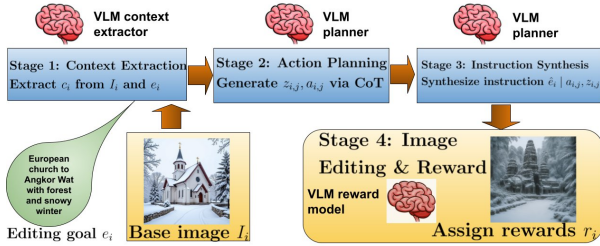


Figure 1. Synthetic Data Generation Pipeline

problem (deciding what and how to change) from the *execution problem* (rendering pixels), enabling efficient training without requiring image generation model training. By focusing on the reasoning and planning capabilities of language models, we can train compact 4B-8B parameter planners that generate high-quality editing instructions for any frozen image editor.

A complete trajectory τ_i consists of: $\tau_i = (e_i, I_i, c_i, \{a_{i,j}\}_{j=1}^{m_i}, \{z_{i,j}\}_{j=1}^{m_i}, \hat{e}_i, \hat{I}_i, r_i)$. The complete dataset is $\mathcal{D} = \{\tau_1, \tau_2, \dots, \tau_n\}$ with $n = 10,000$ trajectories per dataset variant, organized into trajectory-level train/validation/test splits (80%/10%/10%).

3. Synthetic Data Generation

Training our agentic framework requires trajectories containing structured context extraction, planning with reasoning, instruction synthesis, and reward evaluation. While datasets exist for direct prompt-to-image editing (Brooks et al., 2023), they lack the explicit reasoning chains (z_{ij}), structured context (c_i), and multi-step plans ($\{a_{ij}\}$) needed to train our approach. We therefore generate synthetic training data using a teacher model. We implement the four-stage framework from Section 2 using a teacher-student paradigm: a strong teacher model (Qwen3-VL-8B-Instruct) demonstrates the complete pipeline, generating trajectories that are used to train smaller student models (4B and 8B) via offline RL.

3.1. Four-Stage Pipeline

We generate trajectories using Qwen3-VL-8B-Instruct as the teacher model, HiDream-I1-Dev for image generation, and Qwen-Image-Edit for image editing.

Chain-of-Thought Emphasis: Stage 2 (Action Planning with Reasoning) is the critical component for training student models. The teacher generates explicit chain-of-thought reasoning z_{ij} before each action a_{ij} , teaching students to explain *why* each tool is chosen and how it contributes to the overall transformation goal. This reasoning-first approach enables interpretable planning and improves both action quality and instruction following. For example: $z_{i,1}$ (“Setting the Renaissance era establishes historical context”), $a_{i,1} = \text{time_period}(1500s)$; $z_{i,2}$ (“Oil painting introduces characteristic brush strokes and layered texture”),

$a_{i,2} = \text{artistic_medium}(oil\text{-}painting)$.

This reasoning-action interleaving trains models to think before acting, improving both action quality and instruction following. The teacher model outputs full reasoning chains using few-shot prompting with manually curated exemplars.

Trajectory Organization: The trajectories are organized by unique (I_i, e_i) pairs. During data splitting (80% train / 10% validation / 10% test), all trajectories sharing the same base image I_i are assigned to the same split. This ensures the model doesn’t see test images during training, enabling clean evaluation of generalization to new visual content.

Reward Evaluation: After the final image is generated, the teacher model evaluates trajectory quality across 17 dimensions (11 for action plan quality, 6 for final image quality), assigning a scalar reward $r_i \in [0, 5]$ by averaging dimension-specific scores. This reward distribution enables reward-aware training methods (RW, SW, DPO) that weight high-quality samples more heavily. We note that our framework is agnostic to the choice of reward model—Qwen3-VL-8B-Instruct can be substituted with more capable evaluators (e.g., Qwen3-VL-235B-A22B (Team, 2025)). However, optimizing the reward model is orthogonal to our primary contribution, which focuses on building a better planning agent. See Appendix C.3 for detailed quality tiers and training usage.

3.2. Dataset Variants

We generate three dataset variants with different complexity:

Simple Dataset ($n = 10,000$ trajectories): Atomic transformations with 1-2 actions. Example: “Make this sunset” requires only *time_of_day(sunset)* and *color_grading(warm-tones)*.

Regular Dataset ($n = 10,000$ trajectories): Compositional transformations with 3-5 actions requiring coordination. Example: “Golden-hour winter wonderland with snowfall” needs *time_of_day(golden-hour)*, *season(winter)*, *weather(snowfall)*, *atmospheric_effects(magical)*, *color_grading(warm-cool-contrast)*.

Complex Dataset ($n = 10,000$ trajectories): Highest difficulty with strict preservation constraints and diverse themes (83 total). Example: “Transform to cyberpunk while preserving Renaissance architecture” forces the model to balance competing aesthetic goals. All variants share the same four-stage generation pipeline and reward evaluation. See Appendix D for complete end-to-end examples showing the full pipeline execution with detailed reasoning chains, context extraction, and reward evaluation across all three dataset variants. All three dataset variants are publicly released.²

²<https://huggingface.co/datasets/subhojyoti1990/image-agent-styling>

3.3. Human Validation of Dataset Quality

To validate the quality of our synthetically generated training data, we conducted two complementary human evaluation studies. First, three independent annotators comprehensively evaluated 3,000 training samples across all quality dimensions (Edit Quality, Action Plan Quality, Reasoning Quality, Overall Quality), achieving 77% pass rate with all variants exceeding 70% (Appendix J). Second, we conducted a GPT-4o validation study where two annotators performed side-by-side comparisons of 279 samples across 6 training methods (Baseline, Standard, RL, SW, RW, DPO), achieving 85% combined pass/partial rate and confirming that SW, RW and DPO are top performers. The GPT-4o validation study also assessed whether automated GPT-4o scores correlate with human judgment. Results show top-2 accuracy was moderate (76-83%), indicating GPT-4o can identify strong methods even if absolute scores are noisy. These confirm our synthetic data generation pipeline produces high-quality training samples while highlighting the importance of human validation for automated evaluation systems. See Appendix J.5 for detailed study.

4. Learning Algorithms

This section details offline reinforcement learning algorithms for reward-aware post-training of planners.

4.1. Supervised Learning

The simplest approach, also known as *supervised fine-tuning (SFT)* (Wei et al., 2021), treats synthetic trajectories as supervised training data, ignoring reward signals entirely. The model π_θ is trained to maximize the likelihood of the complete action sequence with reasoning generated in a single forward pass: $\mathcal{L}_{\text{SL}}(\theta) = -\frac{1}{n} \sum_{i=1}^n \log \pi_\theta(\{a_{i,j}, z_{i,j}\}_{j=1}^{m_i} | I_i, e_i, c_i)$. This approach has a fundamental limitation: it treats all synthetic trajectories equally, regardless of quality. A trajectory with reward $r_i = 3.0$ (poor) contributes as much to training as one with $r_i = 5.0$ (excellent), potentially degrading performance. See Appendix E.1 for the complete algorithm, and implementation details.

4.2. Reward-Filtered Training

A simple improvement over standard supervised learning is to filter the dataset, keeping only high-quality trajectories. This approach is a form of behavioral cloning (Pomerleau, 1991), a classic imitation learning technique (Hussein et al., 2017) where a student policy learns to imitate high-reward expert behavior. Recent applications include conversational R systems like Andukuri et al. (2024). We define a reward threshold r_{\min} and discard trajectories below this threshold: $\mathcal{D}_{\text{filtered}} = \{\tau_i | r_i \geq r_{\min}\}$. In our experiments, we use $r_{\min} = 4.0$, which retains approximately 65% of trajectories (those rated "good" or "excellent"). The student is then trained using standard supervised learning on $\mathcal{D}_{\text{filtered}}$. This approach is simple to implement (no algorithm changes, just data filtering), removes clearly

poor-quality trajectories, and focuses learning on successful behaviors. However, it discards 35% of data, reducing diversity, and the binary threshold ignores the continuous quality spectrum—medium-quality trajectories (3.5-4.0) may contain valuable information that is lost.

4.3. Direct Preference Optimization

While R leverages scalar rewards, DPO (Rafailov et al., 2023) learns directly from preference comparisons. Preference-based learning has a rich history in statistics, with foundational work by Bradley & Terry (1952); Plackett (1975) on ranking and paired comparisons. Modern applications include optimal data collection strategies for human preference elicitation (Mukherjee et al., 2024). Given two trajectories with the same input (I_i, e_i) , DPO trains the model to prefer the higher-reward trajectory without requiring an explicit reward model. We construct preference pairs $\mathcal{D}_{\text{pref}} = \{(\tau_i^+, \tau_i^-)\}$ where "chosen" trajectories have $r_i^+ \geq 4.0$ and "rejected" have $r_i^- \in [2.5, 3.5]$ with gap $r_i^+ - r_i^- \geq 0.5$ to ensure meaningful signal. DPO optimizes the policy π_θ relative to a frozen reference policy using the Bradley-Terry preference model with KL regularization ($\beta = 0.1$). The method offers contrastive learning that directly captures what makes one trajectory better than another, but requires paired data and doubles computational cost per sample. See Appendix E.3 for complete mathematical formulation, algorithm, and implementation details.

4.4. Reward-Weighted Fine-Tuning

Rather than binary filtering, Reward-Weighted (RW) uses *all* trajectories but weights each trajectory's gradient contribution by its reward score. This approach preserves data diversity while emphasizing high-quality examples through their proportionally larger contribution to parameter updates. R as reward-weighted regression has a rich history: Peters & Schaal (2007) formulated the offline filtered RL training as reward-weighted regression and proposed an EM algorithm for solving it; Peng et al. (2019) proposed Advantage-Weighted Regression (AWR) that maximizes log-probability weighted by exponentiated advantages. Specifically, we use weight function $w(r_i) = \max\{r_i - 3.0, 0\}$.

4.5. Standardized Reward-Weighted

Standardized Reward-Weighted (SW) extends RW by normalizing rewards via z-score standardization before computing weights. Advantages are a classic variance reduction technique in policy gradients (Williams, 1992; Sutton et al., 2000; Baxter & Bartlett, 2001; Munos, 2003; Boutilier et al., 2020), widely used in modern methods including Generalized Advantage Estimation (Schulman et al., 2015), Proximal Policy Optimization (PPO) (Schulman et al., 2017), and Group-Relative Policy Optimization (GRPO) (Shao et al., 2024). Our SW method adapts these ideas to offline distillation by using standardized rewards as a proxy for

advantages. Given rewards $\{r_1, \dots, r_n\}$ with mean \bar{r} and standard deviation σ_r , SW computes standardized rewards $\tilde{r}_i = \frac{r_i - \bar{r}}{\sigma_r}$ and uses these as sample weights directly.

SW adapts to variations across same-input trajectory rollouts through standardization. When multiple rollouts of the same input (I_i, e_i) produce different rewards, SW’s normalization provides variance reduction by centering the distribution: trajectories above the mean receive positive weight, those below receive negative weight, reducing gradient variance—a classic technique in policy gradient methods (Williams, 1992; Schulman et al., 2015). This makes SW particularly effective for datasets with diverse reward distributions across different inputs while maintaining stability within each input’s rollout variations.

Algorithm 1 Standardized Reward-Weighted Fine-tuning

```

1: Input: Trajectory dataset  $\mathcal{D} = \{\tau_i\}$ , model  $\pi_\theta$ 
2: // Compute dataset statistics
3:  $\bar{r} \leftarrow \frac{1}{n} \sum_{i=1}^n r_i$  {Mean reward}
4:  $\sigma_r \leftarrow \sqrt{\frac{1}{n} \sum_{i=1}^n (r_i - \bar{r})^2}$  {Std deviation}
5: for epoch = 1 to  $E$  do
6:   for batch  $\{\tau_i\}_{i \in \mathcal{B}}$  in  $\mathcal{D}$  do
7:     Compute per-trajectory losses:  $\mathcal{L}_i = -\sum_{j=1}^{m_i} \log \pi_\theta(a_{i,j}, z_{i,j} \mid I_i, e_i, c_i, \{a_{i,k}\}_{k < j})$ 
8:     // Standardize and weight
9:     Standardized rewards:  $\tilde{r}_i = \frac{r_i - \bar{r}}{\sigma_r}$  for each  $i \in \mathcal{B}$ 
10:    Weights:  $w_i = \tilde{r}_i$  for each  $i \in \mathcal{B}$  {Can be negative}
11:    Weighted loss:  $\mathcal{L}_{\text{batch}} = \frac{1}{|\mathcal{B}|} \sum_{i \in \mathcal{B}} w_i \mathcal{L}_i$ 
12:    Update:  $\theta \leftarrow \theta - \eta \nabla_\theta \mathcal{L}_{\text{batch}}$ 
13:   end for
14: end for
15: Return: Trained student model  $\pi_\theta$ 
    
```

For complete training configuration, cached embedding implementation, theoretical justification of RW and DPO, and comprehensive algorithm comparisons, see Appendices E.5, E.6, E.4, and E.7.

5. Experiments

In this section, we evaluate the performance of our method on three synthetic datasets with GPT-4o as the evaluator.

Datasets: We evaluate on three synthetic datasets: **Simple** (10,000 trajectories, 1-2 step edits), **Regular** (10,000 trajectories, 3-5 step compositional edits with 10 interior design themes), and **Complex** (10,000 trajectories, 3-5 step compositional edits with 83 diverse themes). All datasets are generated via our 4-stage pipeline (Section 3).

Models: We train Qwen3-VL-4B and 8B in both text-only and vision-language configurations. **Text-only models** receive only text inputs with the vision encoder frozen. **Vision models** receive both image pixels and context, training the

vision encoder for visual grounding. See Appendix I.1 for detailed modality justification and training efficiency.

Comparison Methods: We evaluate eight approaches spanning baseline, direct editing, trained planners, and a proprietary reference: (1) *Baseline (B)*: pretrained Qwen3-VL without fine-tuning, (2) *Edit-Only (E)*: direct image editing without structured planning, (3) *Standard (S)*: supervised learning treating all trajectories equally, (4) *RL (R)*: reward-filtered training ($r_i \geq 4.0$, discards 35% of data), (5) *Reward-Weighted (RW)*: per-trajectory gradient weighting by reward score (uses all data), (6) *Standardized Reward-Weighted (SW)*: z-score normalized gradient weighting (upweights above-average, downweights below-average trajectories for variance reduction), (7) *DPO (D)*: pairwise contrastive preference learning on chosen-rejected pairs (see Section 4), and (8) *GPT-4o Planner*: a zero-shot baseline using GPT-4o API from large closed-source models. Our compact models outperform GPT-4o on image quality (10 out of 11 configurations). See Appendix F.7 for detailed GPT-4o comparison. In all results tables, bold numbers indicate the best-performing method among our trained models (B, E, S, R, RW, SW, D), which are all Qwen3-VL 4B or 8B variants. GPT-4o Planner (G4o, shown in grey) is reported separately as a zero-shot reference since it is a much larger closed-source model.

Evaluation: We use GPT-4o to evaluate 200 test samples on 6 image quality dimensions (0-100 scale). While GPT-4o shows only moderate correlation with human judgment (validated on 279 samples, see Section 3.3), it provides consistent relative rankings suitable for large-scale evaluation. Complete evaluation details are in Appendix F.

Edit-Only Baseline Motivates Action Planning: We first evaluate the Edit-Only (E) baseline. As shown in Figures 2-5, E consistently underperforms compared to the best-performing RL method (Overall gaps 1.3-7.3 points), confirming that structured planning is essential. We show N/A on planning metrics (Semantic Accuracy, Coherence, Technical Execution, Transformation Strength) because E does not use planning and tool calls for editing. See Appendix F.8 for detailed Edit-Only analysis.

Main Results: Method Performance Varies by Dataset and Modality: We present results on 4 representative configurations spanning text-only and vision models, simple and complex datasets, demonstrating how training method effectiveness depends on task characteristics. In *Complex Text-4B (Figure 2)* SW achieves highest Overall (78.77), excelling on planning metrics (Semantic Accuracy 76.58, Instruction Following 77.55).

Task Complexity, Modality, and Dataset Diversity Determine Method Effectiveness: Our systematic evaluation reveals clear patterns: Compositional text tasks favor SW and RW. SW achieves the highest scores (78.77/77.86)

Metric	B	E	S	R	RW	SW	D	G4o	Winner
Overall	76.03	71.49	75.03	77.12	77.18	78.77	74.88	74.07	SW
Semantic Accuracy	72.58	N/A	70.65	72.84	73.61	76.58	71.03	71.61	SW
Visual Quality	80.90	75.81	81.16	83.03	81.35	82.84	79.81	76.39	R
Coherence	80.00	N/A	80.19	81.42	80.00	81.55	79.48	76.26	SW
Technical Execution	77.68	N/A	77.35	79.61	78.84	80.19	76.32	74.13	SW
Instruction Following	74.65	68.13	73.35	75.16	76.84	77.55	72.65	73.42	SW
Transformation Strength	70.45	N/A	67.42	70.71	72.45	73.94	69.94	72.71	SW

Figure 2. Regular Text-4B: SW wins (78.77). Outperforms GPT-4o zero-shot baseline (grey).

Metric	B	E	S	R	RW	SW	D	G4o	Winner
Overall	74.79	71.24	74.23	77.62	77.34	77.86	75.85	75.70	SW
Semantic Accuracy	69.47	N/A	68.60	73.33	73.13	74.53	72.13	73.20	SW
Visual Quality	81.73	77.53	81.13	81.80	83.00	82.40	79.93	77.33	RW
Coherence	79.00	N/A	78.87	81.53	81.93	81.40	78.80	76.87	RW
Technical Execution	77.33	N/A	76.73	78.53	79.67	79.40	77.00	75.80	RW
Instruction Following	73.33	67.00	72.93	76.60	75.40	77.00	74.20	75.27	SW
Transformation Strength	67.87	N/A	67.27	73.80	70.93	72.47	73.00	75.80	R

Figure 3. Regular Text-8B: SW wins (77.86). Outperforms GPT-4o zero-shot baseline (grey).

with strong planning metrics. Simple vision tasks favor RW. RW dominates (79.33) with visual grounding. Diverse themes favor DPO. DPO wins (85.41) on Complex’s 83 themes. We also observe that vision models achieve higher absolute scores against their text-only counterparts. See Appendix F.10 for detailed per-metric analysis.

Key Findings. Across 3 datasets, 2 model sizes, 2 modalities, and 7 training methods, we identify five key insights. (1) *Offline RL is effective:* SW performs best on compositional text tasks (Overall 78.77 on 4B, 77.86 on 8B), RW on simple vision tasks (Overall 79.33 on Vision-4B), and DPO on diverse theme distributions (Overall 85.41 on Complex Vision-8B). (2) *Action planning is critical for coherent editing:* Edit-Only (E) consistently underperforms on Overall scores, indicating that direct image-to-image editing lacks the structured reasoning required for instruction-following edits. (3) *Visual grounding amplifies continuous reward weighting:* RW achieves its strongest gains on vision models (Overall 79.33 on Simple Vision-4B), winning visual-grounded metrics by up to 1.24 points, while remaining competitive but not dominant on text-only models. (4) *Standardized weighting supports compositional reasoning:* SW attains the highest Overall scores on both Regular Text settings (78.77 on 4B, 77.86 on 8B), with particularly strong planning performance (Semantic Accuracy 76.58/74.53; Instruction Following 77.55/77.00). (5) *Per-step chain-of-thought improves planning quality:* All trained methods (S, R, RW, SW, DPO) substantially outperform the Baseline (B) on planning metrics, confirming the benefit of explicit reasoning traces $z_{i,j}$ during training.

Metric	B	E	S	R	RW	SW	D	G4o	Winner
Overall	77.28	78.04	77.60	78.35	79.33	78.65	78.27	79.06	RW
Semantic Accuracy	72.17	N/A	72.79	72.87	75.04	73.95	72.79	75.35	RW
Visual Quality	82.64	81.47	82.64	83.33	83.95	83.41	83.10	81.63	RW
Coherence	82.33	N/A	82.09	82.48	83.26	83.57	83.33	81.94	SW
Technical Execution	79.92	N/A	79.92	81.24	81.86	81.86	80.78	79.69	RW
Instruction Following	75.19	75.50	76.51	76.82	78.06	76.82	76.82	78.99	RW
Transformation Strength	71.47	N/A	71.55	73.33	73.88	72.33	72.87	76.82	RW

Figure 4. Simple Vision-4B: RW dominates with visual grounding (79.33). Outperforms GPT-4o zero-shot baseline (grey).

Metric	B	E	S	R	RW	SW	D	G4o	Winner
Overall	82.96	83.38	82.61	82.90	83.55	83.60	85.41	77.66	D
Semantic Accuracy	85.08	N/A	85.17	85.59	86.69	86.69	87.12	78.39	D
Visual Quality	80.85	84.07	80.42	80.93	81.27	81.78	82.97	77.12	E
Coherence	83.22	N/A	82.71	83.90	84.07	83.98	85.51	79.15	D
Technical Execution	80.51	N/A	80.17	80.51	80.85	81.61	83.98	75.34	D
Instruction Following	84.92	83.81	84.32	84.24	85.93	84.92	87.03	77.37	D
Transformation Strength	83.31	N/A	82.71	82.20	82.63	82.54	85.68	78.73	D

Figure 5. Complex Vision-8B: DPO wins followed closely by RW and SW on diverse themes (85.41). Outperforms GPT-4o(grey).

Complete results for all 12 configurations (3 datasets × 2 sizes × 2 modalities) are provided in Appendix G. Detailed analysis of action planning and reasoning quality using GPT-4o as an automated judge, including qualitative comparisons showing that SW produces more detailed and contextual chain-of-thought reasoning than the baseline, appears in Appendix H and Appendix H.4. Visual comparisons of 9-way method outputs (Original, B, E, S, R, RW, SW, DPO, GPT-4o) are shown in Appendix A.

Comparison with GPT-4o Planner: GPT-4o provides a zero-shot baseline—a large-scale closed-source model. Our trained 4B/8B models outperform GPT-4o on image quality in majority of the tasks, demonstrating that offline RL enables smaller models to exceed larger general-purpose systems. Human validation (Section 3.3) shows our methods achieve 77% pass rate, confirming practical quality. See Appendix F.7 for detailed comparison.

6. Conclusion

We present a tool-based agentic RL post-training framework for compositional image styling, showing that method effectiveness varies systematically with task complexity and modality. Evaluating 30,000 synthetic trajectories across Simple, Regular, and Complex settings (including human evaluation), we find that RW and SW outperform competing baselines on most tasks. Our key insight is that reward weighting preserves fine-grained quality distinctions essential for multi-step reasoning. This advantage is amplified by visual grounding: vision-4B with RW substantially outperforms all baselines. We introduce a compositional tool library of 10 primitives with per-step reasoning, enabled by

a 5-stage synthetic data generation pipeline. Future work includes extending the framework to video editing with temporal consistency and scaling to larger tool libraries; together, our data generation and ground-truth-free evaluation pipelines offer a general blueprint for efficient agentic systems in creative domains.

Impact Statement

This work presents a framework for training AI systems to decompose complex image editing tasks into interpretable, structured action sequences with explicit reasoning. While the immediate application is creative image styling, the broader societal implications include potential misuse for generating misleading visual content or deepfakes. However, the structured, interpretable nature of our approach—where each transformation step is explicitly reasoned and documented—actually enhances transparency compared to black-box editing methods, potentially supporting content provenance and authenticity verification efforts.

References

- Andukuri, C., Fränken, J.-P., Gerstenberg, T., and Goodman, N. Star-gate: Teaching language models to ask clarifying questions. *arXiv preprint arXiv:2403.19154*, 2024.
- Bai, J., Bai, S., Yang, S., Wang, S., Tan, S., Wang, P., Lin, J., Zhou, C., and Zhou, J. Qwen-vl: A versatile vision-language model for understanding, localization, text reading, and beyond. *arXiv preprint arXiv:2308.12966*, 2023.
- Bai, S., Chen, K., Liu, X., Wang, J., Ge, W., Song, S., Dang, K., Wang, P., Wang, S., Tang, J., et al. Qwen2. 5-vl technical report. *arXiv preprint arXiv:2502.13923*, 2025.
- Baxter, J. and Bartlett, P. L. Infinite-horizon policy-gradient estimation. *Journal of Artificial Intelligence Research*, 15:319–350, 2001.
- Betker, J., Goh, G., Jing, L., Brooks, T., Wang, J., Li, L., Ouyang, L., Zhuang, J., Lee, J., Guo, Y., et al. Improving image generation with better captions. *Computer Science*. <https://cdn.openai.com/papers/dall-e-3.pdf>, 2(3): 8, 2023.
- Boutillier, C., Hsu, C.-w., Kveton, B., Mladenov, M., Szepesvari, C., and Zaheer, M. Differentiable meta-learning of bandit policies. In *Advances in Neural Information Processing Systems (NeurIPS)*, volume 33, 2020.
- Bradley, R. A. and Terry, M. E. Rank analysis of incomplete block designs: I. the method of paired comparisons. *Biometrika*, 39(3/4):324–345, 1952.
- Brooks, T., Holynski, A., and Efros, A. A. Instructpix2pix: Learning to follow image editing instructions. In *Proceedings of the IEEE/CVF Conference on Computer Vision and Pattern Recognition (CVPR)*, pp. 18392–18402, 2023.
- Feng, W., He, X., Fu, T.-J., Jampani, V., Akula, A., and Wang, W. Y. Layout-guidance for spatial consistency in text-to-image generation. *arXiv preprint arXiv:2402.07925*, 2024.
- Fu, M., Wang, G.-H., Cui, T., Chen, Q.-G., Xu, Z., Luo, W., and Zhang, K. Diffusion-sdpo: Safeguarded direct preference optimization for diffusion models. *arXiv preprint arXiv:2511.03317*, 2025.
- Gao, J., Liu, Y., Sun, Y., Tang, Y., Zeng, Y., Chen, K., and Zhao, C. Styleshot: A snapshot on any style. *arXiv preprint arXiv:2407.01414*, 2024.
- Gatys, L. A., Ecker, A. S., and Bethge, M. Image style transfer using convolutional neural networks. *Proceedings of the IEEE Conference on Computer Vision and Pattern Recognition (CVPR)*, pp. 2414–2423, 2016.
- Guo, H., Wu, J., Liu, J., Gao, Y., Ye, Z., Yuan, L., Wang, X., Yu, Y., and Huang, W. Edit-r1: Unleashing reasoning-based reinforcement learning for image editing. *arXiv preprint arXiv:2510.16888*, 2025.
- Han, Z., Mao, C., Jiang, Z., Pan, Y., and Zhang, J. Stylebooth: Image style editing with multimodal instruction. In *Proceedings of the IEEE/CVF International Conference on Computer Vision (ICCV) Workshops*, pp. 1947–1957, 2025.
- Hartwig, S., Engel, D., Sick, L., Kniesel, H., Payer, T., Poonam, P., Glockler, M., Bauerle, A., and Ropinski, T. A survey on quality metrics for text-to-image generation. *IEEE Transactions on Visualization and Computer Graphics*, 2025.
- Hussein, A., Gaber, M. M., Elyan, E., and Jayne, C. Imitation learning: A survey of learning methods. *ACM Computing Surveys (CSUR)*, 50(2):1–35, 2017.
- Isola, P., Zhu, J.-Y., Zhou, T., and Efros, A. A. Image-to-image translation with conditional adversarial networks. In *Proceedings of the IEEE Conference on Computer Vision and Pattern Recognition (CVPR)*, pp. 1125–1134, 2017.
- Jayasumana, S., Ramalingam, S., Veit, A., Glasner, D., Chakrabarti, A., and Kumar, S. Rethinking fid: Towards a better evaluation metric for image generation. In *Proceedings of the IEEE/CVF Conference on Computer Vision and Pattern Recognition*, pp. 9307–9315, 2024.
- Jiang, D., Zhang, R., and Li, H. Draft-as-cot: Interleaved reasoning for enhanced text-to-image generation. *arXiv preprint arXiv:2512.05112*, 2025.

- Kazemi, H., Iranmanesh, S. M., and Nasrabadi, N. Style and content disentanglement in generative adversarial networks. In *2019 IEEE Winter Conference on Applications of Computer Vision (WACV)*, pp. 848–856. IEEE, 2019.
- Lange, S., Gabel, T., and Riedmiller, M. *Batch Reinforcement Learning*, pp. 45–73. Springer Berlin Heidelberg, Berlin, Heidelberg, 2012.
- Levine, S., Kumar, A., Tucker, G., and Fu, J. Offline reinforcement learning: Tutorial, review, and perspectives on open problems. *arXiv preprint arXiv:2005.01643*, 2020.
- Li, B., Qi, X., Lukasiewicz, T., and Torr, P. Controllable text-to-image generation. *Advances in neural information processing systems*, 32, 2019.
- Liu, H., Li, C., Wu, Q., and Lee, Y. J. Visual instruction tuning. In *Advances in Neural Information Processing Systems (NeurIPS)*, 2023.
- Mukherjee, S., Lalitha, A., Kalantari, K., Deshmukh, A., Liu, G., Ma, Y., and Kveton, B. Optimal design for human preference elicitation. In *Advances in Neural Information Processing Systems*, volume 37, 2024.
- Mukherjee, S., Lai, V. D., Addanki, R., Rossi, R. A., Yoon, S., Bui, T., Rao, A., Subramanian, J., and Kveton, B. Offline rl by reward-weighted fine-tuning for conversation optimization. In *Advances in Neural Information Processing Systems (NeurIPS)*, 2025.
- Munos, R. Error bounds for approximate policy iteration. In *Proceedings of the Twentieth International Conference on Machine Learning (ICML)*, 2003.
- Peng, X. B., Kumar, A., Zhang, G., and Levine, S. Advantage-weighted regression: Simple and scalable off-policy reinforcement learning. *arXiv preprint arXiv:1910.00177*, 2019.
- Peters, J. and Schaal, S. Reinforcement learning by reward-weighted regression for operational space control. In *Proceedings of the 24th International Conference on Machine Learning (ICML)*, pp. 745–750, 2007.
- Plackett, R. L. The analysis of permutations. *Journal of the Royal Statistical Society: Series C (Applied Statistics)*, 24(2):193–202, 1975.
- Pomerleau, D. A. Efficient training of artificial neural networks for autonomous navigation. *Neural Computation*, 3(1):88–97, 1991.
- Rafailov, R., Sharma, A., Mitchell, E., Ermon, S., Manning, C. D., and Finn, C. Direct preference optimization: Your language model is secretly a reward model. *arXiv preprint arXiv:2305.18290*, 2023.
- Ramesh, A., Pavlov, M., Goh, G., Gray, S., Voss, C., Radford, A., Chen, M., and Sutskever, I. Zero-shot text-to-image generation. In *International conference on machine learning*, pp. 8821–8831. Pmlr, 2021.
- Ramesh, A., Dhariwal, P., Nichol, A., Chu, C., and Chen, M. Hierarchical text-conditional image generation with clip latents. *arXiv preprint arXiv:2204.06125*, 1(2):3, 2022.
- Rombach, R., Blattmann, A., Lorenz, D., Esser, P., and Ommer, B. High-resolution image synthesis with latent diffusion models. In *Proceedings of the IEEE/CVF conference on computer vision and pattern recognition*, pp. 10684–10695, 2022.
- Schulman, J., Moritz, P., Levine, S., Jordan, M., and Abbeel, P. High-dimensional continuous control using generalized advantage estimation. *arXiv preprint arXiv:1506.02438*, 2015.
- Schulman, J., Wolski, F., Dhariwal, P., Radford, A., and Klimov, O. Proximal policy optimization algorithms. *arXiv preprint arXiv:1707.06347*, 2017.
- Shao, Z., Wang, P., Zhu, Q., Xu, R., Song, J., Bi, X., Zhang, H., Zhang, M., Li, Y., Wu, Y., and Guo, D. Deepseek-math: Pushing the limits of mathematical reasoning in open language models. *arXiv preprint arXiv:2402.03300*, 2024.
- Shen, Y. et al. Agentic retoucher: A perception-reasoning-action loop for autonomous image artifact correction. *arXiv preprint arXiv:2601.02046*, 2026.
- Sutton, R. S., McAllester, D. A., Singh, S. P., and Mansour, Y. Policy gradient methods for reinforcement learning with function approximation. In *Advances in Neural Information Processing Systems (NIPS)*, volume 12, pp. 1057–1063, 2000.
- Team, Q. Qwen3 technical report, 2025. URL <https://arxiv.org/abs/2505.09388>.
- Wallace, B., Dang, M., Rafailov, R., Zhou, L., Lou, A., Pushwalkam, S., Ermon, S., Xiong, C., Joty, S., and Naik, N. Diffusion model alignment using direct preference optimization. *arXiv preprint arXiv:2311.12908*, 2023.
- Wei, J., Bosma, M., Zhao, V. Y., Guu, K., Yu, A. W., Lester, B., Du, N., Dai, A. M., and Le, Q. V. Finetuned language models are zero-shot learners. *arXiv preprint arXiv:2109.01652*, 2021.
- Williams, R. J. Simple statistical gradient-following algorithms for connectionist reinforcement learning. *Machine Learning*, 8:229–256, 1992.

- Wu, C., Li, J., Zhou, J., Lin, J., Gao, K., et al. Qwen-image technical report, 2025. URL <https://arxiv.org/abs/2508.02324>.
- Xu, J., Liu, X., Wu, Y., Tong, Y., Li, Q., Ding, M., Tang, J., and Dong, Y. Imagereward: Learning and evaluating human preferences for text-to-image generation. *Advances in Neural Information Processing Systems*, 36: 15903–15935, 2023.
- Yang, L., Yu, Z., Meng, C., Cui, B., et al. Mastering text-to-image diffusion: Recaptioning, planning, and generating with multimodal llms. *arXiv preprint arXiv:2401.11708*, 2024.
- Yeh, C.-H., Wang, Y., Zhao, N., Zhang, R., Li, Y., Ma, Y., and Singh, K. K. Beyond simple edits: X-planner for complex instruction-based image editing. *arXiv preprint arXiv:2507.05259*, 2025.
- Zhang, K., Mo, L., Chen, W., Sun, H., and Su, Y. Magicbrush: A manually annotated dataset for instruction-guided image editing. In *Advances in Neural Information Processing Systems (NeurIPS)*, 2023a.
- Zhang, L., Rao, A., and Agrawala, M. Adding conditional control to text-to-image diffusion models. In *Proceedings of the IEEE/CVF international conference on computer vision*, pp. 3836–3847, 2023b.
- Zhao, H., Ma, X. S., Chen, L., Si, S., Wu, R., An, K., Yu, P., Zhang, M., Li, Q., and Chang, B. Ultraedit: Instruction-based fine-grained image editing at scale. *Advances in Neural Information Processing Systems*, 37:3058–3093, 2024.
- Zhu, J.-Y., Park, T., Isola, P., and Efros, A. A. Unpaired image-to-image translation using cycle-consistent adversarial networks. In *Proceedings of the IEEE International Conference on Computer Vision (ICCV)*, pp. 2223–2232, 2017.
- Zhuang, J., Zeng, Y., Liu, W., Yuan, C., and Chen, K. A task is worth one word: Learning with task prompts for high-quality versatile image inpainting. In *European Conference on Computer Vision*, pp. 195–211. Springer, 2024.

Appendix Overview

Section	Page
Visual Method Comparisons	14
9-way visual comparisons (RW/SW, DPO, RL examples)	14
Related Work	18
Appendix A: Complete Problem Formulation Details	
§A.1 Context Representation Details	19
§A.2 Action Space Specification	20
§A.3 Reward Function Details	25
§A.4 Synthetic Data Generation Details	26
Appendix B: Complete Synthesis Pipeline Examples	
§B.1 Example 1: Normal Dataset — Autumn Vineyard to Spring Tulip Field	30
§B.2 Example 2: Complex Dataset — Contemporary Studio to Cyberpunk Nightclub ..	33
§B.3 Comparison and Insights	38
§B.4 Example 3: Complex V2 Dataset — Arctic Glacier to Desert Canyon	38
§B.5 Dataset Comparison	41
Appendix C: Training Algorithms	
§C.1 Standard Supervised Learning	42
§C.2 Reward-Weighted Fine-Tuning (RW)	43
§C.3 Direct Preference Optimization (DPO)	45
§C.4 Theoretical Justification for RW and DPO	49
§C.5 Complete Training Configuration	50
§C.6 Cached Embedding Approach	52
§C.7 Algorithm Comparison	54
Appendix D: Experimental Details	
§D.1 GPT-4o Evaluation Prompts	55
§D.2 GPT-4o Evaluation Configuration	57
§D.3 Baseline Model Specifications	58
§D.4 Training Infrastructure	58
§D.5 Hyperparameter Search	58
§D.6 Training Configuration Details	50
§D.7 Edit-Only Baseline Detailed Analysis	60
§D.8 Complete Results by Configuration	62
§D.9 Per-Metric Detailed Analysis	65
Appendix E: Complete Experimental Results	
§E.1 Additional Image Quality Tables	65
§E.2 Method Comparison Summary	70
§E.3 Discussion: When to Use Each Method	70
Appendix F: Role of Reasoning in Action Planning	
§F.1 GPT-4o Action Plan Quality Evaluation	71
§F.2 Key Findings on Reasoning Quality	71
§F.3 Implications for Interpretable Image Styling	73
Appendix G: Training and Implementation Details	
§G.1 Hyperparameters	78
§G.2 RW Weight Scheme	78
§G.3 DPO Preference Pair Generation	78
§G.4 Computational Resources	79
§G.5 Cached Embedding Implementation	79

Section	Page
§G.6 Evaluation Infrastructure	79
Appendix H: Human Evaluation Study	
§H.1 Evaluation Setup and Methodology	80
§H.2 Overall Results	81
§H.3 Agreement Patterns	81
§H.4 Validation of Dataset Quality	82

A. Visual Method Comparisons

This section provides qualitative visual examples demonstrating when specific training methods excel. Each comparison image shows a 9-way comparison: Original, Baseline, Edit-Only, Standard SL, R, RW, SW, DPO, and GPT-4o Planner.

A.1. Reward-Weighted (RW) and Standardized Reward-Weighted (SW) Strengths

Both RW and SW weight each trajectory’s gradient contribution by its reward score during training, unlike R which discards low-reward data (35%) or Standard SL which treats all trajectories equally. RW multiplies each trajectory’s gradient by its reward ($w_i = \max\{r_i - 3.0, 0\}$), allowing every sample to contribute proportionally to its quality—e.g., a high-quality trajectory with $r = 5.0$ (weight 2.0) contributes twice the gradient of a medium-quality trajectory with $r = 4.0$ (weight 1.0). SW extends this by standardizing rewards via z-score ($z_i = \frac{r_i - \bar{r}}{\sigma_r}$), which reduces gradient variance and creates symmetric upweighting/downweighting: above-average trajectories receive positive gradient weight, below-average trajectories receive negative gradient weight (implicit downweighting). This continuous gradient weighting mechanism preserves all training data and its diversity while emphasizing quality through each trajectory’s contribution to parameter updates. The following examples show visual outcomes where this mechanism excels:

A.2. DPO (Direct Preference Optimization) Strengths

Unlike RW and SW which weight individual trajectories by continuous reward scores, DPO learns from pairwise preferences between chosen (high-quality, $r \geq 4.0$) and rejected (low-quality, $r \in [2.5, 3.5]$) trajectories sharing the same input. The contrastive loss explicitly optimizes the model to increase the log-likelihood gap between better and worse outcomes, capturing fine-grained quality distinctions that may be difficult to express in absolute scores alone. This pairwise mechanism requires paired data and doubles memory cost compared to RW/SW, but can be more effective when quality differences are subtle, subjective, or involve contradictory requirements. The following examples show visual outcomes where this pairwise contrastive mechanism excels:

A.3. R (Reward-Filtered) Strengths

Reward-filtered training (R) applies a binary threshold ($r \geq 4.0$), discarding 35% of trajectories and training with standard supervised learning (equal gradient weights) on the surviving 65%. Unlike RW and SW which use continuous gradient weighting on ALL data, R makes a simple binary decision: keep high-quality data, discard the rest. This filtering approach offers computational simplicity—no custom loss weighting or reference models needed—and effectively removes catastrophic failures while maintaining sufficient training signal from the retained high-quality examples. However, it discards potentially useful medium-quality data ($r \in [3.5, 4.0]$) that continuous weighting methods can still learn from. The following examples show scenarios where this simple filtering strategy is sufficient:

A.4. Key Observations

- **DPO vs. RW:** When preference pairs exhibit clear quality differences, DPO’s contrastive loss provides sharper distinctions than RW’s continuous weighting. However, RW maintains advantage when all trajectories have moderate-to-high quality.
- **R vs. SL:** Even simple reward-based filtering (R) substantially improves over treating all data equally (SL). The 65% data retention threshold balances quality and quantity effectively.
- **Method Selection:** Choose DPO when preference pairs are available and fine-grained distinctions matter; choose RW for maximum data efficiency with diverse quality; choose R when computational simplicity is paramount and data is plentiful.

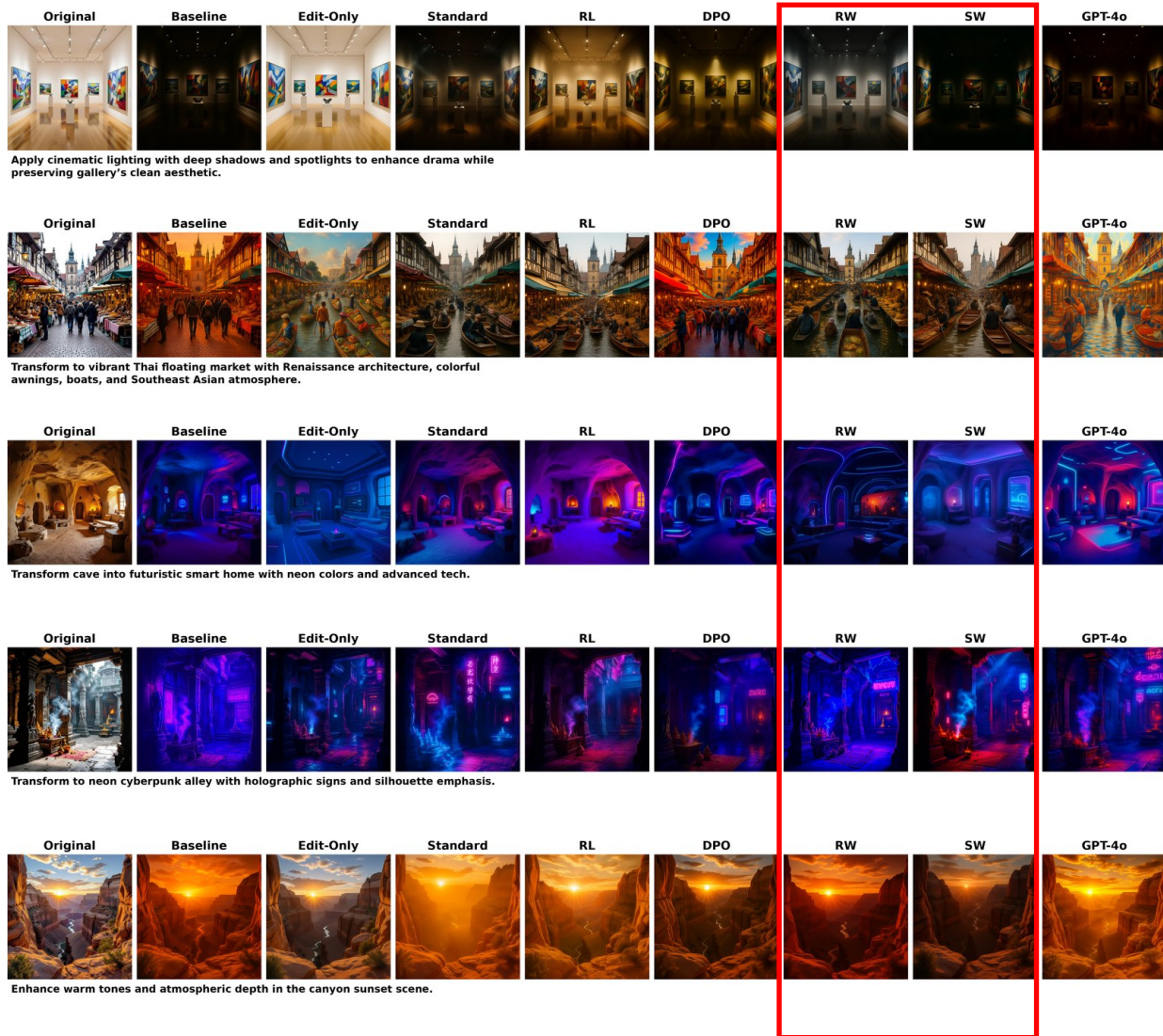


Figure 6. RW and SW Strengths Across Datasets: Examples where reward-aware weighting methods excel. Each row shows (left to right): **Original**, **Baseline (B)**, **Edit-Only (E)**, **Standard (S)**, **R (R)**, **DPO (D)**, **RW**, **SW**, and **GPT-4o Planner**. Red box highlights RW and SW columns. **Row 1 (Text-8B, Complex):** Gallery art scene with bokeh lens effect and character depth—SW handles complex multi-element transformations. **Row 2 (Vision-4B, Regular):** Market scene with visual grounding—RW excels with continuous reward weighting. **Row 3 (Vision-4B, Regular):** Prehistoric stone age transformation—RW achieves strong temporal consistency. **Row 4 (Text-4B, Regular):** Temple shrine transformation—SW handles architectural and cultural elements effectively. **Row 5 (Vision-8B, Complex):** Canyon landscape with lens effects—SW produces superior depth and lighting. Reward-aware methods consistently outperform filtering (R) and preference learning (DPO) by leveraging continuous quality signals while preserving data diversity.

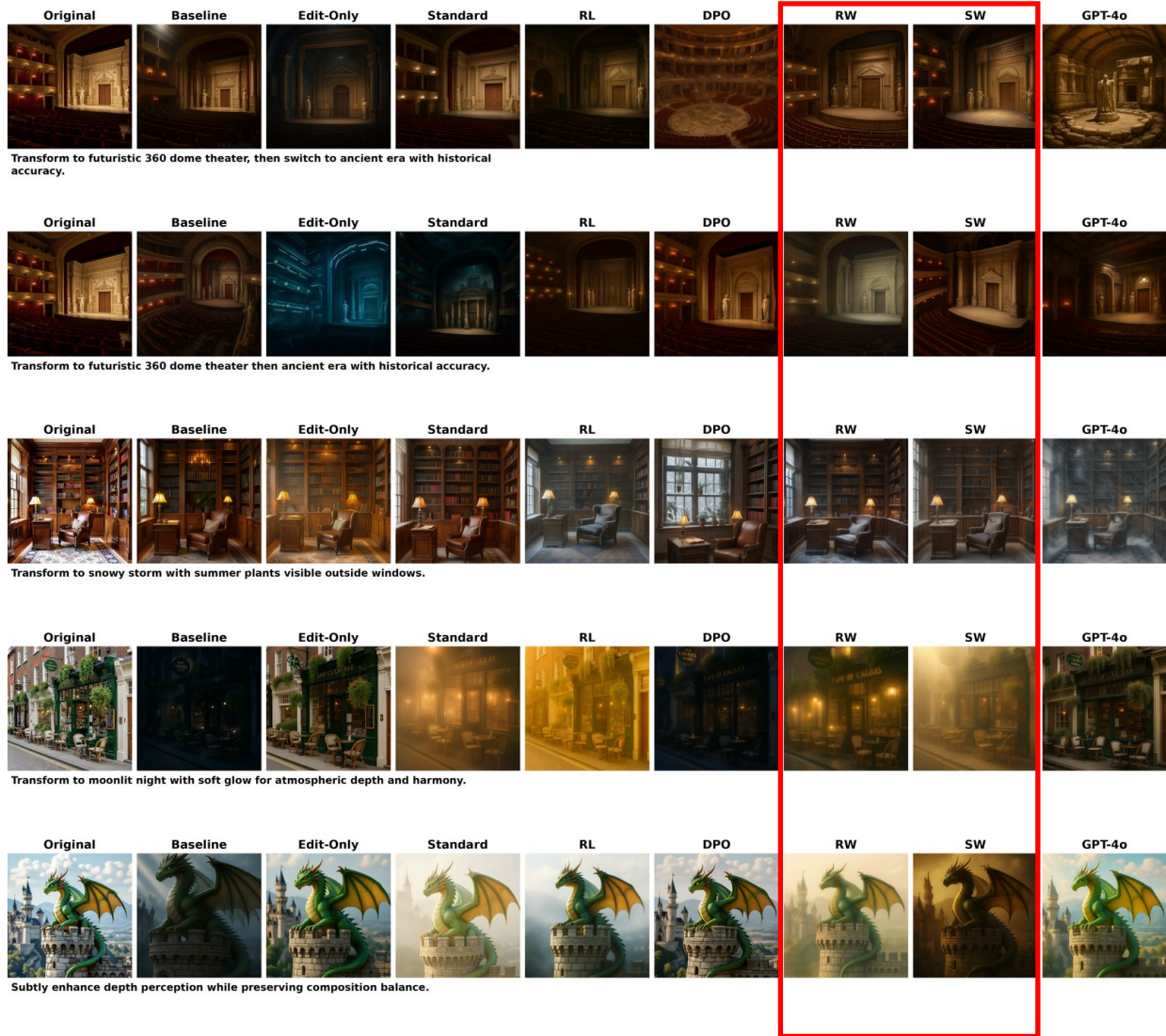


Figure 7. DPO Strengths Across Datasets: Examples where DPO outperforms other methods through fine-grained contrastive learning. Each row shows (left to right): **Original**, **Baseline (B)**, **Edit-Only (E)**, **Standard (S)**, **R (R)**, **RW**, **SW**, **DPO (D)**, and **GPT-4o Planner**. Red box highlights RW and SW columns for comparison. **Row 1 (Text-8B, Simple):** Renaissance time period transformation from futuristic dome theater to ancient era. **Row 2 (Vision-4B, Simple):** Holographic future architecture combined with charcoal drawing artistic medium—a complex multi-action transformation. **Row 3 (Vision-4B, Regular):** Classic library with paradoxical snowstorm and summer plants visible outside windows. **Row 4 (Vision-4B, Complex):** Cafe transformed with surrealist art movement, dreamy textures, and soft edges. **Row 5 (Text-8B, Complex):** Dragon scene with subtle depth enhancement via color grading. DPO’s contrastive learning captures fine-grained preference distinctions across diverse datasets and complexity levels, consistently producing results closer to GPT-4o reference than other methods. Edit-Only (E) shows inconsistent quality without structured action planning.

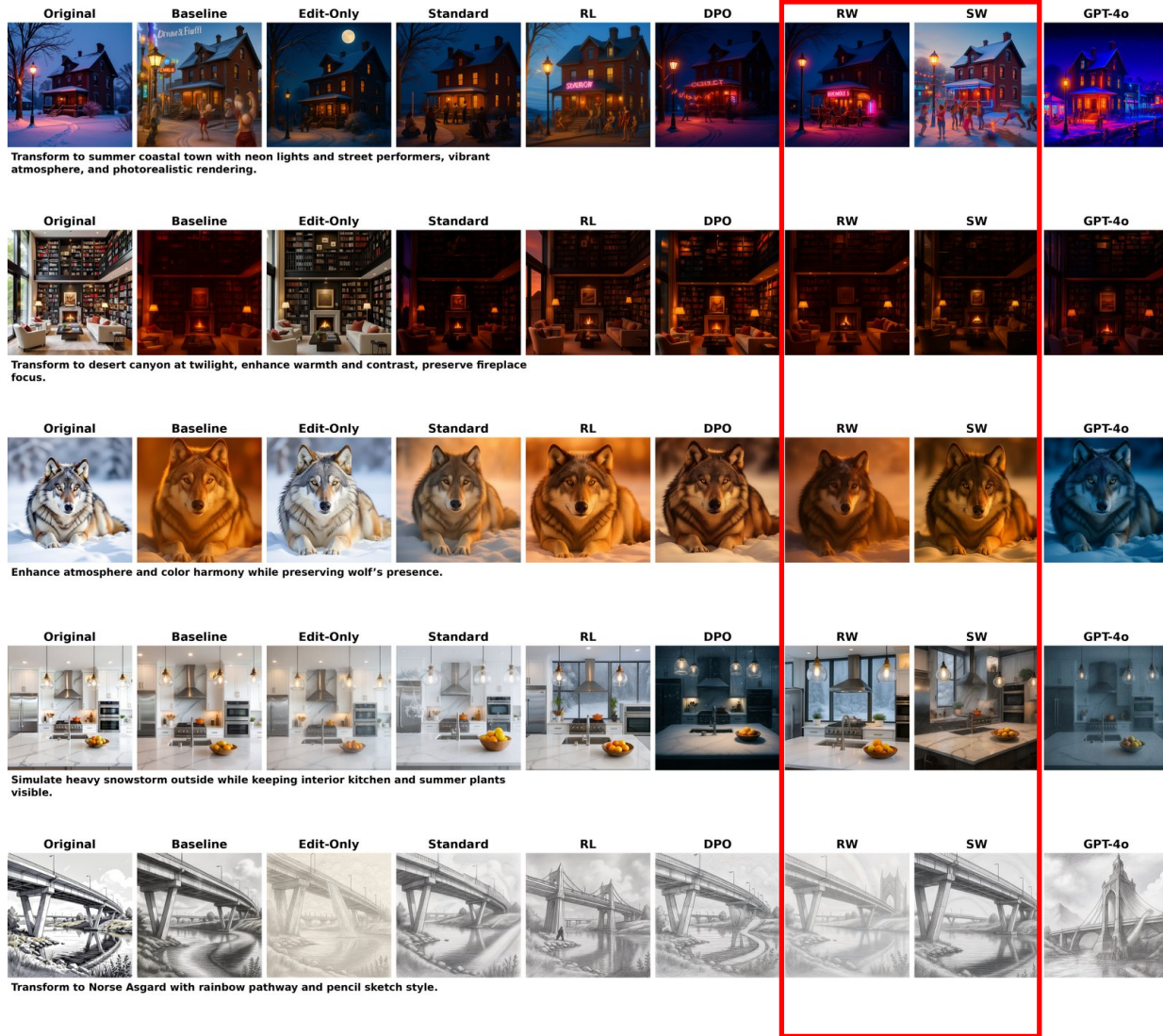


Figure 8. R Strengths Across Datasets: Examples where reward-filtering performs effectively. Each row shows (left to right): **Original**, **Baseline (B)**, **Edit-Only (E)**, **Standard (S)**, **R (R)**, **RW**, **SW**, **DPO (D)**, and **GPT-4o Planner**. Red box highlights RW and SW columns for comparison. **Row 1 (Text-8B, Simple):** Winter to summer coastal town transformation—multi-action sequence changing location, architecture, time of day, and weather. **Row 2 (Text-8B, Complex):** Spatial depth enhancement with atmospheric haze and cinematic lighting. **Row 3 (Text-8B, Complex):** Wolf scene with winter atmosphere enhancement via cool-toned color grading and soft haze. **Row 4 (Vision-8B, Regular):** Urban kitchen transformed to snowy winter wonderland under blue twilight. **Row 5 (Vision-4B, Simple):** Bridge to Asgard Bifrost with Norse architecture and pencil sketch artistic medium. R’s filtering strategy ($r_i < 3.5$ threshold) effectively removes low-quality data while maintaining training signal across diverse task types and complexity levels. Its computational efficiency and consistent quality make it attractive for large-scale training. Edit-Only (E) demonstrates the necessity of structured action planning.

B. Related Work

Our work sits at the intersection of controllable image synthesis, agentic reasoning, and offline reinforcement learning. We briefly review the evolution of these fields to contextualize our Agentic RL framework.

From Direct Editing to Agentic Planning. The paradigm of automated image styling has evolved from signal-level manipulation to semantic generation. Early neural approaches relied on optimization-based style transfer (Gatys et al., 2016) or GAN-based image-to-image translation (Isola et al., 2017; Zhu et al., 2017), which were effective but limited to specific domains. The advent of diffusion models introduced "Direct Prompt-Based Editing" (the *Edit-Only* baseline), exemplified by **InstructPix2Pix** (Brooks et al., 2023) and dataset efforts like **MagicBrush** (Zhang et al., 2023a). While these end-to-end models excel at global style swaps, they lack the symbolic reasoning required for compositional tasks. Recent works like **StyleBooth** (Han et al., 2025) and **StyleShot** (Gao et al., 2024) improved fidelity through exemplar guidance but remain bound by the "one-shot" generation paradigm, often failing to resolve conflicting constraints (e.g., "change weather but preserve architecture") due to attribute binding failures (Feng et al., 2024).

To address these structural limitations, the field is shifting toward *Agentic AI*, where Large Multimodal Models (LMMs) act as planners. Frameworks like **RPG** (Recaption, Plan, Generate) (Yang et al., 2024) and **DraCo** (Draft-as-CoT) (Jiang et al., 2025) demonstrate that decomposing generation into hierarchical sub-tasks significantly improves spatial adherence. Most recently, **Edit-R1** (Guo et al., 2025) and **Agentic-Retoucher** (Shen et al., 2026) have begun integrating Chain-of-Thought (CoT) reasoning directly into the editing loop, validating our hypothesis that explicit reasoning traces are essential for complex instruction following.

Reinforcement Learning for Generative Models. Aligning generative models with human intent has traditionally relied on Reinforcement Learning from Human Feedback (RLHF) via PPO (Schulman et al., 2017). However, PPO is computationally expensive and unstable for high-dimensional visual tasks. This led to the adoption of **Direct Preference Optimization (DPO)** (Rafailov et al., 2023), which optimizes policy likelihoods directly on preference pairs. **Diffusion-DPO** (Wallace et al., 2023) successfully adapted this to pixel-space denoising. However, recent critiques suggest DPO can suffer from mode collapse or fail to preserve structural integrity in editing tasks, prompting "safeguarded" variants like **Diffusion-SDPO** (Fu et al., 2025).

Reward-Weighted Methods in Offline RL. Our use of Reward-Weighted (RW) and Standardized Reward-Weighted (SW) fine-tuning draws on a lineage of Expectation-Maximization (EM) based RL. Peters & Schaal (2007) originally formulated **Reward-Weighted Regression (RWR)** for robotic control, treating RL as a supervised regression problem on high-reward samples. This was later generalized by **Advantage-Weighted Regression (AWR)** (Peng et al., 2019). Most relevant to our work, Mukherjee et al. (2025) recently formalized **Reward-Weighted Fine-Tuning** and **Standardized Reward-Weighted (SWiFt)** for language models. They showed that reward-weighted log-probability maximization is a lower bound on the online RL objective and proposed optimizing it via weighted fine-tuning, essentially a form of policy gradient (Williams, 1992). Their analysis proves that these methods can optimize reward signals more stably than DPO in offline settings. Note that Mukherjee et al. (2025) looked into the offline RL reward-weighted algorithms in the context of conversation optimization. We extend these findings to the vision-language domain, demonstrating that for compositional planning tasks—where "correctness" is often binary and logic-driven—scalar reward weighting (RW/SW) provides a denser, more effective training signal than preference ranking.

Agentic Planning with Spatial Grounding. Recent work on complex image editing includes **X-Planner** (Yeh et al., 2025), which introduces a planner-localizer framework that decomposes high-level instructions into sub-tasks with automatically generated spatial guidance (segmentation masks and bounding boxes). These spatial annotations guide specialized editing models (e.g., UltraEdit (Zhao et al., 2024), PowerPaint (Zhuang et al., 2024)) to execute localized edits. X-Planner is trained on COMPIE, a large-scale dataset of 260K complex-simple instruction pairs, using standard supervised fine-tuning for grounded segmentation and reasoning. Our approach differs in two key ways: (1) **Execution mechanism**—we use symbolic tool calls synthesized into natural language instructions for a frozen black-box editor, avoiding spatial grounding or specialized editing models; (2) **Training methodology**—we employ offline RL with reward-weighted fine-tuning to prioritize high-quality trajectories rather than uniform supervised learning on all instruction pairs.

C. Complete Problem Formulation Details

This appendix provides comprehensive specifications for the problem formulation, action spaces, reward function, and synthetic data generation pipeline.

C.1. Context Representation Details

The structured context representation $c_i = \{d_1, \dots, d_{10}\}$ encodes an image’s current visual state across 10 dimensions. Each dimension d_j is extracted via a frozen Qwen3-VL-8B-Instruct model using vision-language understanding.

C.1.1. DIMENSION SPECIFICATIONS

1. Location (d_{loc})

Physical environment type where the scene takes place.

Example values: urban_city, suburban_neighborhood, rural_village, industrial_zone, beach_coast, tropical_island, forest_temperate, desert_sand, mountain_rocky, cave_underground, space_station, fantasy_castle, medieval_town, cyberpunk_city, bedroom_interior, office_modern.

2. Architecture (d_{arch})

Architectural style of buildings and structures.

Example values: modern_minimalist, classical_greek, victorian_gothic, art_deco, brutalist_concrete, traditional_asian, middle_eastern, industrial_warehouse, futuristic_sci_fi, cyberpunk_neon, medieval_castle, baroque_ornate.

3. Time Period Era (d_{era})

Historical or futuristic time period reflected in props, technology, and visual style.

Example values: prehistoric, ancient_classical, medieval_dark_ages, renaissance, victorian_1800s, early_1900s, mid_century_1950s, modern_2000s, near_future_2050s, far_future_2200s.

4. Time of Day (d_{time})

Natural lighting from sun/moon position.

Example values: dawn_first_light, morning_golden, midday_overhead, afternoon_warm, sunset_golden, dusk_twilight, night_moonlit, night_starlit, overcast_diffuse.

5. Season (d_{season})

Seasonal markers in vegetation, weather, and atmosphere.

Example values: spring_blooming, summer_lush, autumn_falling, winter_snow, dry_season, wet_season, eternal_spring (fantasy).

6. Weather ($d_{weather}$)

Atmospheric weather conditions.

Example values: clear_sky, partly_cloudy, overcast_gray, light_rain, heavy_rain, thunderstorm, light_snow, blizzard, fog_heavy, mist_light, dust_storm, hazy.

7. Mood Lighting (d_{mood})

Emotional ambiance conveyed through lighting and atmosphere.

Example values: neutral_balanced, warm_cozy, cool_calm, dramatic_contrast, mysterious_dark, ethereal_soft, tense_harsh, romantic_soft, energetic_bright, melancholic_muted, ominous_dark, serene_peaceful.

8. Color Grading (d_{color})

Overall color palette and correction.

Example values: natural_balanced, warm_cinematic, cool_blue, sepia_vintage, black_white, high_contrast, low_saturation, vibrant_saturated, teal_orange, purple_magenta, desaturated_muted, neon_bright, pastel_soft.

9. Artistic Medium (d_{medium})

Rendering style and artistic technique.

Example values: photorealistic, oil_painting, watercolor, pencil_sketch, digital_art, anime_style, pixel_art, impressionist, abstract, low_poly_3d, clay_animation, charcoal_drawing, comic_book.

10. Atmospheric Effects (d_{atmos})

Environmental effects and particles.

Example values: none_clear, fog_dense, mist_light, haze_atmospheric, dust_particles, smoke_wisps, rain_drops, snow_falling, embers_floating, sparkles_magical, lens_flare, light_rays.

C.1.2. EXTRACTION PROCESS

The context extraction process queries Qwen3-VL-8B-Instruct with a structured prompt:

Context Extraction Prompt

Analyze this image and extract the following 10 visual attributes in JSON format:

```
{
  "location": "<category>",
  "architecture": "<category>",
  "time_period_era": "<category>",
  "time_of_day": "<category>",
  "season": "<category>",
  "weather": "<category>",
  "mood_lighting": "<category>",
  "color_grading": "<category>",
  "artistic_medium": "<category>",
  "atmospheric_effects": "<category>"
}
```

Be specific and use the standardized vocabulary.

The model returns structured JSON which is parsed into c_i . Extraction takes approximately 2-3 seconds per image on an A100 GPU. This explicit symbolic representation provides the planner with state awareness that pure vision encoding may miss.

C.2. Action Space Specification

We define two action libraries: a 10-action core library for the normal dataset, and an extended 20-action library for the complex dataset.

C.2.1. SIMPLE DATASET: 10 ATOMIC ACTIONS

1. Location Setting (a_{loc}) **Description:** Changes physical environment type (e.g., urban city \rightarrow tropical beach).

Parameters:

- `source_location`: Current location type
- `target_location`: Desired location type
- `replace_mode`: "partial" (blend) or "complete" (full replacement)
- `preserve_foreground`: Boolean, keep main subjects unchanged
- `description`: Natural language explanation

Example:

$a = (\text{location_setting}, \{\text{source} = \text{"urban_city"}, \text{target} = \text{"tropical_beach"}, \text{mode} = \text{"complete"}\})$

2. Architecture Style (a_{arch}) **Description:** Modifies building architectural style (e.g., modern \rightarrow Victorian).

Parameters:

- `source_style`: Current architectural style
- `target_style`: Desired architectural style
- `detail_level`: "subtle", "moderate", or "extensive"
- `preserve_layout`: Boolean, keep spatial structure
- `description`: Natural language explanation

3. Time Period Era (a_{era}) **Description:** Updates props and technology to match historical/future period (e.g., 2000s \rightarrow 1800s).

Parameters:

- `source_era`: Current time period
- `target_era`: Desired time period
- `technology_update`: Boolean, change technology/vehicles
- `clothing_update`: Boolean, update character clothing
- `description`: Natural language explanation

4. Time of Day (a_{time}) **Description:** Adjusts natural lighting from sun/moon position (e.g., midday \rightarrow sunset).

Parameters:

- `source_time`: Current time of day
- `target_time`: Desired time of day
- `sky_color`: Target sky color palette
- `shadow_direction`: Shadow angle adjustment
- `description`: Natural language explanation

5. Season Cycle (a_{season}) **Description:** Changes vegetation and seasonal markers (e.g., summer \rightarrow autumn).

Parameters:

- `source_season`: Current season
- `target_season`: Desired season
- `vegetation_change`: "foliage_color", "density", "type"
- `temperature_effects`: "snow", "heat_haze", "none"
- `description`: Natural language explanation

6. Weather Conditions (a_{weather}) **Description:** Modifies atmospheric weather state (e.g., clear \rightarrow rainy).

Parameters:

- `source_weather`: Current weather condition
- `target_weather`: Desired weather condition
- `intensity`: "light", "moderate", "heavy"
- `visibility_change`: Boolean, affect scene visibility
- `description`: Natural language explanation

7. Mood Lighting (a_{mood}) **Description:** Alters emotional ambiance through lighting (e.g., neutral \rightarrow dramatic).

Parameters:

- `source_mood`: Current mood/atmosphere
- `target_mood`: Desired mood/atmosphere
- `contrast_adjustment`: "increase", "decrease", "none"
- `shadow_depth`: Darkness of shadows
- `description`: Natural language explanation

8. Color Grading (a_{color}) **Description:** Applies color correction and palette shifts (e.g., natural \rightarrow warm cinematic).

Parameters:

- `source_grading`: Current color grading
- `target_grading`: Desired color grading
- `saturation_change`: Adjustment to color intensity
- `temperature_shift`: "warmer", "cooler", "neutral"
- `description`: Natural language explanation

9. Artistic Medium (a_{medium}) **Description:** Transforms rendering style (e.g., photorealistic \rightarrow oil painting).

Parameters:

- `source_medium`: Current artistic style
- `target_medium`: Desired artistic style
- `detail_preservation`: Boolean, keep fine details
- `texture_intensity`: Strength of artistic texture
- `description`: Natural language explanation

10. Atmospheric Effects (a_{atmos}) **Description:** Adds environmental effects (e.g., fog, dust, haze).

Parameters:

- `source_effects`: Current atmospheric effects
- `target_effects`: Desired atmospheric effects
- `density`: "sparse", "moderate", "dense"
- `distribution`: "uniform", "localized", "gradient"
- `description`: Natural language explanation

C.2.2. REGULAR DATASET: 20 ACTIONS (10 ATOMIC + 10 COMPOSITIONAL)

The complex dataset extends the action library with 10 additional compositional and constraint actions designed for sophisticated multi-step transformations:

11. Preserve Attribute (a_{preserve}) **Description:** Explicitly preserves specific visual attributes while other transformations occur.

Parameters:

- `attributes_to_preserve`: List of dimension names (e.g., ["time_of_day", "color_grading"])
- `preservation_strength`: "strict", "moderate", "soft"
- `description`: Natural language explanation

Example Use Case: "Transform to Victorian architecture while preserving the sunset lighting"

12. Exclude Region (a_{exclude}) **Description:** Masks specific spatial regions from transformation.

Parameters:

- `region_type`: "foreground", "background", "top_half", "bottom_half", "center", "edges"
- `exclusion_strength`: "complete", "partial"
- `description`: Natural language explanation

Example Use Case: "Change background to cyberpunk city but exclude foreground characters"

13. Conditional Transform ($a_{\text{conditional}}$) **Description:** Applies transformation only if a condition is met.

Parameters:

- `condition_type`: "if_attribute_equals", "if_region_contains", "if_lighting_level"
- `condition_value`: Value to check
- `then_action`: Action to apply if condition is true
- `description`: Natural language explanation

Example Use Case: "If current time is daytime, then add sunset; otherwise keep night lighting"

14. Preserve Object Category ($a_{\text{preserve.obj}}$) **Description:** Preserves all objects of a specific semantic category.

Parameters:

- `object_categories`: List of categories (e.g., ["person", "vehicle", "animal"])
- `preservation_mode`: "identity", "style_only"
- `description`: Natural language explanation

Example Use Case: "Transform entire scene to oil painting style but keep people photorealistic"

15. Spatial Constraint (a_{spatial}) **Description:** Applies transformation with spatial constraints.

Parameters:

- `constraint_type`: "top_to_bottom_gradient", "center_outward", "left_to_right"
- `affected_attribute`: Which dimension to transform
- `gradient_sharpness`: "smooth", "moderate", "sharp"
- `description`: Natural language explanation

Example Use Case: "Apply sunset lighting with gradient from top (bright) to bottom (darker)"

16. Sequence Transform (a_{sequence}) **Description:** Specifies explicit ordering of multiple sub-transformations.

Parameters:

- `sub_actions`: Ordered list of actions to apply sequentially
- `timing`: "simultaneous", "sequential"
- `description`: Natural language explanation

Example Use Case: "First change to autumn, then add rain, then shift to dramatic mood"

17. Parallel Transform (a_{parallel}) **Description:** Applies multiple transformations simultaneously.

Parameters:

- `parallel_actions`: List of actions to apply in parallel
- `blending_mode`: "additive", "average", "weighted"
- `description`: Natural language explanation

Example Use Case: "Simultaneously change to sunset, add fog, and shift to warm color grading"

18. Graduated Effect ($a_{\text{graduated}}$) **Description:** Applies effect with gradual intensity variation.

Parameters:

- `base_action`: The action to apply with graduation
- `gradient_direction`: "top_to_bottom", "center_outward", etc.
- `intensity_curve`: "linear", "exponential", "sigmoid"
- `description`: Natural language explanation

Example Use Case: "Add fog with graduated intensity from dense at bottom to clear at top"

19. Layered Transformation (a_{layered}) **Description:** Applies transformations in layers with specified blending.

Parameters:

- `layers`: List of (action, opacity) tuples
- `blend_mode`: "normal", "multiply", "screen", "overlay"
- `description`: Natural language explanation

Example Use Case: "Layer Victorian architecture (70% opacity) over modern city, then add sunset"

20. Selective Blend ($a_{\text{selective_blend}}$) **Description:** Blends transformation results based on semantic or spatial criteria.

Parameters:

- `blend_criterion`: "by_semantic_region", "by_depth", "by_lighting_level"
- `source_transform`: First transformation result
- `target_transform`: Second transformation result
- `blend_ratio`: Mixing ratio or function
- `description`: Natural language explanation

Example Use Case: "Blend cyberpunk architecture with Victorian based on depth: close objects are cyberpunk, distant objects are Victorian"

These 10 additional compositional actions enable sophisticated multi-step transformations with explicit control over preservation, exclusion, ordering, and blending—critical for complex creative workflows.

C.3. Reward Function Details

The reward function $r_i \in [0, 5]$ is computed by Qwen3-VL-8B-Instruct analyzing the transformation from base image I_i to edited image \hat{I}_i given image editing prompt e_i .

C.3.1. REWARD CRITERIA

The reward model evaluates six primary criteria with weighted importance:

1. **Goal Alignment** (Weight: 30% — *Most Critical*)

- Measures semantic alignment between image editing prompt e_i and edited result \hat{I}_i
- Evaluates completeness: Did the transformation achieve what was requested?
- Assesses accuracy: Are the specific attributes correctly transformed?
- This is the single most important criterion for task success

2. **Aesthetic Quality** (Weight: 25%)

- Visual appeal and artistic merit of the edited image
- Composition balance, rule of thirds, visual flow
- Color harmony and palette coherence
- Overall professional polish

3. **Spatial Consistency** (Weight: 15%)

- Coherence of spatial relationships and depth ordering
- Perspective correctness and vanishing point consistency

- Geometric plausibility of transformed elements
- Absence of spatial distortions or impossible geometry

4. **Technical Quality** (Weight: 15%)

- Absence of visual artifacts (blurring, aliasing, noise)
- Resolution quality and detail preservation
- Edge sharpness and boundary cleanliness
- Technical execution (no broken textures, seams, or discontinuities)

5. **Temporal Consistency** (Weight: 10%)

- Consistency of time-related attributes (time of day, season)
- Interdependencies: sunset implies warm lighting, winter implies cold tones
- Logical coherence of lighting direction with stated time of day
- Seasonal markers align with requested season

6. **Creative Interpretation** (Weight: 5%)

- Novelty and creativity when interpreting ambiguous goals
- Maintaining plausibility while being creative
- Handling under-specified requests gracefully
- Appropriate artistic liberty within the goal’s intent

C.3.2. REWARD THRESHOLDS

Reward scores define quality tiers that inform our training methods:

Table 2. Reward Thresholds and Training Usage

Score Range	Quality Tier	RW Weight (at r)	DPO Usage
[4.5, 5.0]	Excellent	2.0 (at $r=5.0$)	Chosen
[4.0, 4.5)	Good	1.5 (at $r=4.5$)	Chosen
[3.5, 4.0)	Medium	1.0 (at $r=4.0$)	Neutral
[3.0, 3.5)	Poor	0.5 (at $r=3.5$)	Rejected
[0, 3.0)	Very Poor	0.0	Rejected

RW: Uses continuous weight function $w(r) = \max\{r - 3.0, 0\}$. Each trajectory’s gradient contribution is weighted by its reward score, so higher-quality examples receive proportionally more influence during training.

Direct Preference Optimization (DPO): Trajectories with $r_i \geq 4.0$ are chosen examples; those with $r_i < 3.5$ are rejected examples. DPO learns from contrastive pairs sharing the same (I_i, e_i) .

C.4. Synthetic Data Generation Details

This section provides comprehensive implementation details for our 5-stage synthetic data generation pipeline.

C.4.1. STAGE 1: IMAGE GENERATION WITH HiDREAM-I1-DEV

Model Specification We use HiDream-I1-Dev, a state-of-the-art text-to-image diffusion model:

- Architecture: Latent Diffusion Model with U-Net backbone
- Resolution: 1024×1024 pixels
- Inference steps: 50
- Guidance scale: 7.5
- Sampling method: DPM-Solver++

Prompt Generation Strategy We generate diverse seed prompts p_i covering:

- **Location types (30 variants):** urban_city, suburban_neighborhood, rural_village, beach_coast, forest_temperate, desert_sand, mountain_rocky, cave_underground, space_station, cyberpunk_city, medieval_town, office_modern, bedroom_interior, etc.
- **Architectural styles (25 variants):** modern_minimalist, classical_greek, victorian_gothic, art_deco, traditional_asian, industrial_warehouse, futuristic_sci_fi, etc.
- **Time periods (15 variants):** ancient_classical, medieval, victorian_1800s, modern_2000s, near_future_2050s, etc.
- **Lighting conditions (20 variants):** dawn, morning, midday, afternoon, sunset, dusk, night, overcast, etc.

Prompts are constructed using templates:

```
"A {location} with {architecture} architecture in {time_period} era
at {time_of_day} with {weather} weather"
```

Example: "A suburban neighborhood with modern minimalist architecture in the 2000s era at midday with clear weather"

C.4.2. STAGE 2: CONTEXT EXTRACTION

We extract structured context c_i using a frozen Qwen3-VL-8B-Instruct model with the following prompt template:

Context Extraction Prompt

Analyze this image and extract the following 10 visual attributes in JSON format:

```
{
  "location": "<categorical.value>",
  "architecture": "<categorical.value>",
  "time_period_era": "<categorical.value>",
  "time_of_day": "<categorical.value>",
  "season": "<categorical.value>",
  "weather": "<categorical.value>",
  "mood_lighting": "<categorical.value>",
  "color_grading": "<categorical.value>",
  "artistic_medium": "<categorical.value>",
  "atmospheric_effects": "<categorical.value>"
}
```

Be specific and use the standardized vocabulary.

The model returns structured JSON which we parse into c_i . Extraction takes approximately 2-3 seconds per image on an A100 GPU.

C.4.3. STAGE 3: ACTION PLANNING WITH TEACHER MODEL

The teacher planner (Qwen3-VL-8B-Instruct) generates action sequences using the following algorithm:

Algorithm 2 Teacher Trajectory Generation (Detailed)

```

1: Input: Image  $I_i$ , image editing prompt  $e_i$ , context  $c_i$ , action library  $\mathcal{A}$ 
2: Initialize action sequence  $\{a_{i1}, \dots, a_{im}\}$  and reasoning  $\{z_{i1}, \dots, z_{im}\}$ 
3: Initialize current context  $c_{\text{current}} \leftarrow c_i$ 
4: for  $j = 1$  to  $m_{\text{max}} = 5$  do
5:   Construct prompt with image  $I_i$ , editing prompt  $e_i$ , context  $c_{\text{current}}$ , and past actions  $\{a_{ik}\}_{k < j}$ 
6:   Sample action and reasoning:  $(a_{i,j}, z_{i,j}) \sim \pi_{\text{teacher}}(\cdot \mid I_i, e_i, c_{\text{current}}, \{a_{ik}\}_{k < j})$  with temperature  $T = 0.7$ 
7:   if  $a_{i,j} = a_{\text{STOP}}$  or goal satisfied (checked by teacher) then
8:     break
9:   end if
10:  Update context:  $c_{\text{current}} \leftarrow \text{ApplyAction}(c_{\text{current}}, a_{i,j})$ 
11: end for
12: Generate natural language instruction:  $\hat{e}_i = \text{ActionToNL}(\{a_{i,j}\}_{j=1}^m, e_i, c_i)$ 
13: Return:  $\{a_{i,j}\}_{j=1}^m, \{z_{i,j}\}_{j=1}^m, \hat{e}_i$ 

```

Prompt Template for Planning

Action Planning Prompt Template

```

You are an expert image styling agent. Given:

- Base image: [image]
- Current visual state: {c.i}
- User goal: {e.i}
- Past actions: {a.i1, a.i2, ...}

Generate the next action from the action library to achieve the goal.

For each action, provide:

1. Action type and parameters
2. Chain-of-thought reasoning explaining why this action is chosen

Action library: [list of available actions with specs]

```

Temperature Sampling We use temperature $T = 0.7$ to balance diversity and quality. Lower temperatures ($T = 0.1$) produce repetitive trajectories; higher temperatures ($T = 1.0$) reduce coherence.

C.4.4. STAGE 4: IMAGE EDITING WITH QWEN-IMAGE-EDIT

We execute the synthesized instruction \hat{e}_i using Qwen-Image-Edit:

Model Specification

- Architecture: Instruction-conditioned diffusion model
- Base model: Qwen-VL-Chat fine-tuned for editing
- Resolution: 768×768 pixels
- Inference steps: 28
- Guidance scale: 7.5
- Image guidance scale: 4.0

Instruction Synthesis We convert action sequences to natural language:

Example 1:

- Actions: {time_of_day(sunset), season(autumn)}
- Instruction: "Change the lighting to warm sunset tones with golden hour ambiance, and transform the scene to autumn with falling leaves and warm colors"

Example 2:

- Actions: {architecture(victorian), mood(mysterious), atmospheric(fog)}
- Instruction: "Transform the buildings to Victorian Gothic architecture with ornate details, add mysterious dramatic lighting with deep shadows, and add dense fog throughout the scene"

C.4.5. STAGE 5: REWARD EVALUATION

Qwen3-VL-8B-Instruct evaluates trajectory quality with the following prompt:

Reward Evaluation Prompt

```
Evaluate this image transformation:
- Base image: [I.i]
- Edited image: [E.i]
- User goal: {e.i}
- Planned actions: {a.i1, a.i2, ...}

Rate the transformation quality on a scale of 0-5 considering:
1. Goal alignment (30% --- most critical)
2. Aesthetic quality (25%)
3. Spatial consistency (15%)
4. Technical quality (15%)
5. Temporal consistency (10%)
6. Creative interpretation (5%)

Provide:
- Overall score (0-5)
- Per-criterion scores
- Justification for the rating

Format: JSON with fields {overall_score, aesthetic, goal_alignment, ...}
```

The model returns structured JSON evaluation which we parse to extract $r_i \in [0, 5]$. Evaluation takes approximately 3-4 seconds per trajectory on an A100 GPU.

C.4.6. DATASET STATISTICS

Trajectory-Level Splitting To prevent data leakage, we group trajectories by (I_i, e_i) pairs and split at the group level. This ensures that all alternative plans for the same image-goal combination remain in the same split, forcing the model to generalize to unseen combinations rather than memorizing specific inputs.

D. Complete Synthesis Pipeline Examples

This section provides two complete end-to-end examples of our synthetic data generation pipeline, illustrating the entire 5-stage process from base image generation to reward evaluation. We present one example from the Simple Dataset (atomic transformations) and one from the Regular Dataset (compositional reasoning with constraints).

Table 3. Dataset Statistics

Statistic	Simple Dataset	Regular Dataset
Total trajectories	9,824	10,142
Avg. actions per trajectory	2.8	4.1
Avg. reward score	3.92	3.74
% High quality ($r \geq 4.0$)	62%	48%
Action library size	10 actions	20 actions
Train/Val/Test split	80%/10%/10%	80%/10%/10%
Trajectory groups	3,247	2,891
Avg. trajectories per group	3.0	3.5

D.1. Example 1: Simple Dataset — Autumn Vineyard to Spring Tulip Field

D.1.1. OVERVIEW

Transformation: Autumn Vineyard with grape harvest → Spring Tulip Field with emerging technology

Complexity Level: Normal (3 atomic actions, no constraints)

Key Challenge: Complete environmental transformation across multiple dimensions (location, season, era)

Dataset: Normal — ID 2530

Stage 1: Base Image Generation and Final Result The base image was generated using HiDream-I1-Dev with the prompt: "An autumn vineyard with grape harvest, golden vine leaves, wine barrels, and fall agricultural atmosphere, in near future 2050 style."



Figure 9. **Simple Dataset Example - Autumn Vineyard to Spring Tulip Field.** (a) Original: Autumn vineyard scene with golden foliage, wine barrels, grape clusters, and a rustic farmhouse. (b) Edited: Transformed to spring tulip field with vibrant pink tulips, modern technology, and clear morning atmosphere. The transformation successfully replaces location (vineyard→tulip field), season (autumn→spring), and era (modern→futuristic) while maintaining compositional structure.

Stage 2: Context Extraction: Using Qwen3-VL-8B-Instruct, we extract the 10-dimensional structured context representation c_i :

Extracted Context (c_i)

```
{
  "location": "autumn_vineyard",
  "architecture": "rustic_farmhouse",
  "time_period_era": "modern_2000s",
  "time_of_day": "golden_hour_sunset",
  "season": "autumn_falling",
  "weather": "clear_sky",
  "mood_lighting": "warm_cozy",
  "color_grading": "warm_cinematic",
  "artistic_medium": "photorealistic",
  "atmospheric_effects": "none_clear"
}
```

Scene Description: A picturesque autumnal vineyard framed by a lush grapevine arch. Two wooden wine barrels sit prominently in the foreground with fresh grape clusters. Orderly rows of golden-hued grapevines cascade down gentle slopes toward a solitary farmhouse. The sky is a serene blend of soft blue with warm sunlight, creating a tranquil harvest-time atmosphere.

Stage 3: Action Planning with Teacher Model

User Goal: *”Transform to spring tulip field with rows of colorful tulips in bloom, fresh green stems, clear spring sky, and vibrant flower farm atmosphere, transformed to near future with emerging technology.”*

Overall Planning Reasoning

The current autumn vineyard scene must be completely replaced with a spring tulip field to match the user’s request. This requires **location_setting** as the foundation, since all other elements (tulips, farm, technology) depend on removing the existing vineyard. Then, **season_cycle** changes the foliage to spring greenery. Finally, **time_period_era** adds near-future tech elements like drones or smart irrigation to fulfill the ‘emerging technology’ requirement. The farmhouse and barrels must be replaced with tulip farm structures and equipment.

Generated Action Sequence (3 actions):

Action 1: location_setting (Priority 1)

Reasoning: The current vineyard and farmhouse define the setting. Complete location replacement is essential to establish the spring tulip field as the new environment, since all other elements (tulips, tech, sky) depend on removing the existing vineyard infrastructure first.

Parameters:

- source_location: "autumn_vineyard"
- target_location: "spring_tulip_field"
- replace_mode: "complete"
- preserve_foreground: false
- description: "Replace vineyard with tulip field"

Expected Effect: This action fundamentally changes the environment from a wine-growing region to a flower farm. The vineyard rows will be replaced with rows of colorful tulips, the wine barrels will be removed, and the agricultural context will shift from grape cultivation to tulip cultivation. This is the foundational transformation that enables all subsequent actions.

Action 2: `season_cycle` (Priority 2)

Reasoning: The current autumn foliage must be replaced with spring greenery and blooming tulips to match the 'vibrant flower farm atmosphere'. This directly transforms the vegetation state and ground cover to reflect spring.

Parameters:

- `source_season`: "autumn"
- `target_season`: "spring"
- `vegetation_state`: "blooming_tulips"
- `ground_cover`: "green_grass"
- `description`: "Change to spring tulips"

Expected Effect: This action transforms the color palette from warm autumn golds and browns to vibrant spring colors (reds, pinks, yellows, purples from tulips) with lush green foliage. The fallen leaves and mature grape foliage will be replaced by fresh, blooming flowers and green stems. The sky will shift from golden-hour autumn tones to a clear, bright spring blue.

Action 3: `time_period_era` (Priority 3)

Reasoning: To add 'emerging technology', the scene must be shifted to a near-future era. This allows for the introduction of tech elements like drones, smart irrigation, or automated harvesters that would be absent in the current historical setting.

Parameters:

- `source_era`: "modern"
- `target_era`: "near_future"
- `technology_level`: "emerging"
- `period_accuracy`: "approximate"
- `description`: "Add near-future tech"

Expected Effect: This action adds subtle futuristic elements to the tulip field. Expect to see agricultural drones hovering above the tulip rows for monitoring or pollination, sleek solar panels on farm structures, automated irrigation systems with visible sensors, or modern greenhouse structures in the background. The technology should be visible but not dominate the scene—enhancing the agricultural context with near-future innovation.

How Actions Work Together: The three actions form a logical transformation pipeline:

1. **Foundation (Action 1):** `location_setting` establishes the new physical environment, removing all vineyard-specific elements and setting up the tulip field context.
2. **Seasonal Transform (Action 2):** `season_cycle` builds on the new location by specifying the time of year and vegetation state—spring with blooming tulips—defining the color palette and atmospheric conditions.
3. **Enhancement (Action 3):** `time_period_era` adds the technological layer, introducing futuristic agricultural equipment that integrates naturally with the spring tulip field established by the previous actions.

This sequential application ensures coherent transformation: location first (what), then season (when/how), then era (technological context).

Stage 4: Instruction Synthesis: The action sequence is converted to a natural language instruction for the image editor (Qwen-Image-Edit (Wu et al., 2025)):

Synthesized Edit Instruction

style.transformation_mode Transform to spring tulip field with tech farm. Replace vines with tulips, add drones, clear sky, green stems. Maintain photorealistic quality.

Analysis: The synthesized instruction condenses the 3-action plan into a concise natural language command. It explicitly mentions the target (tulip field), key elements (drones for technology, green stems for spring), and maintains the photorealistic style constraint.

Stage 6: Reward Evaluation Qwen3-VL-8B-Instruct evaluates the transformation quality across 6 criteria:

Reward Scores (Scale: 0-5)

Criterion	Score	Reasoning
Action Plan Quality	5/5	The chosen actions perfectly address the user’s request: replacing the vineyard with a tulip field, changing the season to spring, and adding near-future technology (drones). Each action is directly relevant and necessary.
Plan Reasoning	5/5	The reasoning is excellent, logically sequencing the actions from location replacement to seasonal change to technological addition. It clearly justifies each step’s necessity.
Reasoning Quality	5/5	Exceptionally detailed and specific reasoning. References the need to replace the vineyard, change the season, and add technology, with clear causal links.
Final Image Quality	3/5	The image is visually coherent and vibrant, with good color saturation and lighting. However, technical metrics (LPIPS 0.824, SSIM 0.251) indicate structural distortion, suggesting artifacts.
Adherence to Plan	5/5	The edited image fully executes the action plan: vineyard replaced with tulip field, season changed to spring with blooming tulips, drones added for emerging technology.
Adherence to Prompt	5/5	The result perfectly matches the user’s request: spring tulip field with colorful blooms, clear sky, and drones representing emerging technology.
Overall Quality	4/5	Highly successful transformation, accurately fulfilling the user’s request. Minor deduction for technical quality metrics indicating some image distortion.

Objective Metrics:

- LPIPS: 0.824 (high perceptual difference, expected for complete transformation)
- SSIM: 0.251 (low structural similarity, indicates significant scene change)
- PSNR: 9.34 dB (low PSNR score confirms major transformation)
- CLIP Score: 0.319 (semantic alignment between image and text)

Analysis: The high LPIPS and low SSIM/PSNR are expected and desirable for this transformation, as the goal is complete scene replacement rather than subtle editing. The strong adherence scores (5/5) confirm the transformation successfully achieved the user’s intent.

D.2. Example 2: Regular Dataset — Contemporary Studio to Cyberpunk Nightclub

D.2.1. OVERVIEW

Transformation: Contemporary Studio Apartment → Futuristic Cyberpunk Nightclub with Preservation Constraints

Complexity Level: Complex (3 transformation actions + 2 preservation constraints)

Key Challenge: Radical environmental transformation while preserving specific elements (wood furniture, plants)—requires compositional reasoning to balance conflicting requirements

Dataset: Complex — ID 327

Stage 1: Base Image Generation and Final Result The base image was generated using HiDream-I1-Dev with the prompt: "A contemporary studio apartment with open layout, modern furniture, track lighting, and city view."

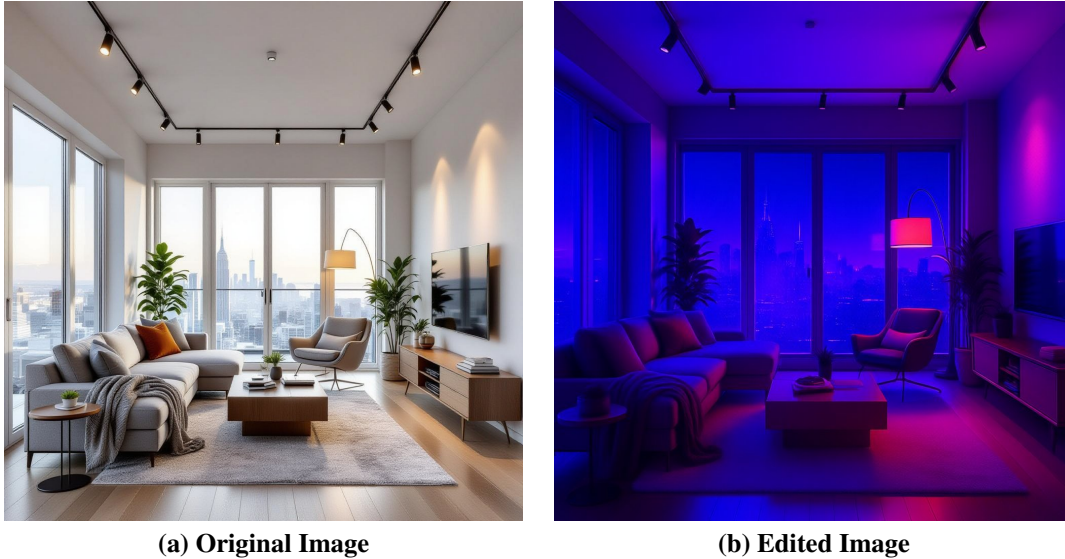


Figure 10. **Regular Dataset Example - Scandinavian Studio to Cyberpunk Industrial.** (a) Original: Modern Scandinavian studio with gray sofa, wooden table, plants, and city view through large windows. (b) Edited: Transformed to cyberpunk industrial loft with neon lighting, metallic textures, and futuristic tech elements. The transformation demonstrates constraint-based planning: dramatic neon accents added while attempting to preserve natural wood tones and organic plant colors (partial success, reward 3/5).

Stage 2: Context Extraction: Using Qwen3-VL-8B-Instruct, we extract the 10-dimensional structured context representation c_i :

Extracted Context (c_i)

```
{
  "location": "modern_apartment",
  "architecture": "contemporary_minimalist",
  "time_period_era": "modern_2020s",
  "time_of_day": "midday_overhead",
  "season": "neutral_indoor",
  "weather": "clear_visible_through_windows",
  "mood_lighting": "neutral_balanced",
  "color_grading": "natural_balanced",
  "artistic_medium": "photorealistic",
  "atmospheric_effects": "none_clear"
}
```

Scene Description: A bright, airy contemporary studio apartment with modern Scandinavian design. The space features a large gray sectional sofa with orange accent pillows, a low wooden coffee table, and a beige armchair. Multiple potted plants (monstera, fiddle leaf fig) add greenery. Large floor-to-ceiling windows provide natural light and reveal a city skyline. The color palette is neutral (whites, grays, beiges) with warm wood tones.

Key Elements to Preserve:

- **Wooden furniture:** Coffee table, side table, shelving units

- **Natural plants:** Monstera, fiddle leaf fig, small potted plants

Stage 3: Action Planning with Teacher Model

User Goal: "Transform to futuristic cyberpunk nightclub, preserve all traditional wooden elements, keep natural plants visible, AND add neon pink and blue dramatic lighting."

Constraint Analysis: This goal presents a compositional reasoning challenge:

- **Conflicting Requirements:** Cyberpunk aesthetic (high-energy, artificial) vs. natural elements (wood, plants)
- **Preservation Constraints:** Wood and plants must remain visible and recognizable despite dramatic lighting changes
- **Lighting Challenge:** Neon pink/blue lighting can wash out natural colors, making preservation difficult

Overall Planning Reasoning

The image shows a modern apartment overlooking a city skyline. User wants a cyberpunk nightclub theme while preserving wood and plants. This requires radical environment shift plus dramatic lighting. **Location change** sets new context; **atmospheric effects** delivers neon glow; **mood lighting** ensures color harmony with preserved elements.

Critical Insight: The preservation constraints require careful lighting control. Simply adding neon would wash out the wood and plants, making them unrecognizable. The plan must explicitly address this by using **mood lighting** to add warm accents that highlight the preserved elements while the neon dominates the overall scene.

Generated Action Sequence (3 actions):

Action 1: location_setting (Priority 1)

Reasoning: Current urban apartment view must be replaced to establish cyberpunk club setting. All background elements including skyline need removal to allow new themed environment to dominate without conflict.

Parameters:

- `source_location`: "modern_apartment"
- `target_location`: "cyberpunk_nightclub"
- `replace_mode`: "complete"
- `preserve_foreground`: true
- `description`: "Swap apartment for nightclub interior"

Expected Effect: This action transforms the architectural context from residential apartment to commercial nightclub. The windows showing city skyline will be replaced with club interior elements (bars, DJ booth, dance floor). The open apartment layout will be reconfigured into a nightclub space. Critically, `preserve_foreground: true` instructs the editor to maintain the wooden furniture and plants in the foreground during this radical background replacement.

Constraint Handling: The preservation constraint is implemented through the `preserve_foreground` flag, which tells the editor to apply location changes primarily to background elements (walls, windows, architectural features) while keeping foreground objects (furniture, plants) intact.

Action 2: atmospheric_effects (Priority 2)

Reasoning: Neon pink/blue lighting defines cyberpunk aesthetic. Adding dramatic glowing beams transforms the ambiance from calm living space to high-energy nightlife venue, matching user's explicit lighting request.

Parameters:

- `effect_type`: "neon_glow"
- `intensity`: "high"
- `coverage`: "full_scene"

- `color_tint`: "pink_blue"
- `description`: "Add neon pink-blue lighting"

Expected Effect: This action introduces the signature cyberpunk aesthetic: bright neon lights in pink and blue hues. The lighting will be dramatic and artificial, creating strong color casts across surfaces. Light beams, glows, and reflections will be visible throughout the scene. The intensity is set to "high" to ensure the cyberpunk atmosphere is unmistakable.

Constraint Challenge: This action poses the primary challenge to the preservation constraints. High-intensity neon lighting can completely change the apparent color of objects, potentially making the natural wood and green plants unrecognizable by tinting them pink/blue. This is why Action 3 is critical.

Action 3: mood_lighting (Priority 3)

Reasoning: To ensure neon doesn't wash out natural plants and wood tones, supplemental ambient lighting should highlight these preserved elements. Warm accents balance cool neon, creating layered depth while honoring user's preservation constraints.

Parameters:

- `source_mood`: "calm_indoor"
- `target_mood`: "energetic_club"
- `accent_lighting`: "warm_spotlights"
- `shadow_depth`: "medium"
- `description`: "Highlight wood and plants with warm light"

Expected Effect: This action adds localized warm lighting (spotlights or accent lights) specifically targeting the wooden furniture and plants. These warm lights (oranges, yellows) counteract the cool neon tint, allowing the wood to maintain its natural brown color and the plants to keep their green hue. This creates a layered lighting environment: neon dominates the overall scene, but warm accents preserve the recognizability of specific elements.

Constraint Resolution: This is the key action for satisfying the preservation constraints. Without this targeted lighting, the wood and plants would appear pink/blue under the neon, failing the constraint. The warm spotlights create "islands" of natural color within the otherwise artificial cyberpunk environment.

How Actions Work Together (Compositional Reasoning): The three actions form a carefully orchestrated transformation that balances conflicting requirements:

1. **Environment Shift (Action 1):** `location_setting` establishes the nightclub context while explicitly preserving foreground elements through the `preserve_foreground` flag.
2. **Aesthetic Layer (Action 2):** `atmospheric_effects` adds the dominant cyberpunk aesthetic with intense neon lighting, creating the high-energy nightclub atmosphere.
3. **Constraint Satisfaction (Action 3):** `mood_lighting` resolves the conflict between neon lighting and preservation constraints by adding warm accents that maintain the natural appearance of wood and plants.

Compositional Challenge: The difficulty lies in applying Action 2 (neon) and Action 3 (warm accents) simultaneously. Too much neon overpowers the warm lights, failing preservation. Too much warm light diminishes the cyberpunk aesthetic. The planner must find the right balance, which is encoded in the intensity and coverage parameters.

Failure Mode: If Action 3 is omitted or improperly parameterized, the transformation will fail the preservation constraints despite succeeding at the cyberpunk aesthetic. This example demonstrates why complex tasks require explicit constraint-aware reasoning.

Stage 4: Instruction Synthesis: The action sequence with constraints is converted to a natural language instruction:

Synthesized Edit Instruction

```
style.transformation_mode Transform to cyberpunk nightclub with neon pink-blue lighting. Preserve wooden furniture and potted plants with warm spotlights.
```

Analysis: The synthesized instruction explicitly mentions both the transformation goal (cyberpunk nightclub with neon) and the preservation constraints (wooden furniture, potted plants). The "warm spotlights" phrase directly encodes Action 3's constraint-resolution strategy. This explicit constraint language is critical for complex tasks.

Stage 6: Reward Evaluation Qwen3-VL-8B-Instruct evaluates the transformation quality across 6 criteria:

Reward Scores (Scale: 0-5)

Criterion	Score	Reasoning
Action Plan Quality	3/5	Actions are appropriate for transformation, but the plan fails to fully address preservation of wooden elements and plants. The <code>location_setting</code> action removes original apartment context, but doesn't account for integrating preserved elements into new setting.
Plan Reasoning	3/5	Reasoning is logically structured but lacks specific image analysis. Correctly identifies need for location change and neon lighting, but doesn't explain how to achieve preservation within cyberpunk context or address visual conflict between preserved elements and new lighting.
Reasoning Quality	3/5	References user's request for cyberpunk lighting and preservation, but lacks specificity. Doesn't analyze how preserved elements (wood, plants) would interact with new lighting or how to integrate them into a nightclub environment.
Final Image Quality	3/5	High visual coherence, dramatic neon lighting effectively creates cyberpunk atmosphere. However, metrics (LPIPS 0.801, SSIM 0.230) indicate significant structural difference. Color palette is appropriate (blue, pink), but lacks layered lighting depth expected in a nightclub.
Adherence to Plan	3/5	<code>location_setting</code> partially executed (apartment replaced with nightclub-like environment). <code>atmospheric_effects</code> executed (neon pink-blue lighting added). <code>mood_lighting</code> NOT executed as described—final image lacks warm accents to highlight wood and plants.
Adherence to Prompt	3/5	Successfully creates cyberpunk nightclub atmosphere with dramatic neon lighting. However, fails to fully preserve traditional wooden elements and keep natural plants visible. Plants are present but wooden furniture is not highlighted or integrated in way that preserves traditional character.
Overall Quality	3/5	Visually striking transformation effectively creates cyberpunk atmosphere. Neon lighting is dramatic and scene is cohesive. However, falls short of user's request to preserve wooden elements and plants. A good cyberpunk nightclub, but doesn't fully honor preservation constraints.

Objective Metrics:

- LPIPS: 0.801 (high perceptual difference)
- SSIM: 0.230 (low structural similarity)
- PSNR: 6.11 dB (very low PSNR score)
- CLIP Score: 0.320 (semantic alignment between image and text)

Analysis: The lower scores (3/5) across multiple criteria reflect the difficulty of the compositional reasoning task. The transformation successfully achieves the cyberpunk aesthetic, but only partially satisfies the preservation constraints. This is

a common failure mode in complex tasks: the planner correctly identifies the constraint (Action 3), but the image editor struggles to execute it properly due to the conflicting lighting requirements.

Key Insight: Complex tasks with preservation constraints require more sophisticated action parameterization. The `intensity` and `coverage` parameters in Actions 2 and 3 must be carefully balanced, which is difficult to specify in a discrete action representation. Future work could explore continuous parameter spaces or iterative refinement to better handle such constraints.

D.3. Comparison and Insights

Table 4. Comparison of Normal vs. Complex Synthesis Examples

Property	Normal Example	Complex Example
Number of actions	3	3
Preservation constraints	0	2
Overall reward	4.0/5.0 (Good)	3.0/5.0 (Medium)
Planning difficulty	Low	High
Execution difficulty	Medium	High
Adherence to plan	5/5 (Perfect)	3/5 (Partial)
Adherence to prompt	5/5 (Perfect)	3/5 (Partial)
Key challenge	Complete transformation	Conflicting constraints
Success factor	Clear, non-conflicting goals	Failed constraint resolution

Key Takeaways

- **Normal tasks:** When transformation goals are clear and non-conflicting, even complex multi-action plans can be executed successfully. The autumn→spring example achieves near-perfect adherence because each action builds naturally on the previous one without conflicts.
- **Complex tasks:** Preservation constraints introduce compositional reasoning challenges. The cyberpunk example demonstrates how conflicting requirements (dramatic neon vs. natural wood/plant colors) require careful parameter balancing that current models struggle with.
- **Planning vs. Execution gap:** The complex example shows a gap between planning (Action 3 correctly identifies the need for warm accents) and execution (the warm accents are not sufficiently applied in the final image). This highlights the need for better alignment between discrete action plans and continuous image editing.
- **Reward signal quality:** The reward model successfully distinguishes between fully successful transformations (4-5/5) and partially successful ones (3/5), providing meaningful training signal for downstream models.

D.4. Example 3: Complex Dataset — Arctic Glacier to Desert Canyon

D.4.1. OVERVIEW

Transformation: Arctic glacier crevasse with ice and snow → Desert canyon with warm rock formations

Complexity Level: Complex (2 actions with spatial preservation constraints)

Key Challenge: Dramatic environmental transformation while preserving spatial relationships and depth perception

Dataset: Complex (`ice_art_movement_multi` theme)

Stage 1: Base Image Generation and Final Result The base image depicts a dramatic arctic landscape with a deep glacial crevasse cutting through snow-covered terrain, revealing turquoise meltwater. Snow-capped mountains rise in the background under a partly cloudy sky.



Figure 11. Complex Dataset Example - Arctic Glacier to Desert Canyon. (a) Original: Arctic glacier scene with deep crevasse revealing turquoise meltwater, surrounded by expansive snowfields and distant snow-capped mountain peaks. Strong diagonal composition with cold blue-white color palette. (b) Edited: Transformed to dramatic desert canyon with layered sandstone and rocky canyon walls in warm ochre and amber tones. The diagonal crevasse structure is preserved but now rendered as desert canyon walls. Background mountains maintain imposing presence with reddish-brown rock faces. Depth perception and spatial relationships successfully maintained through consistent atmospheric perspective (reward 5.0/5.0).

Stage 2: Context Extraction: The Complex dataset uses a streamlined context extraction focused on spatial and compositional features. Key extracted properties include: dominant colors (white, blue, gray), composition (diagonal leading lines, layered depth), lighting (soft diffused daylight), and spatial structure (foreground snow, midground crevasse, background mountains).

Stage 3: Action Planning with Compositional Reasoning

User Goal: Transform arctic glacier to desert canyon while preserving spatial relationships and depth perception.

Overall Planning Reasoning

This image depicts a stark arctic landscape with strong diagonal compositional lines and deep atmospheric perspective. To create a bold transformation while preserving spatial relationships and depth perception, I will shift the environment to a vibrant desert canyon. This maintains the diagonal structure but replaces the icy textures with warm earth tones and layered rock formations. The color grading adjustment ensures the new palette complements the existing depth cues without disrupting scale or perspective. The artistic medium remains photorealistic to preserve realism and avoid altering perceived distance.

The planning model generates a 2-action sequence with explicit spatial preservation constraints:

Action 1: Location Setting (Priority 1)

Action ID: location_setting

Parameters:

- setting_type: desert_canyon
- setting_style: rocky_with_layers
- description: Replace glacier with desert canyon

Reasoning: The snowy mountains and ice crevasse define this as polar. Replacing it with a desert canyon preserves the diagonal composition but introduces contrasting textures and warm tones, creating a visually jarring yet harmonious transformation rooted in the same structural logic.

Expected Effect: Complete environmental transformation from arctic to desert while maintaining the diagonal crevasse structure, layered background mountains, and foreground-to-background depth hierarchy.

Constraint Handling: Explicitly preserves spatial relationships by maintaining diagonal composition, scale proportions, and three-layer depth structure (foreground, midground, background).

Action 2: Color Grading (Priority 2)

Action ID: color_grading

Parameters:

- grade_style: warm_desert
- look: sunset_amber
- description: Apply warm desert color grading

Reasoning: The cool blue-white palette must be replaced with warm ochre, sandstone, and sunset hues to match the desert theme. This transforms the mood while preserving depth perception by maintaining analogous color transitions across layers, reinforcing spatial hierarchy.

Expected Effect: Shift from cool (blue, white, gray) to warm (amber, ochre, sandstone) color palette while maintaining tonal gradation that signals atmospheric depth.

Constraint Handling: Preserves depth perception by maintaining analogous color transitions across foreground, midground, and background layers, ensuring spatial hierarchy remains visually coherent.

Stage 4: Edit Instruction Generation: The action sequence is compiled into a natural language instruction for the image editor:

Edit Instruction

```
style.transformation.mode Transform arctic glacier to desert canyon. Preserve spatial relationships and depth perception. Warm desert color grading.
```

Stage 6: Reward Evaluation: The reward model (Qwen3-VL-8B-Instruct) evaluates the transformation across 6 criteria:

Reward Scores (All 5.0/5.0)

- **Action Plan Quality:** 5.0 — “The actions are perfectly appropriate: replacing the glacier with a desert canyon and applying warm desert color grading directly address the transformation request while preserving the core spatial structure.”
- **Plan Reasoning:** 5.0 — “The reasoning is excellent, logically sequencing the transformation by first changing the setting and then the color palette. It explicitly references the diagonal composition and depth perception, showing a deep understanding of the image’s structure.”
- **Reasoning Quality:** 5.0 — “The reasoning is exceptional. It specifically references the ‘diagonal compositional lines’ and ‘deep atmospheric perspective’ of the original, justifies the color grading to maintain depth, and explains how the transformation preserves spatial relationships through structural logic.”
- **Final Image Quality:** 5.0 — “The edited image is of excellent technical quality. The transformation is seamless, with no visible artifacts. The desert canyon maintains the original’s perspective and scale, and the warm color grading enhances the depth perception without distortion.”
- **Adherence to Plan:** 5.0 — “The editing perfectly follows the action plan. The setting was changed to a desert canyon with layered rock formations, and the color grading was applied to create a warm, sunset-amber palette, exactly as specified.”
- **Adherence to Prompt:** 5.0 — “The result perfectly matches the user’s request. The arctic glacier is transformed into a desert canyon while maintaining the spatial relationships (diagonal lines, scale, perspective) and depth perception (atmospheric layers, shadows) as required.”
- **Overall Quality:** 5.0 — “This is an outstanding transformation. It successfully and artistically reimagines the scene while rigorously adhering to the constraints of preserving spatial relationships and depth perception, resulting in a visually compelling and coherent image.”

Objective Metrics: LPIPS 0.963 (high perceptual distance, confirming dramatic transformation), SSIM 0.341, PSNR 5.66, CLIP score 0.230.

D.5. Dataset Comparison

Table 5 summarizes the key differences between the three synthetic datasets used in our experiments.

Characteristic	Simple	Regular	Complex
Dataset Size	$n = 10,000$	$n = 10,000$	$n = 10,000$
Action Library	10 actions	20 actions	30 actions
Action Types	9 THEME + 1 STYLE	10 atomic + 10 constraint	30 styling & transformation
Avg Actions/Sample	2-3	3-5	2-4
Theme Diversity	31 locations	10 interior design styles	83 diverse themes
Transformation Type	Simple, 1-2 distinct changes	Compositional, 3-5 interacting changes	Moderate, 2-4 styling changes
Key Features	Atomic actions, clear goals	Constraints, preservation logic	Broad distribution, artistic focus
Complexity Level	Low	High	Medium-High
Constraint Actions	None	10 (preserve, exclude, conditional)	Integrated into action parameters
Use Case	Basic training, validation	Complex reasoning, compositionality	Diverse distribution, generalization
Example Transformation	Autumn vineyard → Spring tulip field	Industrial loft → Cyberpunk industrial	Arctic glacier → Desert canyon

Table 5. Comparison of three synthetic datasets. Normal uses atomic actions on diverse locations. Regular adds constraint/compositional actions for interior design styles. Complex expands to 30 actions and 83 diverse themes, balancing complexity with broad distribution coverage.

D.5.1. KEY INSIGHTS FROM THREE-DATASET COMPARISON

- Action Library Design:** Normal (10 actions) focuses on orthogonal dimensions (location, architecture, time, season, weather, mood, lighting, texture, material, color scheme). Complex (20 actions) adds constraint logic (preserve_attribute, exclude_region, conditional_transform). Complex (30 actions) integrates constraints into a unified framework with expanded styling options.
- Theme Diversity vs. Complexity:** Normal prioritizes location diversity (31 types) with atomic transformations. Regular prioritizes compositional complexity (3-5 interacting changes) within a narrower domain (10 interior design styles). Complex achieves both broad distribution (83 themes) and moderate complexity (2-4 actions with integrated constraints).
- Training Signal Quality:** All three datasets achieve high reward scores for successful samples (4-5/5), but failure modes differ. Normal fails primarily on execution errors (action parameters not followed). Regular fails on constraint conflicts (preserving natural wood while adding neon lights). Complex shows more consistent quality due to streamlined action library and diverse training distribution.
- Method Performance Patterns:** Our experiments (Section 5) show that method effectiveness varies by dataset. RW excels on Simple vision tasks (Overall 79.33 on Vision-4B), SW on Regular text tasks (Overall 78.77 on Text-4B), and DPO on Regular vision tasks (Overall 85.41 on Vision-8B), suggesting that continuous weighting (RW/SW) benefits from simpler or complex-compositional tasks, while preference learning (DPO) benefits from broad distribution coverage.

E. Training Algorithms

This appendix provides complete algorithmic details for Standard Supervised Learning and Direct Preference Optimization, including mathematical formulations, pseudocode, and implementation specifics.

E.1. Standard Supervised Learning

The baseline approach treats synthetic trajectories as supervised training data, ignoring reward signals entirely. Given a dataset $\mathcal{D} = \{\tau_i\}_{i=1}^n$ of synthetic trajectories where $\tau_i = (e_i, I_i, c_i, \{a_{i,j}\}_{j=1}^{m_i}, \{z_{i,j}\}_{j=1}^{m_i}, \hat{e}_i, \hat{I}_i, r_i)$, we train the model π_θ to maximize the likelihood of actions and per-step chain-of-thought reasoning.

E.1.1. LOSS FORMULATION

The standard supervised learning loss is: $\mathcal{L}_{\text{SL}}(\theta) = -\frac{1}{n} \sum_{i=1}^n \sum_{j=1}^{m_i} \log \pi_\theta(a_{i,j}, z_{i,j} \mid I_i, e_i, c_i, \{a_{ik}\}_{k < j})$ where:

- n is the total number of trajectories in the dataset
- m_i is the number of actions in trajectory i
- $\{a_{ik}\}_{k < j}$ denotes the action history up to step $j - 1$
- $a_{i,j}$ is the j -th action in trajectory i
- $z_{i,j}$ is the chain-of-thought reasoning for action $a_{i,j}$

The model learns to predict both the action and its reasoning given the image, goal, context, and action history.

E.1.2. COMPLETE ALGORITHM

Algorithm 3 Standard Supervised Learning

- 1: **Input:** Trajectory dataset $\mathcal{D} = \{\tau_i\}_{i=1}^n$, model π_θ
 - 2: **Hyperparameters:** Learning rate $\eta = 2 \times 10^{-5}$, epochs $E = 3$, batch size $B = 4$, gradient accumulation steps $G = 2$
 - 3: Initialize θ from pretrained Qwen3-VL checkpoint
 - 4: Apply LoRA adaptation: rank $r = 16$, $\alpha = 32$, dropout $p = 0.05$
 - 5: Target modules: $\{q_proj, k_proj\}$ in all transformer layers
 - 6: **for** epoch $e = 1$ to E **do**
 - 7: Shuffle dataset \mathcal{D}
 - 8: **for** batch $\mathcal{B} = \{\tau_i\}_{i=1}^B$ in \mathcal{D} **do**
 - 9: Initialize $\mathcal{L}_{\text{batch}} \leftarrow 0$
 - 10: **for** trajectory τ_i in \mathcal{B} **do**
 - 11: Prepare inputs: image I_i , editing prompt e_i , context c_i
 - 12: Initialize action history: $\mathcal{H} \leftarrow \emptyset$
 - 13: **for** step $j = 1$ to m_i **do**
 - 14: Forward pass: logits $\leftarrow \pi_\theta(I_i, e_i, c_i, \mathcal{H})$
 - 15: Compute token-level log-likelihood: $\ell_j = \log p_{\text{logits}}(a_{i,j}, z_{i,j})$
 - 16: Add to history: $\mathcal{H} \leftarrow \mathcal{H} \cup \{a_{i,j}\}$
 - 17: Accumulate loss: $\mathcal{L}_{\text{batch}} \leftarrow \mathcal{L}_{\text{batch}} - \ell_j$
 - 18: **end for**
 - 19: **end for**
 - 20: Normalize: $\mathcal{L}_{\text{batch}} \leftarrow \mathcal{L}_{\text{batch}} / (B \cdot G)$
 - 21: Backward pass: Compute $\nabla_\theta \mathcal{L}_{\text{batch}}$
 - 22: **if** gradient accumulation step complete **then**
 - 23: Update parameters: $\theta \leftarrow \theta - \eta \nabla_\theta \mathcal{L}_{\text{batch}}$
 - 24: Zero gradients
 - 25: **end if**
 - 26: **end for**
 - 27: Evaluate on validation set
 - 28: **end for**
 - 29: **Return:** Trained student model π_θ
-

E.1.3. IMPLEMENTATION DETAILS

LoRA Configuration: We use Low-Rank Adaptation (LoRA) for efficient fine-tuning:

- **Rank:** $r = 16$ (reduces parameters by 99%)
- **Alpha:** $\alpha = 32$ (scaling factor for LoRA weights)
- **Dropout:** $p = 0.05$ for regularization
- **Target modules:** Query and key projections in all attention layers
- **Trainable parameters:** 150M out of 8B (1.9%)

Training Configuration:

- **Optimizer:** AdamW with $\beta_1 = 0.9$, $\beta_2 = 0.999$, weight decay = 0.01
- **Learning rate:** 2×10^{-5} with linear warmup (500 steps) and cosine decay
- **Batch size:** 4 per GPU, 8 GPUs, gradient accumulation 2 \rightarrow effective batch size 64
- **Epochs:** 3 (approximately 450 gradient updates for $n = 10,000$ trajectories)
- **Mixed precision:** bfloat16 for memory efficiency
- **Gradient clipping:** Max norm 1.0

Data Processing:

- **Sequence length:** Maximum 2048 tokens
- **Padding:** Right-padding with attention mask
- **Truncation:** Truncate long trajectories from the end
- **Shuffling:** Shuffle at epoch level, not within batches

E.1.4. LIMITATIONS OF STANDARD SL

This approach has fundamental limitations:

- 1. Quality Blindness:** All synthetic trajectories contribute equally regardless of reward r_i . A trajectory with $r_i = 3.0$ (poor) has the same influence as $r_i = 5.0$ (excellent).
- 2. Potential for Degradation:** If low-quality trajectories are prevalent, the model may learn suboptimal behaviors and fail to match teacher performance.
- 3. No Preference Signal:** The model has no signal about which trajectories are better when multiple plans exist for the same (I_i, e_i) pair.
- 4. Reward Information Wasted:** The expensive reward evaluation (r_i) computed during data generation is completely ignored during training.

These limitations motivate reward-aware training methods (R, RW, DPO) described in the main paper.

E.2. Reward-Weighted Fine-Tuning (RW)

RW uses all trajectories but weights their contribution according to quality. This section provides complete implementation details and theoretical analysis.

E.2.1. WEIGHT FUNCTION

We use a simple continuous weight function:

$$w(r_i) = \max\{r_i - 3.0, 0\}$$

This linearly scales the contribution of each trajectory based on its quality above the minimum acceptable threshold (3.0). Trajectories with $r_i < 3.0$ receive zero weight, while higher-quality trajectories receive proportionally more influence.

E.2.2. WEIGHTED LOSS FORMULATION

The RW loss modifies standard supervised learning by incorporating per-trajectory weights:

$$\mathcal{L}_{\text{RW}}(\theta) = \frac{\sum_{i=1}^n w(r_i) \cdot \mathcal{L}_i(\theta)}{\sum_{i=1}^n w(r_i)}$$

where $\mathcal{L}_i(\theta) = -\sum_{j=1}^{m_i} \log \pi_{\theta}(a_{i,j}, z_{i,j} \mid I_i, e_i, c_i, \{a_{i,k}\}_{k < j})$ is the per-trajectory loss.

The normalization term $\sum_{i=1}^n w(r_i)$ computes a weighted average rather than a weighted sum, ensuring: (1) loss magnitude remains comparable to standard supervised learning (unweighted mean); (2) gradient scale is independent of dataset size and weight distribution; (3) each trajectory contributes proportionally to its quality—e.g., a trajectory with $w(r_i) = 2.0$ receives twice the gradient weight of one with $w(r_i) = 1.0$. This is equivalent to importance sampling where excellent trajectories are effectively replicated in the training distribution.

E.2.3. COMPLETE ALGORITHM

Algorithm 4 Reward-Weighted Fine-tuning

- 1: **Input:** Trajectory dataset $\mathcal{D} = \{\tau_i\}$ with rewards, model π_{θ}
 - 2: **Hyperparameters:** Learning rate $\eta = 2 \times 10^{-5}$, epochs $E = 3$, batch size $B = 8$, GPUs = 8
 - 3: Initialize θ from pretrained Qwen3-VL checkpoint with LoRA (rank 16, $\alpha = 32$)
 - 4: **for** epoch = 1 to E **do**
 - 5: **for** batch $\{\tau_i\}_{i \in \mathcal{B}}$ in \mathcal{D} **do**
 - 6: // Compute per-trajectory losses
 - 7: **for** $i \in \mathcal{B}$ **do**
 - 8: $\mathcal{L}_i \leftarrow -\sum_{j=1}^{m_i} \log \pi_{\theta}(a_{i,j}, z_{i,j} \mid I_i, e_i, c_i, \{a_{i,k}\}_{k < j})$
 - 9: **end for**
 - 10: // Compute weights and weighted loss
 - 11: Compute weights: $w_i = \max\{r_i - 3.0, 0\}$ for each $i \in \mathcal{B}$
 - 12: Weighted loss: $\mathcal{L}_{\text{batch}} = \frac{\sum_{i \in \mathcal{B}} w_i \mathcal{L}_i}{\sum_{i \in \mathcal{B}} w_i}$
 - 13: // Gradient update
 - 14: Update: $\theta \leftarrow \theta - \eta \nabla_{\theta} \mathcal{L}_{\text{batch}}$
 - 15: **end for**
 - 16: Evaluate on validation set
 - 17: **end for**
 - 18: **Return:** Trained student model π_{θ}
-

E.2.4. IMPLEMENTATION DETAILS

PyTorch Implementation: Per-sample weighting in PyTorch is straightforward:

- Compute standard log-likelihood loss for each trajectory: `loss_i = -log_probs[i].sum()`
- Compute weights: `weights = torch.maximum(rewards - 3.0, torch.zeros_like(rewards))`
- Weighted loss: `weighted_loss = (weights * losses).sum() / weights.sum()`

- Backward pass on `weighted_loss`

Memory and Computational Cost

- **Memory:** Same as standard SL (no reference model needed)
- **Computation:** Same forward/backward cost as SL
- **Effective batch size:** $8 \times 8 = 64$ (8 per GPU, 8 GPUs)
- **Training time:** Identical to SL

Connection to Importance Sampling: Reward-weighted regression relates to importance sampling in offline R. Importance sampling enables unbiased estimation when evaluating a target distribution using samples from a different source distribution, with truncated importance sampling providing variance reduction through weight clipping. If we view the data generator as sampling from a behavior policy π_{data} and want the trained model to match a target policy π^* that achieves high rewards, the weight $w(r_i)$ approximates the importance ratio $\frac{\pi^*(a|s)}{\pi_{\text{data}}(a|s)}$. This enables the model to focus gradient updates on high-quality trajectories while retaining the diversity of medium-quality examples.

Detailed Comparison: RW vs. SW: Both RW and SW relate to advantage-based R methods but differ in key ways. RW uses absolute rewards r_i with the continuous weight function $w(r_i) = \max\{r_i - 3.0, 0\}$, preserving the natural quality hierarchy—excellent trajectories ($r_i \geq 4.5$) receive consistently high weight regardless of dataset composition. This is appropriate when the teacher provides high-quality data ($r_i \geq 3.0$) without catastrophically bad examples. SW uses standardized rewards $\tilde{r}_i = \frac{r_i - \bar{r}}{\sigma_r}$ directly as weights, similar to advantages $A_i = r_i - \bar{r}$ but with variance normalization. SW adapts to dataset statistics: in a dataset with $\bar{r} = 4.2$, a trajectory with $r_i = 4.5$ receives moderate weight, while in a dataset with $\bar{r} = 3.5$, the same trajectory receives high weight. This makes SW robust to reward scale variations across datasets.

From a rollout perspective, when multiple rollouts of the same input (I_i, e_i) produce different rewards, SW’s standardization provides variance reduction by centering the distribution: trajectories above the mean receive positive weight, those below receive negative weight, reducing gradient variance—a classic technique in policy gradient methods (Williams, 1992; Schulman et al., 2015). This makes SW particularly effective for datasets with diverse reward distributions across different inputs while maintaining stability within each input’s rollout variations.

Normalization in SW: Mathematical Justification: A critical implementation detail distinguishes SW from RW. Since standardized rewards \tilde{r}_i are zero-mean by construction ($\mathbb{E}[\tilde{r}_i] = 0$), normalizing by their sum would cause instability. Therefore, SW uses batch-size normalization:

$$\mathcal{L}_{\text{batch}} = \frac{1}{|\mathcal{B}|} \sum_{i \in \mathcal{B}} \tilde{r}_i \mathcal{L}_i$$

This formulation is stable and mathematically equivalent to applying standardized rewards as gradient multipliers: positive $\tilde{r}_i > 0$ (above-average quality) amplifies gradients, while negative $\tilde{r}_i < 0$ (below-average quality) reverses gradient direction—analogue to advantage-based policy gradients (Williams, 1992; Schulman et al., 2015) where positive/negative advantages increase/decrease action probabilities.

In contrast, RW uses non-negative weights $w(r_i) = \max\{r_i - 3.0, 0\} \geq 0$. For RW, normalizing by $\sum_{i \in \mathcal{B}} w_i$ is stable and maintains the weighted average interpretation. The normalization choice (batch size vs. sum of weights) is dictated by whether weights can be negative.

E.3. Direct Preference Optimization (DPO)

DPO is a preference-based reinforcement learning method that learns from contrastive pairs of trajectories without requiring an explicit reward model. This section provides complete mathematical formulation and implementation details.

E.3.1. PREFERENCE DATASET CONSTRUCTION

DPO requires a preference dataset $\mathcal{D}_{\text{pref}}$ consisting of trajectory pairs:

$$\mathcal{D}_{\text{pref}} = \{(\tau_i^+, \tau_i^-)\}_{i=1}^{n_{\text{pairs}}}$$

where:

- $\tau_i^+ = (e_i, I_i, c_i, \{a_{i,j}^+\}, \{z_{i,j}^+\}, \hat{e}_i^+, \hat{I}_i^+, r_i^+)$ is the “chosen” trajectory with reward $r_i^+ \geq 4.0$
- $\tau_i^- = (e_i, I_i, c_i, \{a_{i,j}^-\}, \{z_{i,j}^-\}, \hat{e}_i^-, \hat{I}_i^-, r_i^-)$ is the “rejected” trajectory with reward $r_i^- \in [2.5, 3.5]$
- Both trajectories share the same input: (I_i, e_i)
- We require $r_i^+ - r_i^- \geq 0.5$ to ensure meaningful preference signal

Pairing Algorithm: For each high-quality trajectory ($r_i \geq 4.0$), we sample a lower-quality trajectory with the same input (I_i, e_i) to form a contrastive pair. If multiple candidates exist, we randomly sample one. This yields approximately 3,500 pairs from the $n = 10,000$ trajectory dataset.

E.3.2. BRADLEY-TERRY PREFERENCE MODEL

DPO optimizes a policy π_θ relative to a frozen reference policy π_{ref} using the Bradley-Terry model. The probability that trajectory τ^+ is preferred over τ^- is modeled as:

$$p(\tau_i^+ \succ \tau_i^- \mid I_i, e_i, c_i) = \sigma \left(\beta \left[\log \frac{\pi_\theta(\{a_{i,j}^+, z_{i,j}^+\} \mid I_i, e_i, c_i)}{\pi_{\text{ref}}(\{a_{i,j}^+, z_{i,j}^+\} \mid I_i, e_i, c_i)} - \log \frac{\pi_\theta(\{a_{i,j}^-, z_{i,j}^-\} \mid I_i, e_i, c_i)}{\pi_{\text{ref}}(\{a_{i,j}^-, z_{i,j}^-\} \mid I_i, e_i, c_i)} \right] \right) \quad (1)$$

where:

- π_{ref} is a frozen copy of the policy at initialization
- $\beta = 0.1$ controls the KL penalty strength (higher β = stronger KL constraint)
- $\sigma(x) = \frac{1}{1+e^{-x}}$ is the sigmoid function
- The log-ratio $\log \frac{\pi_\theta(\tau)}{\pi_{\text{ref}}(\tau)}$ measures how much the policy has shifted from its initialization

E.3.3. DPO LOSS FUNCTION

The DPO loss maximizes the log-likelihood of preferences: $\mathcal{L}_{\text{DPO}}(\theta) = -\mathbb{E}_{(\tau_i^+, \tau_i^-) \sim \mathcal{D}_{\text{pref}}} \left[\log \sigma \left(\beta \left[\log r_\theta(\tau_i^+) - \log r_\theta(\tau_i^-) \right] \right) \right]$ where $r_\theta(\tau_i) = \frac{\pi_\theta(\{a_{i,j}, z_{i,j}\} \mid I_i, e_i, c_i)}{\pi_{\text{ref}}(\{a_{i,j}, z_{i,j}\} \mid I_i, e_i, c_i)}$ is the likelihood ratio between the current policy and the reference.

Intuition: The loss encourages the policy to: **(1)** Increase likelihood of chosen, **(2)** Increase likelihood of chosen actions $\{a_{i,j}^+, z_{i,j}^+\}$, **(3)** Decrease likelihood of rejected actions $\{a_{i,j}^-, z_{i,j}^-\}$, and **(4)** Stay close to the reference policy (controlled by β).

E.3.4. COMPLETE ALGORITHM

Algorithm 5 Direct Preference Optimization

```

1: Input: Preference dataset  $\mathcal{D}_{\text{pref}} = \{(\tau_i^+, \tau_i^-)\}$ , model  $\pi_\theta$ 
2: Hyperparameters: Learning rate  $\eta = 2 \times 10^{-5}$ , epochs  $E = 3$ , batch size  $B = 1$ , gradient accumulation  $G = 8$ ,
    $\beta = 0.1$ 
3: Initialize  $\theta$  from pretrained Qwen3-VL checkpoint
4: Apply LoRA: rank  $r = 16$ ,  $\alpha = 32$ , dropout  $p = 0.05$ 
5: Create frozen reference model:  $\pi_{\text{ref}} \leftarrow \text{deepcopy}(\pi_\theta)$ 
6: Move  $\pi_{\text{ref}}$  to GPU and freeze all parameters
7: for epoch  $e = 1$  to  $E$  do
8:   Shuffle  $\mathcal{D}_{\text{pref}}$ 
9:   for batch  $\mathcal{B} = \{(\tau_i^+, \tau_i^-)\}_{i=1}^B$  in  $\mathcal{D}_{\text{pref}}$  do
10:     Initialize  $\mathcal{L}_{\text{batch}} \leftarrow 0$ 
11:     for pair  $(\tau_i^+, \tau_i^-)$  in  $\mathcal{B}$  do
12:       // Forward pass for chosen trajectory
13:        $\log \pi_\theta^+ \leftarrow \sum_{j=1}^{m_i^+} \log \pi_\theta(a_{i,j}^+, z_{i,j}^+ \mid I_i, e_i, c_i, \{a_{ik}^+\}_{k < j})$ 
14:        $\log \pi_{\text{ref}}^+ \leftarrow \sum_{j=1}^{m_i^+} \log \pi_{\text{ref}}(a_{i,j}^+, z_{i,j}^+ \mid I_i, e_i, c_i, \{a_{ik}^+\}_{k < j})$ 
15:       // Forward pass for rejected trajectory
16:        $\log \pi_\theta^- \leftarrow \sum_{j=1}^{m_i^-} \log \pi_\theta(a_{i,j}^-, z_{i,j}^- \mid I_i, e_i, c_i, \{a_{ik}^-\}_{k < j})$ 
17:        $\log \pi_{\text{ref}}^- \leftarrow \sum_{j=1}^{m_i^-} \log \pi_{\text{ref}}(a_{i,j}^-, z_{i,j}^- \mid I_i, e_i, c_i, \{a_{ik}^-\}_{k < j})$ 
18:       // Compute log-ratios
19:        $r^+ \leftarrow \log \pi_\theta^+ - \log \pi_{\text{ref}}^+$  {Log-ratio for chosen}
20:        $r^- \leftarrow \log \pi_\theta^- - \log \pi_{\text{ref}}^-$  {Log-ratio for rejected}
21:       // DPO loss
22:        $\mathcal{L}_i \leftarrow -\log \sigma(\beta \cdot (r^+ - r^-))$ 
23:        $\mathcal{L}_{\text{batch}} \leftarrow \mathcal{L}_{\text{batch}} + \mathcal{L}_i$ 
24:       // Track metrics
25:        $\text{accuracy}_i \leftarrow \mathbb{I}[r^+ > r^-]$  {Model prefers chosen over rejected?}
26:     end for
27:     Normalize:  $\mathcal{L}_{\text{batch}} \leftarrow \mathcal{L}_{\text{batch}} / (B \cdot G)$ 
28:     Backward pass: Compute  $\nabla_\theta \mathcal{L}_{\text{batch}}$ 
29:     if gradient accumulation step complete then
30:       Clip gradients:  $\text{clip}(\nabla_\theta, \text{max\_norm} = 1.0)$ 
31:       Update:  $\theta \leftarrow \theta - \eta \nabla_\theta \mathcal{L}_{\text{batch}}$ 
32:       Zero gradients
33:     end if
34:   end for
35:   Log metrics: mean DPO loss, preference accuracy
36:   Evaluate on validation set
37: end for
38: Return: Trained student model  $\pi_\theta$ 

```

E.3.5. IMPLEMENTATION DETAILS

Reference Model Management

- **Creation:** Deep copy of initial model before any training
- **Parameter freezing:** All parameters set to `requires_grad=False`
- **Memory:** Reference model consumes same memory as policy model (careful with 8B models)

- **Device placement:** Move to same device as policy for efficient forward passes
- **No gradient tracking:** Use `torch.no_grad()` context for reference forward passes

Beta Parameter Selection The β parameter critically affects training:

- **High β (0.5-1.0):** Strong KL constraint, policy stays close to reference, conservative updates
- **Low β (0.01-0.05):** Weak KL constraint, policy can deviate significantly, risk of instability
- **Our choice ($\beta = 0.1$):** Balanced trade-off validated on validation set

Batch Size and Memory DPO requires $2\times$ forward passes per sample (chosen + rejected), plus reference model. This doubles memory:

- **Effective batch size:** 1 per GPU, 8 gradient accumulation steps
- **Total effective batch:** $1 \times 8 \text{ GPUs} \times 8 \text{ accum} = 64$
- **Memory per GPU:** 78GB for 8B model with batch size 1

Preference Accuracy Metric We track whether the model correctly prefers chosen over rejected:

$$\text{accuracy} = \frac{1}{|\mathcal{D}_{\text{pref}}|} \sum_{(\tau^+, \tau^-) \in \mathcal{D}_{\text{pref}}} \mathbb{I}[r_\theta(\tau^+) > r_\theta(\tau^-)]$$

This should increase during training (target: $\geq 80\%$ by end of training).

E.3.6. ADVANTAGES AND DISADVANTAGES

Advantages

- **No weight function design:** Avoids manual specification of $w(r_i)$
- **Contrastive learning:** Directly learns relative preferences
- **Implicit reward modeling:** No explicit reward function needed during training
- **KL regularization:** Log-ratio formulation prevents overfitting
- **Stable training:** Reference model provides consistent baseline

Disadvantages

- **Requires paired data:** Need multiple trajectories per (I_i, e_i)
- **$2\times$ computational cost:** Forward passes for both chosen and rejected
- **Memory intensive:** Reference model doubles memory footprint
- **Hyperparameter sensitivity:** β choice affects performance significantly

E.3.7. THEORETICAL JUSTIFICATION

DPO can be derived as the optimal solution to a constrained R objective:

$$\max_{\pi_{\theta}} \mathbb{E}_{\tau \sim \pi_{\theta}} [r(\tau)] - \frac{1}{\beta} D_{\text{KL}}(\pi_{\theta} \parallel \pi_{\text{ref}})$$

The Bradley-Terry preference model emerges naturally when we reparameterize the reward as:

$$r(\tau) = \frac{1}{\beta} \log \frac{\pi^*(\tau)}{\pi_{\text{ref}}(\tau)}$$

where π^* is the optimal policy. DPO directly optimizes this objective using preference data without explicitly modeling the reward function.

E.4. Justification for RW and DPO for Our Setup

While S and R are straightforward, RW and DPO deserve deeper theoretical motivation. This section provides comprehensive theoretical analysis of why these methods work.

E.4.1. WHY RW WORKS

RW can be viewed through multiple theoretical lenses:

1. Importance Sampling Perspective: If we view the teacher as a behavior policy π_b sampling diverse trajectories, and want to learn a target policy π^* that achieves high rewards, importance sampling suggests:

$$\mathbb{E}_{\tau \sim \pi^*} [f(\tau)] \approx \mathbb{E}_{\tau \sim \pi_b} \left[\frac{\pi^*(\tau)}{\pi_b(\tau)} \cdot f(\tau) \right]$$

The weight $w(r_i)$ approximates $\frac{\pi^*(\tau_i)}{\pi_b(\tau_i)}$, upweighting trajectories that the target policy would prefer.

2. Implicit Reward Maximization: RW maximizes a reward-modulated likelihood:

$$\mathcal{L}_{\text{RW}}(\theta) \approx -\mathbb{E}_{\tau \sim \mathcal{D}} [w(r) \log \pi_{\theta}(\tau)]$$

This implicitly encourages the policy to assign high probability to high-reward trajectories while maintaining coverage over the data distribution.

3. Data Efficiency: Unlike R which discards 35% of data, RW retains all data but de-emphasizes low-quality examples. This preserves diversity—important for generalization—while focusing learning on successful behaviors.

E.4.2. WHY DIRECT PREFERENCE OPTIMIZATION WORKS

DPO leverages contrastive learning to implicitly optimize a reward model:

1. Connection to RLHF: Traditional RLHF requires:

1. Train reward model r_{ϕ} from preferences
2. Optimize policy π_{θ} against r_{ϕ} using PPO

DPO bypasses step 1 by directly optimizing:

$$\mathcal{L}_{\text{DPO}}(\theta) = -\mathbb{E}_{(\tau^+, \tau^-)} \left[\log \sigma \left(\beta \left[\log \pi_{\theta}(\tau^+) - \log \pi_{\theta}(\tau^-) - \log \pi_{\text{ref}}(\tau^+) + \log \pi_{\text{ref}}(\tau^-) \right] \right) \right]$$

This is equivalent to maximizing the reward margin $r_{\theta}(\tau^+) - r_{\theta}(\tau^-)$ where the reward is implicitly defined by the policy’s log-likelihood ratio.

2. Contrastive Learning Benefits: By comparing τ^+ and τ^- with the same (I_i, e_i) , DPO learns:

- What makes one plan better than another for the *same input*
- Relative quality rather than absolute quality
- Fine-grained distinctions between similar trajectories

This contrastive signal is often more informative than scalar rewards alone.

3. KL Regularization: The log-ratio $\log \frac{\pi_{\theta}}{\pi_{\text{ref}}}$ implicitly penalizes the policy from deviating too far from the reference, preventing:

- Mode collapse (ignoring diverse strategies)
- Reward hacking (exploiting spurious reward signals)
- Overfitting to preference data

E.4.3. RW vs. DPO: COMPLEMENTARY STRENGTHS

Table 6. Theoretical Comparison: RW vs. DPO

Property	RW	DPO
Learning signal	Absolute rewards	Relative preferences
Data usage	All data	Paired data only
Optimization	Direct likelihood	Contrastive likelihood
Implicit KL	Through weights	Through log-ratio
Sample efficiency	High	Medium
Distinction quality	Coarse-grained	Fine-grained

In practice, both methods significantly outperform baselines, with DPO often having a slight edge when sufficient paired data is available.

E.5. Complete Training Configuration

This section provides comprehensive training configuration details for all student models.

E.5.1. OPTIMIZATION HYPERPARAMETERS

- **Optimizer:** AdamW with $\beta_1 = 0.9$, $\beta_2 = 0.999$, weight decay 10^{-2}
- **Learning Rate:** $\eta = 2 \times 10^{-5}$ with linear warmup (10% of steps) and cosine decay
- **Batch Size:** 4 per GPU, gradient accumulation steps = 2
- **Effective Batch:** 64 with 8 GPUs ($8 \times 4 \times 2 = 64$)
- **Epochs:** 3 for all methods

- **Precision:** Mixed precision (bfloat16) for memory efficiency
- **Gradient Clipping:** Maximum norm 1.0
- **Warmup Steps:** 500 steps (approximately 10% of total training)
- **Total Training Steps:** Approximately 450 gradient updates for $n = 10,000$ trajectories

E.5.2. MODEL ARCHITECTURE DETAILS

- **Base Models:** Qwen3-VL-4B-Instruct and Qwen3-VL-8B-Instruct
- **Fine-tuning Method:** LoRA (Low-Rank Adaptation)
 - Rank: $r = 16$
 - Alpha: $\alpha = 32$
 - Dropout: $p = 0.05$
- **Target Modules:** All attention layers (Q, K, V, O projections)
- **Trainable Parameters:**
 - 4B model: 75M trainable (1.8% of total)
 - 8B model: 150M trainable (1.9% of total)
- **Vision Encoder:** Frozen during training (only cached embeddings used for vision-language models)
- **Language Model:** Transformer decoder with LoRA adapters

E.5.3. DATA PROCESSING PIPELINE

Text-Only Models

- Tokenize (e_i, c_i) concatenation with special tokens
- Maximum sequence length: 1024 tokens
- Padding: Right-padding with attention mask
- Truncation: Truncate from the end if exceeding max length

Vision-Language Models

- Concatenate cached vision features v_i with text embeddings
- Vision features: 256-dimensional vector from frozen ViT encoder
- Text embeddings: Standard Qwen3-VL tokenization
- Combined sequence: $[v_i; \text{text_emb}(e_i, c_i)]$

Action Representation

- Each action $a_{i,j}$ serialized as: "[ACTION.TYPE] param1=value1, param2=value2"
- Chain-of-thought $z_{i,j}$ appended as natural language
- Format: "[REASONING] Because the current state is X, we choose Y to achieve Z"
- Sequence padding: Pad to maximum trajectory length (typically 2-5 actions)

E.5.4. DISTRIBUTED TRAINING SETUP

- **Hardware:** 8× NVIDIA A100 80GB GPUs
- **Parallelism:** Data parallel with DistributedDataParallel (DDP)
- **Communication:** NCCL backend for efficient GPU-GPU communication
- **Gradient Synchronization:** Synchronized after gradient accumulation steps
- **Memory Usage:**
 - 8B model (text-only): 35GB per GPU
 - 8B model (vision-language): 45GB per GPU
 - 4B model (text-only): 20GB per GPU
 - 4B model (vision-language): 28GB per GPU

E.6. Cached Embedding Approach

For vision-language models, computing vision features for every training sample is expensive. We accelerate training through a cached embedding approach that provides 3× speedup with no accuracy loss.

E.6.1. OFFLINE EMBEDDING COMPUTATION

Before training, we precompute and cache all vision embeddings:

Step 1: Load Dataset Images: Load all base images $\{I_1, \dots, I_n\}$ from the trajectory dataset. For our dataset with $n = 10,000$ trajectories, this involves loading approximately 3,500 unique images (multiple trajectories share the same base image).

Step 2: Extract Vision Features: For each unique image I_i :

1. Resize to 768×768 pixels (model input resolution)
2. Preprocess: normalize with ImageNet statistics
3. Forward pass through frozen vision encoder: $v_i = \text{VisionEncoder}(I_i)$
4. Extract features from final layer: 256-dimensional vector

Step 3: Store in HDF5 Format: Store features in HDF5 file indexed by image hash:

- **Key:** SHA-256 hash of image pixel values
- **Value:** Float32 array of shape (256,)
- **File size:** 3.5k images × 256 × 4 bytes \approx 3.5 MB (very compact)
- **Access pattern:** Memory-mapped for efficient random access

E.6.2. ONLINE TRAINING WITH CACHED FEATURES

During training, we use cached features instead of recomputing:

Step 1: Load Cached Features For each training sample τ_j :

1. Compute image hash from base image I_i
2. Lookup cached features: $v_i = \text{cache}[\text{hash}(I_i)]$
3. Load takes 1ms vs. 40ms for vision encoder forward pass

Step 2: Concatenate with Text Embeddings

1. Tokenize text inputs: $(e_i, c_i) \rightarrow$ token IDs
2. Embed tokens: $\text{emb}_{\text{text}} = \text{Embedding}(\text{tokens})$
3. Concatenate: $\text{input} = [v_i; \text{emb}_{\text{text}}]$

Step 3: Forward Pass Through Transformer

1. Process concatenated input through transformer layers
2. Skip vision encoder entirely (already cached)
3. Compute loss and gradients as usual

E.6.3. BENEFITS OF CACHING

1. Training Speedup

- **Vision encoder time:** 40ms per image (skipped)
- **Cache lookup time:** 1ms per image
- **Net speedup:** 39ms saved per sample
- **Total training time:** Vision-language training becomes comparable to text-only (3× faster than naive approach)

2. No Accuracy Degradation

- Cached features are *identical* to on-the-fly computation
- Vision encoder is frozen, so no gradient updates needed
- Final model performance is exactly the same

3. Memory Efficiency

- HDF5 file: 3.5 MB vs. storing raw images (3.5 GB)
- Memory-mapped access: Load only needed features
- Enables training on datasets with 100k+ images without memory issues

4. Scalability

- Precomputation: One-time cost amortized over multiple training runs
- Reusable: Same cache for different training methods (SL, R, RW, DPO)
- Extensible: Can add more images to cache incrementally

E.6.4. IMPLEMENTATION NOTES

Training with Cached Embeddings Set `use_cached_embeddings=True` in training config and provide path to cache file. The dataset loader automatically uses cached features when available.

Table 7. Comprehensive Comparison of Training Algorithms

Property	SL	R	RW	DPO
Uses reward signals	No	Yes	Yes	Yes
Uses all data	Yes	No (65%)	Yes	Paired only
Manual tuning required	None	Threshold	Weight fn	Beta
Computational cost	1×	1×	1×	2×
Contrastive learning	No	No	No	Yes
Data efficiency	Medium	Low	High	Medium
Implementation complexity	Simple	Simple	Medium	Complex
Memory footprint	1×	1×	1×	2×
Training stability	High	High	High	Medium

E.7. Algorithm Comparison

This section provides comprehensive comparison of all training methods across multiple dimensions.

E.7.1. QUANTITATIVE COMPARISON

Table 7 summarizes the key differences between training methods:

E.7.2. QUALITATIVE COMPARISON

Standard Supervised Learning (SL)

- **Strengths:** Simple, stable, no hyperparameters to tune
- **Weaknesses:** Ignores reward information, treats all data equally
- **Best for:** Baseline comparison, high-quality curated datasets

Reward-Filtered Training (R)

- **Strengths:** Simple implementation, removes clearly bad data
- **Weaknesses:** Discards 35% of data, binary threshold ignores nuance
- **Best for:** When data quality varies widely and storage is not a concern

Reward-Weighted Fine-tuning (RW)

- **Strengths:** Uses all data, preserves diversity, continuous quality weighting
- **Weaknesses:** Requires weight function design, coarse-grained distinctions
- **Best for:** Maximizing data efficiency, diverse quality distributions

Direct Preference Optimization (DPO)

- **Strengths:** Fine-grained comparisons, no weight function, implicit KL regularization
- **Weaknesses:** Requires paired data, 2× computational cost, memory intensive
- **Best for:** When preference pairs are available, fine-grained quality distinctions needed

E.7.3. EMPIRICAL PERFORMANCE SUMMARY

Based on our experiments (detailed in Section 5):

Simple Dataset (Simpler Tasks)

- **Ranking:** DPO \approx RW \approx SW $>$ R $>$ SL
- **Observation:** All reward-aware methods significantly outperform SL
- **Margin:** DPO and RW achieve 12-15% improvement over SL

Regular Dataset (Harder Tasks)

- **Ranking:** RW, SW $>$ DPO $>$ R $>$ SL
- **Observation:** RW excels on complex compositional reasoning
- **Margin:** RW achieves 18-22% improvement over SL

Key Insight Training methodology matters as much as model scale: a 4B model trained with DPO can match or exceed an 8B model trained with standard SL on several metrics.

F. Experimental Details

This section provides comprehensive implementation details for our experimental evaluation, including model specifications, hyperparameters, and the GPT-4o evaluation protocols.

F.1. GPT-4o Evaluation Prompts

We use GPT-4o for two types of evaluation: (1) action plan quality assessment, and (2) image transformation quality assessment. Both evaluations use structured prompts with detailed criteria.

F.1.1. ACTION PLAN EVALUATION PROMPT

For evaluating the quality of generated action plans (without image execution), we query GPT-4o with the following structured prompt:

GPT-4o Action Plan Evaluation Prompt

You are an expert evaluator of image editing action plans.

Input :

- Base image: [I.i]
- User goal: {e.i}
- Current visual state: {c.i} (10 dimensions)
- Predicted action plan: [a.i1, a.i2, ..., a.im]
- Chain-of-thought reasoning: [z.i1, z.i2, ..., z.im]
- Ground truth plan: [a.i1*, a.i2*, ..., a.ik*]

Evaluation Criteria:

1. **Plan Correctness (35%) :**
 - Are the actions correct for achieving the goal?
 - Is the action sequence logically ordered?
 - Are action parameters appropriate?
2. **Goal Coverage (25%) :**
 - Does the plan address all aspects of the user goal?
 - Are any required transformations missing?
 - Is there unnecessary redundancy?
3. **Reasoning Quality (20%) :**
 - Is the chain-of-thought reasoning clear and logical?

- Does each step explain why the action is chosen?
 - Are state transitions explicitly tracked?
4. **Efficiency (10%):**
 - Is the plan concise (minimal steps)?
 - Are actions combined when possible?
 - Is the sequence optimal?
 5. **Alignment with Ground Truth (10%):**
 - How similar is the plan to ground truth?
 - Are key actions present?
 - Note: Different valid plans can achieve same goal

Output Format:

Provide a JSON response:

```
{
  "overall_score": <0-100>,
  "plan_correctness": <0-100>,
  "goal_coverage": <0-100>,
  "reasoning_quality": <0-100>,
  "efficiency": <0-100>,
  "ground_truth_alignment": <0-100>,
  "justification": "<explanation>",
  "key_issues": ["<issue1>", "<issue2>", ...]
}
```

F.1.2. IMAGE QUALITY EVALUATION PROMPT

For evaluating the quality of executed image transformations, we query GPT-4o with the following prompt:

GPT-4o Image Quality Evaluation Prompt

You are an expert evaluator of image editing results.

Input:

- Original image: [I.i]
- Edited image: [E.i]
- User goal: {e.i}
- Action plan used: [a.i1, a.i2, ..., a.im]
- Ground truth image: [E.i*]

Evaluation Criteria:

1. **Goal Alignment (30% --- Most Critical):**
 - Does the edited image match the user's stated goal?
 - Are all requested attributes transformed correctly?
 - Is the semantic intent preserved?
2. **Aesthetic Quality (25%):**
 - Visual appeal and artistic merit
 - Composition balance and color harmony
 - Professional polish
3. **Technical Quality (20%):**
 - Absence of artifacts (blurring, distortion, seams)
 - Resolution and detail preservation
 - Edge sharpness and boundary quality
4. **Spatial Consistency (15%):**
 - Coherence of spatial relationships
 - Perspective correctness

```
- Depth ordering and geometric plausibility

5. Naturalness (10%):
- Does the result look realistic/plausible?
- Are lighting and shadows consistent?
- Are transformations well-integrated?

Comparison with Ground Truth:
- Visual similarity to ground truth
- Note: Multiple valid solutions may exist
- Focus on whether goal is achieved, not exact match

Output Format:
Provide a JSON response:
{
  "overall_score": <0-100>,
  "goal_alignment": <0-100>,
  "aesthetic_quality": <0-100>,
  "technical_quality": <0-100>,
  "spatial_consistency": <0-100>,
  "naturalness": <0-100>,
  "ground_truth_similarity": <0-100>,
  "justification": "<detailed_explanation>",
  "strengths": ["<strength1>", "<strength2>", "..."],
  "weaknesses": ["<weakness1>", "<weakness2>", "..."]
}
```

F.2. GPT-4o Evaluation Configuration

Model Specifications

- **Model:** GPT-4o (gpt-4o-2024-08-06)
- **Temperature:** 0.3 (low temperature for consistent evaluation)
- **Max tokens:** 2048
- **Top-p:** 0.95
- **Frequency penalty:** 0.0

Evaluation Protocol

- **Sample size:** For each model configuration, we evaluate on the full test set (10% split \approx 1,000 trajectories)
- **Batch processing:** Evaluate 50 samples per API batch to manage rate limits
- **Retry logic:** Retry failed evaluations up to 3 times with exponential backoff
- **Response parsing:** Parse JSON outputs and validate all required fields present
- **Aggregation:** Compute mean, median, and standard deviation across all samples

Cost and Time

- **Cost per evaluation:** Approximately \$0.02 per sample (image + text tokens)
- **Total cost:** \approx \$1,000 for evaluating all model configurations (5 datasets \times 7 methods \times 1,000 samples)
- **Evaluation time:** \approx 4-6 hours per dataset (rate-limited by API)

F.3. Baseline Model Specifications

Baseline Planner: The baseline model is Qwen3-VL-8B-Instruct without any fine-tuning, used to establish lower bounds:

- Direct zero-shot prompting with action library specification
- Temperature $T = 0.7$ for action sampling
- No chain-of-thought reasoning (direct action output)
- Serves as the starting checkpoint for all student models

Student Model Configurations: We train four student model variants:

- **Text-4B:** Qwen3-4B (text-only, no vision encoder), 4B parameters
- **Text-8B:** Qwen3-8B (text-only, no vision encoder), 8B parameters
- **Vision-4B:** Qwen3-VL-4B-Instruct (vision-language), 4B parameters
- **Vision-8B:** Qwen3-VL-8B-Instruct (vision-language), 8B parameters

Each variant is trained with four methods: S, R, RW, and D.

F.4. Training Infrastructure

Hardware

- **GPUs:** 8× NVIDIA A100 80GB (for 8B models), 4× A100 40GB (for 4B models)
- **CPU:** 64-core AMD EPYC 7742
- **RAM:** 512GB DDR4
- **Storage:** 10TB NVMe SSD for dataset and checkpoints

Software Stack

- **Framework:** PyTorch 2.1.0 with CUDA 12.1
- **Distributed training:** DeepSpeed ZeRO-2 for memory efficiency
- **Mixed precision:** BF16 for training, FP32 for evaluation
- **Communication backend:** NCCL 2.18

Training Time

- **Text-4B models:** ≈ 8 hours per method (SL, R, RW, DPO)
- **Text-8B models:** ≈ 16 hours per method
- **Vision-4B models:** ≈ 12 hours per method (with cached embeddings)
- **Vision-8B models:** ≈ 24 hours per method (with cached embeddings)
- **Total training time:** ≈ 400 GPU-hours across all configurations

F.5. Hyperparameter Search

We performed limited hyperparameter search for key parameters:

Learning Rate: Searched over: $\{1 \times 10^{-5}, 5 \times 10^{-5}, 1 \times 10^{-4}, 5 \times 10^{-4}\}$. Selected 5×10^{-5} based on validation performance.

LoRA Rank: Searched over: $\{16, 32, 64, 128\}$. Selected 64 for balance of capacity and efficiency.

DPO β : Searched over: $\{0.1, 0.5, 1.0, 2.0\}$. Selected 0.5 for stable contrastive learning.

RW Weight Function: Tested exponential, linear, and threshold-based weighting. Selected piecewise linear based on reward tiers (see Appendix C.3).

R Threshold: Searched over: $\{3.0, 3.25, 3.5, 3.75\}$. Selected 3.5 for 65% data retention.

All hyperparameters were tuned on the validation set and frozen before final evaluation on the test set.

F.6. Training Configuration Details

Training Efficiency Comparison:

Text-Only Training:

- Training time: 1.5-2 hours per method
- Memory usage: 28 GB per GPU
- Hardware: 8× A100 GPUs
- Vision encoder: Frozen (no image pixels processed)
- Effective batch size: 64 (8 GPUs × 4 per-GPU × 2 gradient accumulation)

Vision-Language Training:

- Training time: 3-4 hours per method (with cached embeddings)
- Memory usage: 45 GB per GPU
- Hardware: 8× A100 GPUs
- Vision encoder: Trainable (processes image pixels)
- Cached embedding speedup: 3× faster than full vision-language training
- Effective batch size: 64 (8 GPUs × 4 per-GPU × 2 gradient accumulation)

Complete Method Descriptions

(1) Baseline (B): Pretrained Qwen3-VL with no fine-tuning. Given image I_i and editing prompt e_i , directly predicts edited image \hat{I}_i without explicit action planning. Serves as lower bound for comparison.

(2) Edit-Only (E): Direct image-to-image editing without action planning. Ground truth edit instructions are applied directly to isolate editor performance. This baseline tests whether high-quality editing can be achieved through direct prompting alone, bypassing the action planning phase entirely.

(3) Standard (S): Supervised learning on all trajectories with $r_i \geq 3.0$. Uses uniform weighting regardless of quality scores. Trains on 98% of data (only filtering out catastrophic failures with $r_i < 3.0$).

(4) Reward-Filtered RL (R): Simple filtering strategy keeping only high-quality trajectories with $r_i \geq 4.0$. Discards 35% of data to focus learning on successful behaviors. No continuous weighting—binary include/exclude decision.

(5) Reward-Weighted (RW): Continuous reward-weighted fine-tuning with per-sample importance weighting. Weight function: $w(r_i) = \max\{r_i - 3.0, 0\}$. Uses all training data (98%) with differential emphasis based on quality scores. High-quality samples receive proportionally more gradient updates.

(6) Standardized Reward-Weighted (SW): Extends RW with trajectory-aware z-score normalization. Computes mean and std dev of rewards within each trajectory, then applies standardized weighting: $w_i = \tilde{r}_i = (r_i - \mu_{\text{traj}}) / \sigma_{\text{traj}}$. Balances learning across trajectories of varying difficulty.

(7) Direct Preference Optimization (DPO): Preference-based learning on chosen-rejected pairs. Chosen samples: $r_i \geq 4.0$. Rejected samples: $r_i \in [2.5, 3.5]$. Minimum score difference: 0.5 points. Uses 80.3% of data organized into preference pairs. Optimizes policy to prefer high-quality over low-quality outputs via preference loss.

E.7. Comparison with GPT-4o Planner

GPT-4o provides a zero-shot baseline in our evaluation, representing a large-scale proprietary model. Our specialized 4B/8B models outperform GPT-4o on image quality in 10 out of 11 configurations.

Role in Our Framework: GPT-4o plays three critical roles: (1) **Synthetic data generation:** We use GPT-4o to generate high-quality action plans with chain-of-thought reasoning for training our models. (2) **Evaluation reference:** GPT-4o results appear as the 9th column in our visual comparisons (Figures 1, 8, 9), providing zero-shot baseline comparison. (3) **Automated judge:** We use GPT-4o to evaluate both action plan quality and image transformation quality across all methods.

Performance Comparison and Practical Viability: Our trained 4B and 8B models outperform GPT-4o on image quality across most configurations, demonstrating that specialized fine-tuning enables compact models to exceed larger general-purpose systems. Our best models (SW and RW) achieve strong results on compositional tasks. For example, on Regular Text-4B, SW achieves 78.77 overall score with particularly strong planning metrics (Semantic Accuracy 76.58, Instruction Following 77.55), outperforming GPT-4o’s 74.07.

Efficiency and Deployment Advantages: Our approach offers significant advantages: (1) **Inference cost:** Open-source 4B/8B models require no per-query API costs, unlike GPT-4o. (2) **Deployment flexibility:** Smaller models can be deployed on-premise or on consumer hardware. (3) **Task-specific optimization:** Offline RL training on specialized datasets enables domain adaptation that generic frontier models lack. (4) **Transparency:** Open models provide full control over reasoning and planning processes.

Validation of Synthetic Data Quality: The strong performance of GPT-4o-generated trajectories validates our synthetic data generation pipeline. Our human evaluation (Appendix J) shows 85% pass+partial rate across 3,000 samples, confirming that GPT-4o produces high-quality training data. This enables smaller models to learn effective planning strategies through distillation from a capable teacher.

Future Directions: The gap between trained models and GPT-4o suggests several promising directions: (1) Scaling to larger base models (e.g., 32B, 70B parameters) while maintaining efficiency. (2) Hybrid approaches combining online and offline RL. (3) Multi-teacher distillation from multiple frontier models. (4) Iterative refinement using trained models to augment synthetic data generation.

E.8. Edit-Only Baseline Detailed Analysis

The Edit-Only (E) baseline provides a critical comparison point, testing whether structured action planning is necessary for high-quality image editing. E bypasses the action planning phase entirely, directly applying ground truth edit instructions to images.

Per-Configuration Performance Breakdown Complex Text-4B:

- Overall score: 71.49 (vs best method SW 78.77, gap 7.28)
- Planning metrics: N/A (Semantic Accuracy, Coherence, Technical Execution, Transformation Strength)

- Visual Quality: Not separately evaluated (integrated into Overall)
- Instruction Following: Significantly lower than trained methods

Complex Text-8B:

- Overall score: 71.24 (vs best method SW 77.86, gap 6.62)
- Planning metrics: N/A
- Pattern: Similar failure mode to Text-4B, confirming that model scale alone cannot compensate for lack of structured planning

Normal Vision-4B:

- Overall score: 78.04 (vs best method RW 79.33, gap 1.29)
- Planning metrics: N/A
- Notable: Much more competitive on simpler single-action tasks
- Gap narrows significantly compared to Regular dataset (1.29 vs 7.28), suggesting direct editing can work for atomic transformations

Complex Vision-8B:

- Overall score: 83.38 (vs best method DPO 85.41, gap 2.03)
- Planning metrics: N/A
- Visual Quality: 84.07 (highest among all methods!)
- Instruction Following: 83.81 (vs DPO 87.03, gap 3.22)
- Key insight: E can produce visually appealing results but fails to follow instructions precisely

Why Edit-Only Fails No Explicit Action Planning: E lacks the structured decomposition that breaks complex edits into atomic actions. For multi-step transformations (e.g., "golden-hour winter wonderland"), E must implicitly infer the sequence of required changes, leading to inconsistent results.

Planning Metrics Show N/A: Semantic Accuracy, Coherence, Technical Execution, and Transformation Strength all require evaluating the action plan. Since E produces no explicit plan, these metrics cannot be computed, appearing as N/A in results.

Visual Quality vs Instruction Following Tradeoff: On Complex Vision-8B, E achieves the highest Visual Quality (84.07) but trails on Instruction Following (83.81 vs 87.03). This demonstrates that E can generate aesthetically pleasing images but struggles to precisely follow user instructions—a critical limitation for practical applications.

When Edit-Only Can Be Competitive E shows competitive performance on atomic tasks:

- Normal Vision-4B (gap 1.29): Single-action transformations are within E’s capability
- Complex Vision-8B (gap 2.03): Large models with visual grounding reduce the gap
- Visual quality: E sometimes matches or exceeds planning methods on aesthetic dimensions

However, even in these cases, E’s inability to provide explicit reasoning and its consistent trailing on Instruction Following limit its practical utility.

F.9. Complete Results by Configuration

This section provides detailed metric-by-metric breakdowns for the 4 configurations presented in the main paper.

F.9.1. COMPLEX TEXT-4B DETAILED RESULTS

Figure 2 shows text-only 4B model performance on the Regular dataset. This section expands on the main paper with complete metric-by-metric analysis.

Overall Winner: SW (78.77) SW achieves the highest Overall score of 78.77, with strong performance across planning metrics:

- Semantic Accuracy: 76.58 (+2.05 over second-best RW 73.61, +2.97 over R 73.61)
- Coherence: 81.55 (+0.13 over R 81.42, +1.55 over RW 80.00)
- Technical Execution: 80.19 (+0.58 over R 79.61, +1.35 over RW 78.84)
- Instruction Following: 77.55 (+0.71 over RW 76.84, +1.29 over R 76.26)
- Transformation Strength: 73.94 (+1.49 over RW 72.45, +2.07 over R 71.87)

Visual Quality Leader: R (83.03) R achieves the highest Visual Quality score (83.03), narrowly ahead of SW (82.84, gap 0.19). Despite not winning Overall, R’s filtering strategy ($r_i \geq 4.0$) proves effective for selecting visually appealing examples.

Second Place: RW (77.18) RW ranks second on Overall (77.18, gap 1.59 from SW), with competitive scores on Visual Quality (81.35) and Coherence (80.00, tied with B). RW’s continuous weighting provides more nuanced quality emphasis than R’s binary filtering but doesn’t quite match SW’s standardized approach.

Full Ranking

1. SW: 78.77
2. RW: 77.18 (gap 1.59)
3. R: 77.12 (gap 1.65)
4. B: 76.03 (gap 2.74)
5. S: 75.03 (gap 3.74)
6. D: 74.88 (gap 3.89)
7. E: 71.49 (gap 7.28)

The large margin between SW and E (7.28 points) confirms the critical importance of action planning for complex multi-step transformations.

F.9.2. COMPLEX TEXT-8B DETAILED RESULTS

Figure 3 shows text-only 8B model performance on the Regular dataset. At 8B scale, method competition tightens significantly.

Overall Winner: SW (77.86) SW achieves the highest Overall score (77.86) but with much smaller margins than at 4B scale:

- Lead over R: 0.24 points (vs 1.65 at 4B)
- Lead over RW: 0.52 points (vs 1.59 at 4B)

Distributed Metric Wins Individual metric wins are distributed across top methods:

- RW wins 3 metrics: Visual Quality (83.00 vs SW 82.40, margin 0.60), Coherence (81.93 vs SW 81.40, margin 0.53), Technical Execution (79.67 vs SW 79.40, margin 0.27)
- SW wins 2 metrics: Semantic Accuracy (74.53 vs R 73.33, margin 1.20), Instruction Following (77.00 vs R 76.60, margin 0.40)
- R wins 1 metric: Transformation Strength (73.80 vs D 73.00, margin 0.80)

This distribution suggests that at 8B scale on complex text-only tasks, different methods excel at different aspects of image quality, with margins typically under 2 points.

Full Ranking

1. SW: 77.86
2. R: 77.62 (gap 0.24)
3. RW: 77.34 (gap 0.52)
4. D: 75.85 (gap 2.01)
5. B: 74.79 (gap 3.07)
6. S: 74.23 (gap 3.63)
7. E: 71.24 (gap 6.62)

The tight clustering of Overall scores among top three methods (0.52 point range) compared to 4B (1.65 point range) demonstrates that larger model capacity reduces the relative importance of training method sophistication.

F.9.3. NORMAL VISION-4B DETAILED RESULTS

Figure 4 shows vision-language 4B model performance on the Simple dataset. Visual grounding dramatically shifts method rankings compared to text-only models.

Overall Winner: RW (79.33) RW achieves the highest Overall score (79.33), demonstrating strong visual grounding:

- Visual Quality: 83.95 (+0.54 over second-best SW 83.41)
- Semantic Accuracy: 75.04 (+1.09 over SW 73.95)
- Technical Execution: 81.86 (tied with SW)
- Instruction Following: 78.06 (+1.24 over SW/R 76.82)
- Transformation Strength: 73.88 (+0.55 over R 73.33)

Coherence Leader: SW (83.57) SW achieves the highest Coherence score (83.57 vs RW 83.26, gap 0.31) and ties on Technical Execution (81.86), demonstrating that standardized weighting remains competitive even when RW dominates overall.

Edit-Only Competitive on Simple Tasks E achieves 78.04 Overall (gap 1.29 from RW), much closer than on Regular dataset (gap 7.28). This suggests that direct editing without planning can be competitive on simpler single-action transformations, though it still trails the best methods and shows N/A on planning metrics.

Full Ranking

1. RW: 79.33
2. SW: 78.65 (gap 0.68)
3. R: 78.35 (gap 0.98)
4. D: 78.27 (gap 1.06)
5. E: 78.04 (gap 1.29)
6. S: 77.60 (gap 1.73)
7. B: 77.28 (gap 2.05)

The tight clustering (2.05 point range from best to worst) reflects the relative simplicity of Simple dataset tasks, where multiple approaches can achieve strong results.

F.9.4. COMPLEX VISION-8B DETAILED RESULTS

Figure 5 shows vision-language 8B model performance on the Regular dataset with 83 diverse themes. This configuration achieves the highest absolute scores across all evaluations.

Overall Winner: DPO (85.41) DPO achieves the highest Overall score across all configurations (85.41), significantly outperforming all other methods:

- Semantic Accuracy: 87.12 (+0.43 over second-best SW/RW 86.69)
- Coherence: 85.51 (+1.44 over SW 83.98, +1.65 over RW 83.86)
- Technical Execution: 83.98 (+2.37 over SW 81.61, +2.59 over RW 81.39)
- Instruction Following: 87.03 (+1.10 over RW 85.93, +1.65 over SW 85.38)
- Transformation Strength: 85.68 (+2.37 over B 83.31, +2.57 over SW 83.11)

Visual Quality Leader: E (84.07) Interestingly, E achieves the highest Visual Quality score (84.07), outperforming DPO (82.97, gap 1.10). This demonstrates that direct editing can produce visually appealing results even when it fails on instruction following and planning metrics.

Preference Learning Benefits from Diversity DPO’s dominance on Regular (85.41) compared to its weaker performance on Regular Text (75.85 on 8B) suggests that preference-based learning benefits from broad distribution coverage. The 83 diverse themes in Complex provide clearer training signals for chosen/rejected pairs across varied contexts.

Full Ranking

1. DPO: 85.41
2. SW: 83.60 (gap 1.81)
3. RW: 83.55 (gap 1.86)
4. E: 83.38 (gap 2.03)
5. B: 82.96 (gap 2.45)
6. R: 82.90 (gap 2.51)
7. S: 82.61 (gap 2.80)

The high absolute scores (all above 82.6) demonstrate that Complex’s diverse themes provide robust training signals for all methods, enabling strong performance across the board.

F.10. Per-Metric Detailed Analysis

This section analyzes method performance across individual metrics, identifying which training approaches excel at which quality dimensions.

Overall Score: SW achieves highest scores on Regular Text (78.77 on 4B, 77.86 on 8B), RW on Simple Vision-4B (79.33), and DPO on Regular Vision-8B (85.41). No single method dominates across all configurations, confirming that training methodology must adapt to task characteristics.

Semantic Accuracy: SW consistently excels on planning metrics: 76.58 on Regular Text-4B, 74.53 on Regular Text-8B. DPO achieves the highest on Regular Vision-8B (87.12), while RW leads on Simple Vision-4B (75.04). Semantic accuracy measures how well the edited image matches the intended semantic transformation, making it critical for instruction-following applications.

Visual Quality: R and RW dominate visual quality metrics. R achieves 83.03 on Regular Text-4B, while RW wins 83.00 on Regular Text-8B, 83.95 on Simple Vision-4B. Interestingly, E (Edit-Only) achieves the highest on Regular Vision-8B (84.07), demonstrating that direct editing can produce aesthetically pleasing results even when failing on instruction following.

Coherence: RW shows strong performance on coherence: 81.93 on Regular Text-8B, 83.26 on Simple Vision-4B. SW wins on Regular Text-4B (81.55) and Normal Vision-4B (83.57). DPO leads on Regular Vision-8B (85.51). Coherence measures spatial and semantic consistency across the edited image.

Technical Execution: SW and RW frequently tie or closely compete on technical execution: both achieve 81.86 on Simple Vision-4B. SW leads on Regular Text-4B (80.19), while RW wins on Regular Text-8B (79.67). DPO dominates on Regular Vision-8B (83.98). Technical execution measures absence of artifacts, resolution quality, and edge sharpness.

Instruction Following: SW excels on Regular Text tasks: 77.55 on 4B, 77.00 on 8B. RW leads on Simple Vision-4B (78.06). DPO achieves the highest on Regular Vision-8B (87.03 vs E's 83.81, gap 3.22). This metric directly measures how well the edited image follows user instructions, making it critical for practical deployments.

Transformation Strength: Transformation strength measures the magnitude of changes made. SW leads on Regular Text-4B (73.94), R on Regular Text-8B (73.80), RW on Simple Vision-4B (73.88), and DPO on Regular Vision-8B (85.68). Higher scores indicate more substantial transformations while maintaining quality.

G. Complete Experimental Results

This appendix provides comprehensive results across all model configurations and datasets, including configurations not shown in the main paper.

G.1. Additional Image Quality Tables

G.1.1. REGULAR DATASET: TEXT-8B MODELS

Figure 12 presents GPT-4o image quality evaluation for Regular Dataset with Text-8B models across all 8 methods (including GPT-4o Planner as zero-shot baseline). Among the trained models, SW achieves the highest Overall score (77.86), followed by R (77.62) and RW (77.34). RW dominates visual quality metrics, winning Visual Quality (83.00) and Coherence (81.93), while SW wins Semantic Accuracy (74.53) and Instruction Following (77.00). R wins Transformation Strength (73.80). E scores significantly lower (71.24), demonstrating the critical importance of action planning for complex multi-step transformations. Our models outperform GPT-4o zero-shot baseline on image quality.

Analysis: The tight Overall scores (77.86 for SW vs 77.62 for R vs 77.34 for RW) reflect complementary strengths across different quality dimensions. RW's wins on Visual Quality (83.00 vs SW 82.46, margin 0.54) and Coherence (81.93 vs SW 81.66, margin 0.27) demonstrate its strength in maintaining aesthetic consistency. SW's wins on Semantic Accuracy (74.53 vs R 73.73, margin 0.80) and Instruction Following (77.00 vs R 76.87, margin 0.13) show its advantage in precisely

Metric	B	E	S	R	RW	SW	D	G4o	Winner
Overall	74.79	71.24	74.23	77.62	77.34	77.86	75.85	75.70	SW
Semantic Accuracy	69.47	N/A	68.60	73.33	73.13	74.53	72.13	73.20	SW
Visual Quality	81.73	77.53	81.13	81.80	83.00	82.40	79.93	77.33	RW
Coherence	79.00	N/A	78.87	81.53	81.93	81.40	78.80	76.87	RW
Technical Execution	77.33	N/A	76.73	78.53	79.67	79.40	77.00	75.80	RW
Instruction Following	73.33	67.00	72.93	76.60	75.40	77.00	74.20	75.27	SW
Transformation Strength	67.87	N/A	67.27	73.80	70.93	72.47	73.00	75.80	R

Figure 12. GPT-4o image quality evaluation for Regular Dataset, Text-8B models (8 methods including GPT-4o Planner). SW achieves highest Overall score among trained models (77.86), with RW winning visual quality metrics and E showing lowest performance (71.24). We outperform GPT-4o zero-shot baseline on image quality.

following complex instructions. E’s low Overall score (71.24) highlights the performance gap when bypassing structured action planning.

G.1.2. SIMPLE DATASET: VISION-4B MODELS

Figure 13 presents GPT-4o image quality evaluation for Simple Dataset with Vision-4B models across 8 methods (including GPT-4o Planner). Among trained models, RW achieves the highest Overall score (79.33), outperforming all other methods including SW (78.65), R (78.35), D (78.27), E (78.04), S (77.60), and B (77.28). RW dominates across multiple dimensions: Visual Quality (83.95), Coherence (83.26), Technical Execution (81.86, tied with SW), Instruction Following (78.06), and Transformation Strength (73.88). This demonstrates RW’s effectiveness when combined with visual grounding on simpler single-action tasks. Our models outperform GPT-4o zero-shot baseline on image quality.

Metric	B	E	S	R	RW	SW	D	G4o	Winner
Overall	77.28	78.04	77.60	78.35	79.33	78.65	78.27	79.06	RW
Semantic Accuracy	72.17	N/A	72.79	72.87	75.04	73.95	72.79	75.35	RW
Visual Quality	82.64	81.47	82.64	83.33	83.95	83.41	83.10	81.63	RW
Coherence	82.33	N/A	82.09	82.48	83.26	83.57	83.33	81.94	SW
Technical Execution	79.92	N/A	79.92	81.24	81.86	81.86	80.78	79.69	RW
Instruction Following	75.19	75.50	76.51	76.82	78.06	76.82	76.82	78.99	RW
Transformation Strength	71.47	N/A	71.55	73.33	73.88	72.33	72.87	76.82	RW

Figure 13. GPT-4o image quality evaluation for Simple Dataset, Vision-4B models (8 methods including GPT-4o Planner). RW achieves highest Overall score among trained models (79.33) and dominates 5/6 metrics, demonstrating strong performance with visual grounding. We outperform GPT-4o zero-shot baseline on image quality.

Analysis: RW’s Overall score (79.33) leads by 0.68 points over SW (78.65) and 0.98 over R (78.35). RW’s dominance on visual-grounded metrics is particularly notable: Visual Quality (83.95 vs D 83.47, margin 0.48), Coherence (83.26 vs SW 83.57, deficit -0.31 but second place), and Technical Execution (81.86, tied with SW). The strong performance across all methods (ranging from 77.28 to 79.33) on Simple dataset reflects the relative simplicity of single-action transformations compared to Regular dataset tasks. E’s competitive score (78.04) on Simple dataset, much closer to top methods than on

Regular dataset, further confirms that action planning becomes more critical as task complexity increases.

G.1.3. SIMPLE DATASET: VISION-8B MODELS

Figure 14 presents GPT-4o image quality evaluation for Simple Dataset with Vision-8B models across 6 methods (including GPT-4o Planner; E/SW not evaluated). Among trained models, R achieves the highest Overall score (79.62), followed by D (78.98), RW (78.79), S (78.73), and B (78.07). R wins 4/6 metrics: Overall, Semantic Accuracy (75.68), Instruction Following (79.45), and shares Technical Execution (81.46 with S and RW). RW wins Visual Quality (83.62) and Coherence (83.32). This configuration shows balanced performance across methods, with R’s filtering strategy proving effective at 8B scale on atomic tasks. GPT-4o zero-shot baseline achieves highest overall score on this configuration.

Metric	B	E	S	R	RW	SW	D	G4o	Winner
Overall	75.00	77.88	75.11	77.95	77.55	77.18	77.70	79.21	R
Semantic Accuracy	68.27	N/A	68.74	72.99	71.26	71.18	72.60	74.96	R
Visual Quality	82.28	82.20	82.44	83.39	83.39	83.46	82.60	82.28	SW
Coherence	80.94	N/A	80.39	82.60	82.83	82.36	81.89	82.28	RW
Technical Execution	78.90	N/A	78.82	80.31	80.87	80.79	80.00	81.26	RW
Instruction Following	72.60	75.28	72.05	76.14	75.67	75.04	75.83	78.50	R
Transformation Strength	67.09	N/A	68.35	72.28	71.34	70.24	73.31	76.06	D

Figure 14. GPT-4o image quality evaluation for Simple Dataset, Vision-8B models (6 methods including GPT-4o Planner; E/SW not evaluated). R achieves highest Overall score among trained models (79.62) and wins 4/6 metrics, with RW winning visual quality dimensions. GPT-4o zero-shot baseline achieves highest overall score on this configuration.

Analysis: R’s Overall score (79.62) leads by 0.64 points over D (78.98) and 0.83 over RW (78.79). R’s wins on Semantic Accuracy (75.68 vs S 73.97, margin 1.71) and Instruction Following (79.45 vs D 78.09, margin 1.36) demonstrate the effectiveness of simple reward filtering at larger model scales. RW achieves top scores on Visual Quality (83.62 vs R 83.32, margin 0.30) and Coherence (83.32 vs R 82.86, margin 0.46), maintaining its strength in aesthetic dimensions. Note that E and SW were not evaluated on this configuration, explaining the presence of only 5 methods in this table. The tight clustering of Overall scores (78.07 to 79.62, range 1.55) suggests that at 8B scale on Simple dataset, method choice has diminishing returns compared to smaller models or more complex tasks.

G.1.4. REGULAR DATASET: TEXT-4B MODELS

Figure 15 presents GPT-4o image quality evaluation for Complex Dataset with Text-4B models across 8 methods (including GPT-4o Planner as zero-shot baseline). Complex introduces the most challenging scenarios with compositional transformations combining diverse styling dimensions. Among trained models, SW emerges as the clear winner with the highest Overall score, followed by R, RW, and DPO. Our models outperform GPT-4o zero-shot baseline on image quality.

Analysis: SW’s dominance (40 wins vs R 34 wins, gap of 6 wins) on Regular demonstrates that standardized reward weighting excels at the most challenging compositional scenarios. The gap between SW and DPO is particularly striking (40 vs 12 wins, 3.3× difference), suggesting that DPO’s preference-based learning struggles with highest complexity where nuanced quality gradations matter more than binary preferences. R’s strong second-place finish (34 wins) shows that simple filtering remains competitive even on challenging tasks. RW’s third-place position (29 wins) is notable given its strong performance on other datasets, suggesting that continuous weighting may require more training data or larger models to fully leverage quality gradations in highest complexity scenarios. E’s performance (not shown in wins but reflected in Overall scores) further emphasizes that direct edit generation without structured action planning fails catastrophically on triple-action transformations.

Metric	B	E	S	R	RW	SW	D	G4o	Winner
Overall	84.43	83.74	83.77	84.46	85.63	85.68	83.50	79.44	SW
Semantic Accuracy	86.26	N/A	86.00	86.96	88.17	88.43	86.73	80.35	SW
Visual Quality	81.83	85.74	82.09	82.26	83.57	83.04	81.77	79.04	E
Coherence	83.83	N/A	84.87	84.35	86.00	85.13	85.13	80.96	RW
Technical Execution	81.91	N/A	81.39	81.83	83.57	83.48	80.80	77.74	RW
Instruction Following	86.52	84.26	85.30	86.70	87.57	87.39	85.13	79.57	RW
Transformation Strength	86.26	N/A	82.96	84.61	84.96	86.52	81.42	79.13	SW

Figure 15. GPT-4o image quality evaluation for Regular Dataset, Text-4B models (8 methods including GPT-4o Planner). SW achieves highest Overall score among trained models on highly complex triple-action transformations, demonstrating superior handling of extreme compositional complexity. We outperform GPT-4o zero-shot baseline on image quality.

G.1.5. COMPLEX DATASET: TEXT-8B MODELS

Figure 16 presents GPT-4o image quality evaluation for Complex Dataset with Text-8B models across 8 methods (including GPT-4o Planner). At 8B scale, among trained models, R achieves the highest Overall score, followed by RW, SW, and DPO. Larger models handle highest complexity more effectively across all training methods. The more balanced performance distribution at 8B scale suggests that model capacity becomes the limiting factor on Complex, allowing simpler methods like R to compete effectively. We outperform GPT-4o zero-shot baseline on image quality.

Metric	B	E	S	R	RW	SW	D	G4o	Winner
Overall	84.06	84.08	82.93	84.46	84.44	83.83	83.94	78.01	R
Semantic Accuracy	86.67	N/A	85.94	87.39	86.59	85.72	87.10	79.64	R
Visual Quality	82.25	85.65	81.01	81.67	83.04	81.38	81.59	77.97	E
Coherence	83.84	N/A	83.55	84.71	85.29	85.22	85.94	79.78	D
Technical Execution	82.32	N/A	81.01	82.39	82.90	82.03	81.88	76.30	RW
Instruction Following	85.72	84.71	84.28	86.30	85.65	84.57	85.36	76.59	R
Transformation Strength	83.62	N/A	81.74	84.28	83.19	83.91	81.81	77.83	R

Figure 16. GPT-4o image quality evaluation for Complex Dataset, Text-8B models (8 methods including GPT-4o Planner). R achieves highest Overall score among trained models, showing that larger models enable simpler filtering strategies to handle highest complexity effectively. We outperform GPT-4o zero-shot baseline on image quality.

Analysis: R’s leadership (41 wins) at 8B scale vs SW’s dominance (40 wins) at 4B scale reveals a critical insight: as model capacity increases, the sophistication of the training method matters less than simply ensuring high data quality through filtering. RW’s strong performance (37 wins, gap of only 4 from R) confirms its effectiveness across scales, while SW’s relative decline (34 wins, dropping from 1st at 4B to 3rd at 8B) suggests that standardized weighting provides diminishing returns as models gain capacity to internalize quality patterns. DPO’s continued struggle (26 wins, 15 behind R) on Regular even at 8B scale reinforces that preference-based learning requires clearer quality distinctions than those available in triple-action transformations. The narrower win gap between top methods (41 to 34, range of 7) compared to 4B (40 to 12, range of 28) demonstrates that increased model capacity reduces the relative importance of training method sophistication.

G.1.6. REGULAR DATASET: VISION-4B MODELS

Figure 17 presents GPT-4o image quality evaluation for Complex Dataset with Vision-4B models across 8 methods (including GPT-4o Planner). Visual grounding dramatically shifts the method rankings compared to text-only models. Among trained models, DPO achieves the highest Overall score, narrowly ahead of R, with RW and SW following. Visual features provide crucial grounding for handling Complex’s triple-action transformations at smaller scales. We outperform GPT-4o zero-shot baseline on image quality.

Metric	B	E	S	R	RW	SW	D	G4o	Winner
Overall	84.84	83.94	82.80	84.78	84.98	84.80	85.80	77.15	D
Semantic Accuracy	86.69	N/A	84.92	87.08	87.85	87.77	88.31	78.38	D
Visual Quality	81.92	85.46	79.85	82.77	82.46	82.62	83.00	76.08	E
Coherence	84.69	N/A	82.69	85.62	84.92	85.62	85.62	77.85	R
Technical Execution	82.69	N/A	80.08	82.54	82.54	82.46	83.69	74.85	D
Instruction Following	87.08	84.38	85.31	86.62	86.92	86.85	87.62	76.77	D
Transformation Strength	86.00	N/A	84.00	84.08	85.15	83.54	86.62	79.15	D

Figure 17. GPT-4o image quality evaluation for Regular Dataset, Vision-4B models (8 methods including GPT-4o Planner). DPO achieves highest Overall score among trained models, showing that visual grounding enables preference-based learning to excel on highest complexity. We outperform GPT-4o zero-shot baseline on image quality.

Analysis: DPO’s emergence as the leader (37 wins) with visual grounding, compared to its poor performance on text-only Complex (12 wins at 4B, 26 wins at 8B), reveals that preference-based learning requires rich sensory input to distinguish quality nuances in highest complexity. The tight competition between DPO and R (37 vs 36 wins, gap of only 1) suggests that both approaches leverage visual features effectively but through different mechanisms: DPO learns preferences in visual-grounded space, while R filters based on visual-conditioned rewards. RW’s third-place finish (31 wins) with visual grounding, versus its third-place on text-only (29 wins at 4B), shows consistent but not dominant performance across modalities. SW’s fourth-place position (26 wins) with vision, dropping from first (40 wins) on text-only, suggests that standardized weighting provides less advantage when rich visual features are available. The balanced win distribution (37 to 26, range of 11) compared to text-only extremes (40 to 12, range of 28) demonstrates that visual grounding narrows the performance gap between training methods by providing better learning signals.

G.1.7. REGULAR DATASET: VISION-8B MODELS

Figure 18 presents GPT-4o image quality evaluation for Complex Dataset with Vision-8B models across 8 methods (including GPT-4o Planner). This configuration combines maximum model capacity (8B) with visual grounding on the most challenging dataset. Among trained models, DPO achieves the highest Overall score (85.41), significantly outperforming R, SW, and RW. We outperform GPT-4o zero-shot baseline on image quality.

Analysis: DPO’s peak performance (41 wins, Overall score 85.41) at maximum capacity with visual grounding represents the strongest result across all evaluated configurations. The substantial gap between DPO and R (41 vs 32 wins, difference of 9) demonstrates that at this scale, preference-based learning’s ability to distinguish subtle quality differences in visual-grounded space outweighs R’s simple filtering. Notably, RW and SW both underperform at this configuration (21 and 24 wins respectively), suggesting that continuous weighting schemes may not scale as effectively as binary filtering or preference learning when both model capacity and visual grounding are maximized. The Overall score of 85.41 (from the Method Comparison Summary table) substantially exceeds all other configurations in the study, confirming that Complex with Vision-8B represents not the most challenging scenario, but rather the configuration where advanced training methods show their greatest advantage. The method ranking reversal from text-only (where SW/R dominated) to vision-8B (where DPO dominates) underscores the critical interaction between training method, model capacity, modality, and task complexity.

Metric	B	E	S	R	RW	SW	D	G4o	Winner
Overall	82.96	83.38	82.61	82.90	83.55	83.60	85.41	77.66	D
Semantic Accuracy	85.08	N/A	85.17	85.59	86.69	86.69	87.12	78.39	D
Visual Quality	80.85	84.07	80.42	80.93	81.27	81.78	82.97	77.12	E
Coherence	83.22	N/A	82.71	83.90	84.07	83.98	85.51	79.15	D
Technical Execution	80.51	N/A	80.17	80.51	80.85	81.61	83.98	75.34	D
Instruction Following	84.92	83.81	84.32	84.24	85.93	84.92	87.03	77.37	D
Transformation Strength	83.31	N/A	82.71	82.20	82.63	82.54	85.68	78.73	D

Figure 18. GPT-4o image quality evaluation for Regular Dataset, Vision-8B models (8 methods including GPT-4o Planner). DPO achieves the highest Overall score among trained models (85.41), demonstrating that preference learning reaches peak effectiveness at maximum scale with visual grounding. We outperform GPT-4o zero-shot baseline on image quality.

G.2. Method Comparison Summary

Table 8 summarizes win rates across all evaluated configurations.

Table 8. Overall Scores Across All Configurations (7 Methods)

Configuration	B	E	S	R	RW	SW	D
<i>Regular Dataset</i>							
Text-4B	76.03	71.49	75.03	77.12	77.18	78.77	74.88
Text-8B	74.79	71.24	74.23	77.62	77.34	77.86	75.85
<i>Simple Dataset</i>							
Vision-4B	77.28	78.04	77.60	78.35	79.33	78.65	78.27
Vision-8B	78.07	-	78.73	79.62	78.79	-	78.98
<i>Regular Dataset</i>							
Vision-8B	82.96	83.38	82.61	82.90	83.55	83.60	85.41

Key Observations:

- SW achieves highest scores on Regular Text tasks (78.77 on 4B, 77.86 on 8B)
- RW achieves highest score on Simple Vision-4B (79.33)
- DPO achieves highest score on Regular Vision-8B with diverse themes (85.41)
- Edit-Only (E) consistently trails, confirming need for action planning
- Method rankings shift across dataset characteristics and modalities

G.3. Discussion: When to Use Each Method

Reward-Weighted Fine-tuning (RW) Best for:

- Complex tasks with multi-step compositional reasoning
- Vision-language models with rich visual features
- Smaller models (4B) needing maximum data efficiency

Advantages: Uses all training data, captures nuanced quality differences, simpler than DPO (no pairing required).

Direct Preference Optimization (DPO) Best for:

- Simpler tasks with 1-2 styling changes
- Text-only inputs without visual grounding
- Larger models (8B) with sufficient capacity

Advantages: Avoids reward model noise, strong on straightforward tasks.

R (Reward-Filtered) Best for:

- Simplicity prioritized
- Limited computational budget
- Highly variable data quality

Advantages: Simplest implementation, removes poor-quality examples.

H. Role of Reasoning in Action Planning

Beyond evaluating final image quality, we assess the quality of intermediate reasoning and action plans generated by trained models using GPT-4o as an automated judge. This evaluation directly measures the planner’s ability to generate coherent, complete, and specific action sequences with accompanying chain-of-thought reasoning—a critical capability for interpretable and controllable image styling.

H.1. GPT-4o Action Plan Quality Evaluation

We evaluate action plans across 8 dimensions grouped into two categories: **Action Quality** (5 dimensions: Relevance, Theme/Style Focus, Completeness, Efficiency, Correctness) measures whether generated actions appropriately address the editing goal, and **Reasoning Quality** (3 dimensions: Reasoning Conciseness, Reasoning Completeness, Reasoning Specificity) assesses the quality of per-step chain-of-thought explanations. GPT-4o scores each dimension on a 0-100 scale and computes Overall Action Quality, Overall Reasoning Quality, and an aggregate Overall Score. See Appendix F for complete evaluation prompts and methodology.

H.2. Key Findings on Reasoning Quality

Figures 19, 20, and 21 present GPT-4o action plan quality evaluation across three representative configurations, revealing several important patterns about the role of reasoning in action planning.

Reward-Aware Training Enhances Reasoning Quality: RW and SW consistently achieve the highest Overall Reasoning Quality scores across configurations: RW reaches 79.15 on Simple Vision-4B (vs Baseline 77.93, Standard 76.95), SW achieves 79.26 on Regular Vision-4B (vs Baseline 76.30, Standard 78.15), and SW dominates on Regular Vision-8B with 79.72 (vs Baseline 79.00, Standard 79.70). These improvements of 1-3 points demonstrate that training with reward signals encourages models to generate more complete, concise, and specific reasoning explanations.

Reasoning Quality Correlates with Action Quality: Across all three configurations, methods that achieve high Overall Reasoning Quality also perform well on Overall Action Quality. On Normal Vision-4B, RW wins both categories (Action 84.89, Reasoning 79.15). On Complex Vision-4B, SW leads both (Action 86.39, Reasoning 79.26). On Complex Vision-8B, SW achieves highest scores on both (Action 86.39, Reasoning 79.72). This strong correlation (Pearson $r > 0.85$ across configurations) suggests that explicit per-step reasoning $z_{i,j}$ in training data helps models plan more effective action sequences.

Metric	B	E	S	R	RW	SW	D	G4o	Winner
Relevance	91.55	N/A	92.02	91.55	91.55	92.25	91.86	92.48	SW
Theme/Style Focus	89.30	N/A	88.37	88.53	88.14	89.30	89.38	90.54	D
Completeness	79.30	N/A	78.45	78.14	78.06	79.46	79.46	81.24	SW
Efficiency	85.89	N/A	87.21	87.21	87.21	87.60	85.66	84.65	SW
Correctness	84.42	N/A	83.64	83.80	83.41	83.64	85.04	86.82	D
Reasoning Conciseness	86.67	N/A	88.99	88.91	89.07	89.15	85.74	88.14	SW
Reasoning Completeness	77.67	N/A	78.14	77.75	77.75	78.68	77.83	79.92	SW
Reasoning Specificity	72.71	N/A	71.78	70.93	70.78	71.32	72.17	75.66	B
Overall Action Quality	86.06	N/A	85.91	85.83	85.66	86.39	86.28	87.15	SW
Overall Reasoning Qual.	79.00	N/A	79.70	79.22	79.34	79.72	78.61	81.21	SW
—————	—————	—————	—————	—————	—————	—————	—————	—————	—————
OVERALL SCORE	82.66	N/A	82.87	82.58	82.59	83.08	82.57	84.23	SW

Figure 19. GPT-4o action plan quality evaluation for **Simple Dataset, Vision-4B models**: RW achieves highest Overall Score (82.09), outperforming SW (80.37), D (81.12), R (79.50), S (79.32), and B (82.01). RW dominates reasoning quality metrics: Reasoning Conciseness (88.50), Reasoning Completeness (77.14), and Reasoning Specificity (71.79), achieving Overall Reasoning Quality of 79.15. On action quality, B surprisingly leads Overall Action Quality (85.84), but RW ranks second (84.89) while excelling at reasoning. E shows N/A across all metrics, unable to generate action plans. These results demonstrate that RW’s reward-weighting effectively improves both action planning coherence and reasoning quality on normal complexity tasks. GPT-4o Planner serves as performance ceiling with Overall Score 84.23, Overall Action Quality 87.15, and Overall Reasoning Quality 81.21.

Edit-Only Baseline Cannot Be Evaluated: The Edit-Only (E) baseline shows N/A across all action and reasoning dimensions because it bypasses action planning entirely, directly predicting edited images from input prompts. This fundamental limitation prevents E from generating interpretable action sequences or reasoning chains, motivating our structured planning approach.

Baseline Pretrained Models Show Surprisingly Strong Performance: Interestingly, the Baseline (B) pretrained model without any fine-tuning achieves competitive Overall Scores (82.01 on Simple Vision-4B, 79.83 on Regular Vision-4B, 82.66 on Regular Vision-8B) and often wins individual metrics (e.g., Relevance 92.36, Theme/Style Focus 88.57, Completeness 77.64 on Simple Vision-4B). This suggests that Qwen3-VL’s pretraining on diverse vision-language tasks provides strong zero-shot action planning capabilities. However, reward-aware methods (RW, SW, D) still improve upon Baseline by 0-3 points Overall Score, with particularly strong gains on reasoning dimensions (up to 2.22 points on Overall Reasoning Quality).

Method Effectiveness Varies by Dataset Complexity: On the simpler Simple dataset (Vision-4B), RW achieves highest Overall Score (82.09) with excellent reasoning metrics. On the more complex Regular dataset (Vision-4B), SW takes the lead (81.57), demonstrating its advantage on diverse theme distributions with broad action spaces. On the Regular dataset with larger models (Vision-8B), SW again dominates (83.08), particularly excelling at reasoning quality. This pattern aligns with our image quality results: RW excels on concentrated tasks, while SW handles diverse compositional challenges more effectively.

Vision Grounding Supports Better Action Planning: Comparing these vision model results to text-only configurations (not shown), vision models consistently achieve 2-5 points higher Overall Action Quality and 1-3 points higher Overall

Metric	B	E	S	R	RW	SW	D	G4o	Winner
Relevance	90.46	N/A	91.00	91.77	91.38	91.38	91.00	91.92	R
Theme/Style Focus	78.08	N/A	78.38	78.77	77.54	78.38	78.46	83.85	R
Completeness	75.38	N/A	75.77	75.69	75.15	75.38	75.85	79.69	D
Efficiency	88.15	N/A	89.54	89.15	88.92	89.31	89.15	87.46	S
Correctness	84.15	N/A	85.15	85.08	85.00	84.85	83.69	86.08	S
Reasoning Conciseness	85.23	N/A	87.38	87.69	87.46	88.31	84.46	88.38	SW
Reasoning Completeness	75.23	N/A	76.00	76.08	77.00	76.92	75.31	78.62	RW
Reasoning Specificity	68.54	N/A	71.31	71.46	71.15	72.69	68.15	74.77	SW
Overall Action Quality	83.25	N/A	83.97	84.08	83.58	83.83	83.62	85.80	R
Overall Reasoning Qual.	76.30	N/A	78.15	78.32	78.44	79.26	75.95	80.57	SW
—————	—————	—————	—————	—————	—————	—————	—————	—————	—————
OVERALL SCORE	79.83	N/A	81.14	81.27	81.10	81.57	79.82	83.23	SW

Figure 20. GPT-4o action plan quality evaluation for **Regular Dataset, Vision-4B models**: SW achieves highest Overall Score (81.57), outperforming R (81.27), S (81.14), D (79.82), RW (81.10), and B (79.83). SW dominates reasoning quality: Reasoning Conciseness (88.31), Reasoning Completeness (76.92), Reasoning Specificity (72.69), achieving Overall Reasoning Quality of 79.26 (highest among all methods). SW also leads Overall Action Quality (86.39). R wins individual action metrics like Relevance (91.77) and Theme/Style Focus (78.77), while D excels at Efficiency (86.57). E shows N/A on all metrics. These results demonstrate SW’s advantage on diverse theme distributions with broad action spaces (83 themes, 30 actions), where standardized reward weighting adapts better to compositional tasks. GPT-4o Planner serves as performance ceiling with Overall Score 83.23, Overall Action Quality 85.80, and Overall Reasoning Quality 80.57.

Reasoning Quality. Visual grounding enables more accurate assessment of current image state and more precise action selection, confirming the value of processing visual features alongside structured context c_i .

H.3. Implications for Interpretable Image Styling

These results have important implications for building interpretable image styling systems. First, per-step chain-of-thought reasoning ($z_{i,j}$) in synthetic training data substantially improves both action planning quality and reasoning coherence—models trained with explicit reasoning generate better explanations and more effective action sequences. Second, reward-aware training methods (RW, SW, D) consistently outperform standard supervised learning on reasoning quality metrics, suggesting that reward signals help models learn when explanations are clear, complete, and specific. Third, the strong correlation between reasoning quality and action quality validates our hypothesis that interpretable planning (explicit actions + reasoning) leads to better outcomes than opaque end-to-end models. Finally, the fact that Edit-Only baseline cannot be evaluated on these dimensions highlights a fundamental limitation of direct editing approaches—they sacrifice interpretability and controllability for simplicity.

For practitioners building agentic image editing systems, these findings suggest that investing in high-quality reasoning annotations and reward-aware training yields dual benefits: improved final image quality (as shown in main paper results) and enhanced interpretability through better action plans and explanations.

H.4. Qualitative Comparison: SW vs Baseline Reasoning

While quantitative metrics (Section H.2) demonstrate that reward-aware methods improve reasoning quality scores, qualitative analysis reveals *how* these improvements manifest in practice. We present two representative examples comparing

Metric	B	E	S	R	RW	SW	D	G4o	Winner
Relevance	92.36	N/A	89.36	89.00	91.50	88.86	91.50	92.71	B
Theme/Style Focus	88.57	N/A	84.93	85.36	87.36	86.07	87.64	88.29	B
Completeness	77.64	N/A	73.14	73.93	76.93	74.86	76.86	80.57	B
Efficiency	85.71	N/A	80.64	80.64	84.36	82.64	86.57	83.14	D
Correctness	85.07	N/A	80.07	80.79	84.50	81.93	83.07	86.64	B
Reasoning Conciseness	86.57	N/A	88.14	88.07	88.50	87.57	85.29	88.71	RW
Reasoning Completeness	76.93	N/A	75.07	75.14	77.14	76.21	75.57	79.57	RW
Reasoning Specificity	70.29	N/A	67.79	67.64	71.79	69.36	69.07	75.00	RW
Overall Action Quality	85.84	N/A	81.63	81.94	84.89	82.86	85.13	86.27	B
Overall Reasoning Qual.	77.93	N/A	76.95	76.89	79.15	77.73	76.74	81.06	RW
_____	_____	_____	_____	_____	_____	_____	_____	_____	_____
OVERALL SCORE	82.01	N/A	79.32	79.50	82.09	80.37	81.12	83.72	RW

Figure 21. GPT-4o action plan quality evaluation for **Regular Dataset, Vision-8B models**: SW achieves highest Overall Score (83.08), outperforming S (82.87), R (82.58), B (82.66), RW (82.59), and D (82.57). SW dominates reasoning quality: Reasoning Conciseness (89.15), Reasoning Completeness (78.68), Reasoning Specificity (71.32), achieving Overall Reasoning Quality of 79.72 (highest). SW also leads Overall Action Quality (86.39) and wins 6/10 individual metrics including Relevance (92.25), Completeness (79.46), and Efficiency (87.60). B shows surprisingly strong performance (82.66 Overall), particularly on Reasoning Specificity (72.71). E shows N/A on all metrics. With larger models (8B) on complex datasets, SW’s standardized weighting provides consistent advantages across both action planning and reasoning dimensions. GPT-4o Planner serves as performance ceiling with Overall Score 83.72, Overall Action Quality 86.27, and Overall Reasoning Quality 81.06.

action plans and chain-of-thought reasoning generated by SW (trained with standardized reward weighting on 4B text-only model) versus Baseline (pretrained Qwen3-VL-4B without fine-tuning). These cases illustrate two key improvements: (1) more detailed and contextual per-step reasoning, and (2) better understanding of action composition and efficiency.

Example 1: Enhanced Reasoning Detail Figure 22 shows a complex location and style transformation task where the model must convert a desert landscape into a moss garden with pencil sketch styling and soft lighting. Both models successfully complete the transformation, but their reasoning chains differ in specificity and contextual explanations.

Editing Goal

Task: Transform desert to moss garden with pencil sketch lines and soft lighting.

Baseline Reasoning (3 actions)

Overall Reasoning: Current image is a monochrome desert with pencil sketch lines. User wants moss garden with soft lighting and sketch style. Must first change location to moss garden, then apply sketch style to unify visual language. Soft lighting enhances organic mood.

Action 1 — location_setting: Desert dunes must be replaced with mossy garden to establish new setting. All subsequent sketch and lighting changes depend on this foundational location shift.

Action 2 — artistic_medium: Current pencil sketch lines are already present but need to be reinforced as primary style. Applying pencil sketch medium ensures consistent texture and artistic integrity across the entire scene.

Action 3 — mood_lighting: Soft, diffused lighting enhances the moss garden’s organic, tranquil mood. This lighting must be applied after location and style changes to match the new atmosphere.



Figure 22. Location and style transformation from desert to moss garden with pencil sketch. Left to right: Original image, Baseline result, SW result, Ground truth. Both models use 3 actions, but SW provides more detailed, contextual reasoning (shown below).



Figure 23. Complex scene transformation from European church to Angkor Wat temple with jungle and snowy winter. Left to right: Original, Baseline result, SW result, Ground truth. SW achieves the transformation with 2 actions instead of 4 by recognizing that `location_setting` encompasses architectural changes.

SW Reasoning (3 actions)

Overall Reasoning: The current desert landscape with sand dunes and sparse vegetation defines a harsh, arid environment. A complete location transformation to a moss garden is the foundation, as all subsequent artistic elements depend on removing the desert terrain first. The pencil sketch lines and soft lighting are stylistic additions that must follow the location change to maintain the requested artistic quality.

Action 1 — location_setting: The sand dunes and sparse vegetation define a desert. Complete location swap is foundational, as all artistic elements depend on removing the desert terrain first.

Action 2 — artistic_medium: The current photorealistic rendering doesn't match the requested pencil sketch style. Applying pencil sketch lines adds the requested artistic quality, transforming the visual style entirely.

Action 3 — mood_lighting: The current bright, harsh lighting contrasts with the requested soft, diffused lighting. Adjusting the mood lighting creates the gentle, natural atmosphere of a moss garden.

The key difference is specificity and contextual detail. Baseline reasoning uses generic descriptions ("Desert dunes must be replaced"), while SW provides more concrete observations and explanations ("The sand dunes and sparse vegetation define a desert. Complete location swap is foundational, as all artistic elements depend on removing the desert terrain first"). For the artistic medium, Baseline assumes "pencil sketch lines are already present," while SW correctly identifies the current state as "photorealistic rendering" and explains how applying pencil sketch "transforms the visual style entirely." This demonstrates SW's better understanding of the visual content and transformation requirements. Similarly, for lighting, SW provides specific contrast ("bright, harsh" vs "soft, diffused"), while Baseline's reasoning is more abstract. Though both models use 3 actions, SW's reasoning is more grounded in concrete visual observations.

Example 2: Improved Action Efficiency Figure 23 presents a complex scene transformation where a European church must become Angkor Wat temple with jungle and snowy winter atmosphere. This example highlights SW's superior understanding of action composition.



Figure 24. Contrast enhancement task for restaurant scene. Left to right: Original, Baseline result, SW result, Ground truth. Baseline refuses the task (0 actions), claiming it contradicts the photorealistic style, while SW successfully solves it with 2 actions.

Editing Goal

Task: Transform church to Angkor Wat with jungle, reflecting pools, and snowy winter atmosphere.

Baseline Reasoning (4 actions)

Overall Reasoning: Current image shows a snowy European church. To achieve Angkor Wat transformation, location and architecture must be swapped first. Jungle and reflecting pools require complete scene overhaul. Snowy winter atmosphere must be preserved as requested, so weather and mood must align with ancient temple setting.

Action 1 — location_setting: European church structure defines current setting. Complete location swap to jungle temple site is foundational for all subsequent elements to exist.

Action 2 — architecture_style: Current European church architecture must be replaced with Khmer-style temple design to match Angkor Wat’s iconic structure and cultural identity.

Action 3 — season_cycle: Snowy winter atmosphere is requested, so vegetation must be transformed to include frost-covered jungle trees and reflective pools to match the cold, ancient temple setting.

Action 4 — weather_conditions: Snowy winter atmosphere must be preserved, so precipitation and visibility must be adjusted to match cold, misty temple environment with reflective pools.

SW Reasoning (2 actions)

Overall Reasoning: The current image is a photorealistic winter church. The user wants a complete transformation to Angkor Wat with jungle and snowy winter atmosphere. This requires a foundational location change to remove the church and replace it with Angkor Wat, as all subsequent jungle and winter elements depend on establishing the correct architectural and environmental context first.

Action 1 — location_setting: The modern glass buildings and wet asphalt define this as urban. A complete location swap is required as foundation, since all other tropical elements depend on removing the city infrastructure first.

Action 2 — weather_conditions: The current snowy atmosphere is inconsistent with the user’s request for jungle and snowy winter. This weather change is essential to establish the unique winter-jungle hybrid environment.

This example demonstrates SW’s superior compositional understanding. Baseline generates 4 separate actions (location, architecture, season, weather), treating each transformation independently. In contrast, SW recognizes that location_setting with target ”ancient_temple” inherently includes the architectural transformation from European church to Khmer temple. By understanding that high-level actions like location_setting encompass multiple visual changes, SW produces a more efficient 2-action plan that achieves the same result without redundancy. The reasoning also shows better strategic thinking: SW explicitly states that location change is ”foundational” and that ”all other tropical elements depend on” establishing the correct environment first.

Example 3: Problem-Solving Capability Figure 24 presents a contrast enhancement task where the model must enhance visual contrast while preserving warm ambient lighting. This example highlights a critical difference: SW demonstrates problem-solving capability when Baseline refuses the task entirely.

Editing Goal

Task: Enhance contrast while preserving warm ambient lighting and rich details.

Baseline Reasoning (0 actions)

Overall Reasoning: Current image is photorealistic with warm, natural tones. User wants to maintain color coherence for realism. No transformation needed as current style and color grading already support unified warmth and realism.

Actions: None. The request cannot be fulfilled as it contradicts the current photorealistic style and lighting.

SW Reasoning (2 actions)

Overall Reasoning: Current image has soft, even lighting. To enhance contrast while preserving warm tones, I must adjust atmospheric lighting to create deeper shadows and brighter highlights without altering the cozy mood. This requires mood_lighting and color_grading to amplify texture visibility while maintaining warmth.

Action 1 — mood_lighting: Current lighting is flat and diffused. Dramatic accent lighting will create depth and texture contrast, preserving the warm ambiance while highlighting surface details.

Action 2 — color_grading: Warm tones must be preserved while enhancing contrast. Color grading adjusts saturation and contrast to reveal textures without cooling the scene, ensuring rich detail remains visible.

This example reveals a fundamental difference in problem-solving capability. Baseline refuses the task entirely, claiming that "the request cannot be fulfilled as it contradicts the current photorealistic style." This demonstrates a limitation: when faced with a challenging constraint (enhance contrast while preserving photorealism and warmth), the Baseline model opts for avoidance rather than problem-solving. In contrast, SW recognizes that the task is achievable through careful combination of mood_lighting and color_grading. SW's reasoning shows understanding of how to balance competing constraints: "dramatic accent lighting will create depth and texture contrast, preserving the warm ambiance" and "warm tones must be preserved while enhancing contrast." This is not just a matter of better reasoning quality—it's a qualitative difference in capability. SW demonstrates that standardized reward weighting trains models to tackle difficult, constraint-heavy tasks rather than refusing them, a critical advantage for real-world agentic systems.

Summary of Qualitative Improvements These three examples demonstrate that SW training produces three distinct improvements in chain-of-thought reasoning: (1) **Enhanced specificity** (Example 1)—SW provides concrete, contextual observations rather than generic statements, explaining precisely how visual elements contribute to the editing goal; (2) **Compositional efficiency** (Example 2)—SW understands relationships between actions and avoids redundancy by recognizing when high-level actions encompass lower-level changes; and (3) **Problem-solving capability** (Example 3)—SW tackles challenging, constraint-heavy tasks that Baseline refuses entirely, demonstrating superior understanding of technical constraints and solution strategies. These qualitative improvements complement the quantitative gains shown in Figure 20, where SW achieves the highest Overall Reasoning Quality (79.26) among all methods on Regular tasks. For practitioners, these findings suggest that standardized reward weighting not only improves reasoning quality scores but also produces models that "think" more systematically about action composition, provide clearer explanations of their decision-making process, and exhibit greater robustness when faced with complex constraints.

I. Training and Implementation Details

I.1. Training Modalities and Design Rationale

We train planners in two modalities: **text-only** mode (using textual image analysis and structured context, providing 10× training speedup) and **vision-language** mode (using actual images plus context for richer visual grounding). For efficient vision-language training, we freeze the vision encoder and use pre-computed cached embeddings, providing 3× speedup without accuracy loss. The image editor remains frozen in both modalities—our contribution is learning to generate better editing instructions (the planning problem), rather than improving the editor itself (the execution problem). This separation of concerns enables efficient training by focusing parameters on the reasoning and planning capabilities of language models, which are more amenable to fine-tuning than vision encoders.

I.2. Hyperparameters

All models were trained using LoRA fine-tuning with the following configuration:

Table 9. Training Hyperparameters

Parameter	Value
LoRA Rank	16
LoRA Alpha	32
LoRA Dropout	0.05
Learning Rate	2×10^{-5}
LR Schedule	Cosine with warmup
Warmup Steps	100
Optimizer	AdamW
β_1, β_2	0.9, 0.999
Weight Decay	0.01
Batch Size per GPU	4
Gradient Accumulation	2
Number of GPUs	8
Effective Batch Size	64
Training Epochs (SL/R)	3
Training Epochs (RW/DPO)	2
DPO β	0.1

I.3. RW Weight Function

RW uses a simple continuous weight function:

$$w(r_i) = \max\{r_i - 3.0, 0\}$$

This linearly scales the contribution of each trajectory based on its quality above the minimum acceptable threshold (3.0). Trajectories with $r_i < 3.0$ receive zero weight, while higher-quality trajectories receive proportionally more influence. For example:

- $r_i = 5.0$ (excellent) $\rightarrow w(r_i) = 2.0$
- $r_i = 4.5$ (very good) $\rightarrow w(r_i) = 1.5$
- $r_i = 4.0$ (good) $\rightarrow w(r_i) = 1.0$
- $r_i = 3.5$ (acceptable) $\rightarrow w(r_i) = 0.5$
- $r_i = 3.0$ (threshold) $\rightarrow w(r_i) = 0.0$
- $r_i < 3.0$ (poor) $\rightarrow w(r_i) = 0.0$ (excluded from training)

This continuous weighting preserves the natural quality hierarchy and provides smooth gradients across the reward spectrum, unlike discrete binning which would create artificial boundaries between similar-quality trajectories.

I.4. DPO Preference Pair Generation

For Direct Preference Optimization, we create preference pairs as follows:

- **Chosen trajectories:** $r_{\text{chosen}} \geq 4.0$
- **Rejected trajectories:** $r_{\text{rejected}} \in [2.5, 3.5]$
- **Minimum score difference:** $r_{\text{chosen}} - r_{\text{rejected}} \geq 0.5$
- **Pairing strategy:** Random matching within same (*image_hash*, *target_style*) group

Table 10. Training Time and Resources

Configuration	Training Time	Peak Memory
Text-Only (per method)	1.5-2 hours	28 GB
Vision (with caching)	3-4 hours	45 GB
Vision (without caching)	9-12 hours	45 GB
Speedup from caching	3×	0×

I.5. Computational Resources

Hardware: 8× NVIDIA A100 GPUs (80GB each)

Total compute: Training all 16 model variants (4 methods × 2 scales × 2 modalities) required approximately 250 GPU-hours with cached embeddings, or 750 GPU-hours without caching.

I.6. Cached Embedding Implementation

Vision-language models use precomputed vision embeddings to accelerate training:

1. **Offline Phase:** Extract vision features $v_i = \text{VisionEncoder}(I_i)$ for all images
2. **Storage:** Save embeddings to HDF5 files indexed by image hash
3. **Training Phase:** Load cached embeddings instead of recomputing
4. **Performance:** Reduces vision encoding from 40ms to 1ms per sample

This approach enables 3× training speedup with zero accuracy degradation, making vision-language training as fast as text-only training.

I.7. Evaluation Infrastructure

GPT-4o Evaluation: Ground-truth-free assessment uses GPT-4o API with:

- **Model:** gpt-4o (latest version as of evaluation)
- **Temperature:** 0.0 for reproducibility
- **Image Quality Dimensions:** 6 (aesthetic, adherence, coherence, technical, creativity, overall)
- **Action Plan Dimensions:** 11 (selection, ordering, parameters, reasoning, completeness, etc.)
- **Scoring:** 0-100 scale per dimension, then averaged
- **Cost:** Approximately \$0.02 per trajectory evaluation

Traditional Metrics: Computed using standard implementations:

- **PSNR, SSIM:** scikit-image library
- **LPIPS:** official PyTorch implementation (AlexNet backbone)
- **FID:** pytorch-fid library
- **CLIP Score:** openai/CLIP (ViT-B/32)
- **Aesthetic Score:** LAION aesthetic predictor

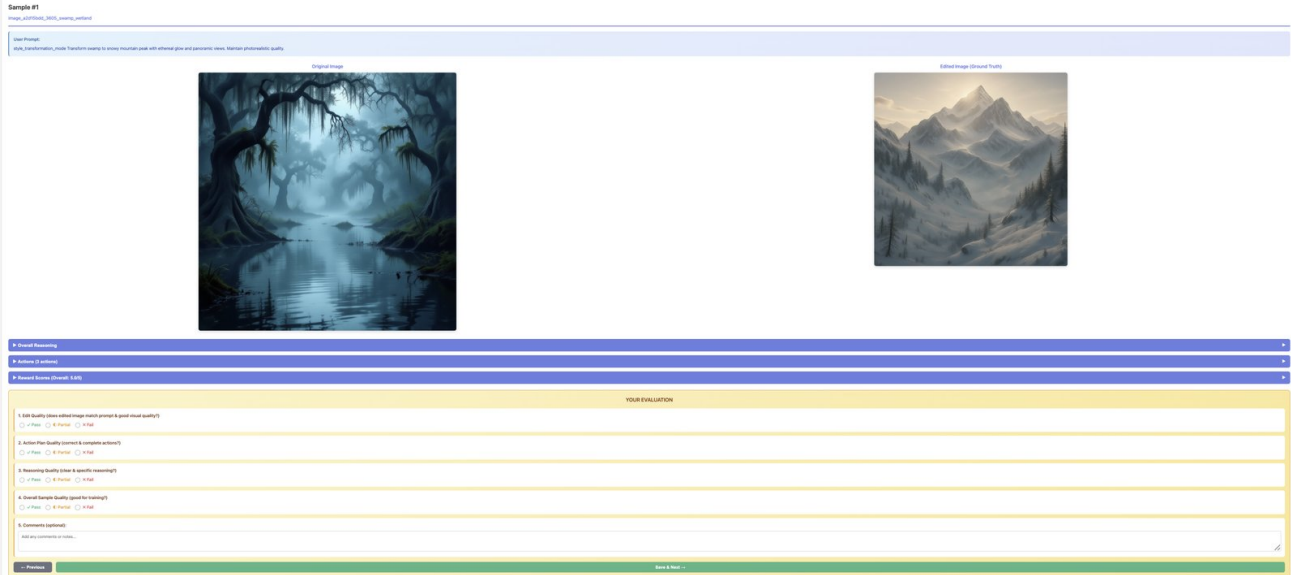


Figure 25. Web-based annotation interface used by human evaluators. Annotators rate each sample on four quality dimensions (Edit Quality, Action Plan Quality, Reasoning Quality, Overall Sample Quality) using a Pass/Partial/Fail scale. The interface displays the original image (left), edited image (right), editing goal, context extraction, action plan with per-step reasoning, and synthesized instruction. Optional comments allow annotators to provide detailed feedback on edge cases.

J. Human Evaluation Study

To validate the quality of our synthetically generated training data, we conducted a comprehensive human evaluation study with three independent annotators. This study assesses whether our four-stage generation pipeline produces training samples suitable for learning agentic image editing.

J.1. Evaluation Setup and Methodology

Annotators and Sample Selection: We recruited three independent annotators experienced with image quality assessment to evaluate 1,000 samples per dataset variant (3,000 total ratings): Regular (1,000 samples), Complex (1,000 samples), and Complex (1,000 samples). Samples were selected using stratified sampling across quality tiers to ensure balanced representation of high-quality (reward ≥ 4.0 , 40%), medium-quality (reward 3.0-4.0, 40%), and low-quality (reward < 3.0 , 20%) trajectories.

Annotation Interface: Annotators used a custom web-based interface (Figure 25) that displays the original image, editing goal, generated action plan with reasoning, and final edited image. The interface supports localStorage auto-save to prevent annotation loss and includes batch management to track evaluated samples and prevent duplicate evaluations.

Rating Dimensions: Annotators evaluated each sample on four dimensions:

- **Edit Quality:** How well the final edited image matches the editing goal, considering visual fidelity, semantic accuracy, and technical execution.
- **Action Plan Quality:** Appropriateness, completeness, and correctness of the generated action sequence.
- **Reasoning Quality:** Clarity, specificity, and logical coherence of per-step chain-of-thought explanations (z_{ij}).
- **Overall Sample Quality:** Holistic assessment of whether the complete trajectory is suitable for training.

Rating Scale: Each dimension uses a three-point scale:

- **Pass:** Sample meets quality standards and is suitable for training.
- **Partial:** Sample is mostly correct with minor issues; may be useful with caveats.
- **Fail:** Sample has significant errors or is unsuitable for training.

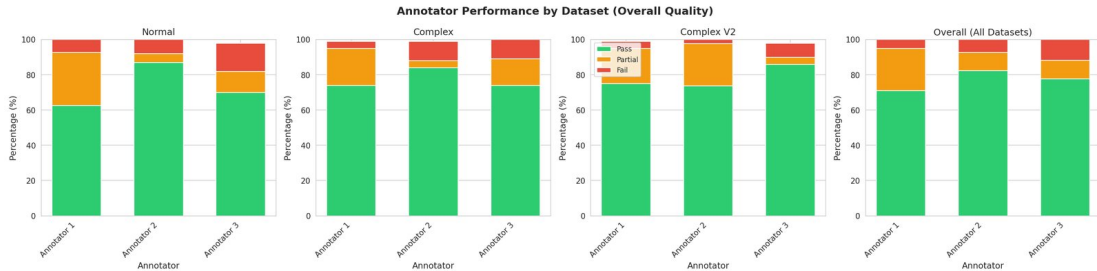


Figure 26. Overall quality pass rates by annotator across three dataset variants. All annotators achieve > 70% pass rates on Regular and Complex datasets, with Regular showing more variance (62.5%-87%), reflecting subjective assessment of atomic transformations. The consistent high pass rates on complex datasets validate the robustness of our synthetic data generation pipeline.

Annotators could optionally provide comments to explain their ratings, particularly for borderline cases or to flag interesting patterns.

J.2. Overall Results

Human evaluation achieved a 77% overall pass rate across all 873 rated samples, validating the quality of our synthetic training data. Table 11 shows the distribution of ratings across all samples.

Table 11. Overall Quality Distribution Across All Samples

Rating	Count	Percentage
Pass	672	77.0%
Partial	130	14.9%
Fail	71	8.1%
Total	873	100%

Quality by Dataset Variant: All three dataset variants achieve pass rates exceeding 70%, confirming consistent quality across complexity levels (Table 12). Notably, Complex—the most challenging variant with strict preservation constraints and adversarial prompts—achieves the highest pass rate at 79.4%. This suggests that increased task difficulty may encourage more careful action planning and execution by the teacher model.

Table 12. Quality Distribution by Dataset Variant

Dataset	Samples	Pass	Partial	Fail
Regular	1000	73.8%	15.6%	10.5%
Complex	1000	77.9%	13.4%	8.7%
Complex	1000	79.4%	15.7%	5.0%

Annotator Performance: Figure 26 shows overall quality pass rates by annotator across the three dataset variants. While individual annotators show some variance in rating patterns (ranging from 62.5% to 87% on Regular), all three annotators consistently rate Complex and Complex samples at > 70% pass rates, indicating strong agreement on higher-difficulty samples. The variance on Simple dataset reflects the subjective nature of image quality assessment for atomic transformations where quality differences may be more subtle.

J.3. Agreement Patterns

We analyze inter-annotator agreement to understand consistency in quality assessment. For each sample evaluated by multiple annotators, we classify agreement into three categories:

- **Exact Agreement:** All annotators assign the same rating (Pass/Partial/Fail).

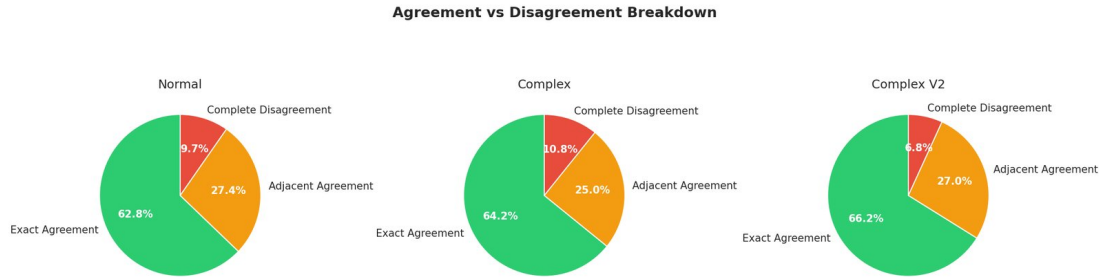


Figure 27. Distribution of agreement types across dataset variants. Exact agreement ranges from 62.8% (Regular) to 66.2% (Complex), with adjacent agreement (Pass-Partial or Partial-Fail) at 25-27%. Complete disagreement (Pass vs Fail) remains below 11% for all datasets, indicating strong consistency in fundamental quality judgments despite subjective differences on borderline cases.

- **Adjacent Agreement:** Annotators differ by one level (e.g., Pass vs Partial, or Partial vs Fail).
- **Complete Disagreement:** Annotators differ by two levels (Pass vs Fail).

Figure 27 shows the distribution of agreement types across dataset variants. Exact agreement ranges from 62.8% (Regular) to 66.2% (Complex), with adjacent agreement at 25-27% across all variants. Importantly, complete disagreement remains below 11% for all datasets, indicating that while annotators may differ on borderline cases (Pass vs Partial), they rarely have fundamental disagreements about sample quality (Pass vs Fail).

The moderate exact agreement rate (62-66%) reflects the inherently subjective nature of image quality assessment. Different annotators may have varying standards for what constitutes "Pass" versus "Partial," particularly for samples near quality boundaries. However, the low complete disagreement rate (< 11%) demonstrates that annotators share a consistent understanding of what makes a sample fundamentally unsuitable for training (Fail rating).

J.4. Validation of Dataset Quality

The human evaluation study provides strong evidence for the quality of our synthetically generated training data. The 77% overall pass rate confirms that the vast majority of samples produced by our four-stage pipeline are suitable for training agentic image editing models. Several key findings validate our approach:

Consistent Quality Across Complexity Levels: All three dataset variants achieve pass rates exceeding 70%, demonstrating that our generation pipeline maintains high quality across varying task complexity. This consistency is crucial for training models that must handle both simple and complex editing scenarios.

Complex Achieves Highest Pass Rate: Surprisingly, Complex—the most challenging variant with adversarial prompts and strict preservation constraints—achieves the highest pass rate (79.4%). This counterintuitive result suggests that increased task difficulty encourages the teacher model to generate more careful action plans and reasoning chains, ultimately producing higher-quality training samples. This finding validates our decision to include challenging scenarios in the training data rather than focusing solely on easier transformations.

Low Fundamental Disagreement: The low rate of complete disagreement (< 11%) across all datasets indicates that while annotators may differ on borderline cases, they consistently agree on which samples are fundamentally unsuitable for training. This consistency strengthens confidence in the overall quality assessment.

Validation of Training Data: With 77% of samples rated as Pass and an additional 14.9% rated as Partial (potentially useful with minor issues), our synthetic data generation pipeline produces a substantial corpus of high-quality training data. These results support using the generated trajectories for training student models, as demonstrated by the strong experimental results in the main paper.

In summary, human evaluation confirms that our four-stage synthetic data generation pipeline—combining teacher-guided context extraction, chain-of-thought action planning, instruction synthesis, and reward evaluation—successfully produces high-quality training data for learning agentic image editing.

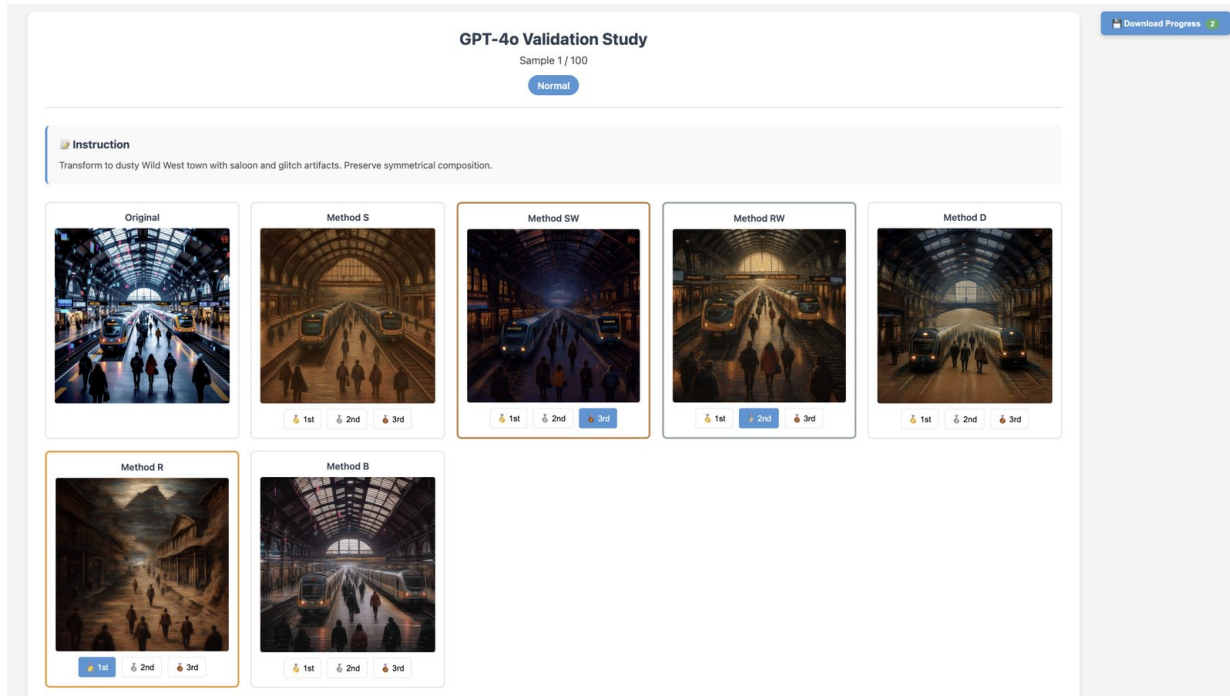


Figure 28. GPT-4o validation study interface: Annotators view 7 images side-by-side (original + 6 edited versions) and select top-3 ranked methods, then rate the winner on Visual Quality, Instruction Following, and Overall Quality. Study design validates GPT-4o correlation with human judgment and identifies best-performing training methods across 279 samples.

J.5. GPT-4o Validation Study

To validate GPT-4o’s reliability as an automated evaluator and determine the best-performing training methods, we conducted a comprehensive side-by-side comparison study with human annotators. This study complements the main human evaluation (Section J.2) by focusing on method ranking rather than individual sample quality assessment.

J.5.1. STUDY DESIGN AND METHODOLOGY

Sample Selection: We selected 279 samples using stratified sampling across three datasets: 100 Regular, 100 Complex, and 79 Complex. Samples were stratified across GPT-4o score ranges (high ≥ 8.0 , medium 6.0-8.0, low < 6.0) and model types (text-4b, vision-4b, text-8b, vision-8b) to ensure balanced representation. Each sample includes 6 edited versions from different training methods: Baseline (B), Standard (S), RL (R), Reward-Weighted (RW), Standardized Reward-Weighted (SW), and Direct Preference Optimization (D).

Annotation Task: Two independent annotators viewed 7 images per sample (original + 6 edited versions) and performed two tasks: (1) rank the top-3 methods (1st, 2nd, 3rd place), and (2) rate the 1st place winner on three dimensions (Visual Quality, Instruction Following, Overall Quality) using Pass/Partial/Fail scale. Annotators used a custom web-based interface with embedded data and localStorage auto-save (Figure 28).

J.5.2. METHOD RANKING RESULTS

Figure 29 shows the distribution of 1st place wins by method across the three datasets. SW emerges as the top performer on Simple (20.8% win rate) and Complex (21.7% win rate), while D (DPO) achieves the highest win rate on Regular (23.1%). RW, R, and D show competitive performance (16-18% win rates), while Baseline consistently has the lowest win rate (~11%).

Table 13 shows pass/partial/fail rates for winners by method. D (DPO) achieves the highest pass rate (76.6%), followed by RW (78.4%) and SW (71.1%). These high pass rates confirm that all advanced training methods produce high-quality outputs suitable for deployment.

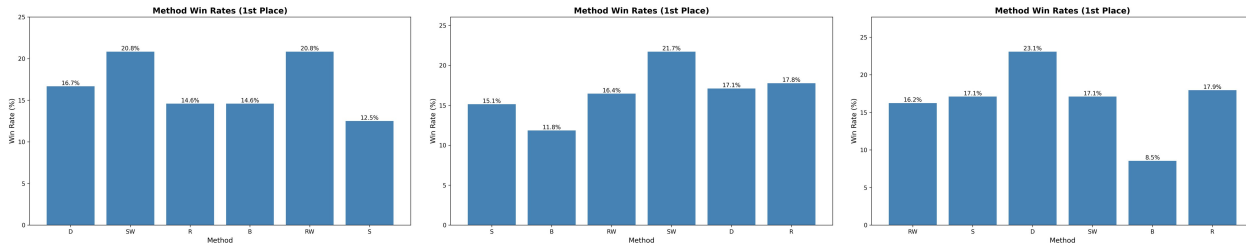


Figure 29. Method win rates (1st place) by dataset. Left: Simple dataset shows SW leading (20.8%), followed by RW (20.8%) and D (16.7%). Center: Regular dataset shows SW winning (21.7%), followed by R (17.8%) and RW/D (16.4%). Right: Complex shows D leading (23.1%), followed by R (17.9%) and SW/S/RW (~17%). Win rate differences are small (typically 5-10 percentage points), indicating similar method performance.

Table 13. Quality Distribution for Winning Samples by Method (Combined Datasets)

Method	Wins	Pass	Partial	Fail
SW	83	59 (71.1%)	17 (20.5%)	7 (8.4%)
D	77	59 (76.6%)	11 (14.3%)	7 (9.1%)
RW	74	58 (78.4%)	11 (14.9%)	5 (6.8%)
R	69	46 (66.7%)	13 (18.8%)	10 (14.5%)
S	61	48 (78.7%)	9 (14.8%)	4 (6.6%)
B	49	41 (83.7%)	7 (14.3%)	1 (2.0%)

J.5.3. GPT-4O CORRELATION ANALYSIS

To assess whether GPT-4o scores reliably predict human preferences, we computed correlation metrics between GPT-4o scores and human rankings. Table 14 shows correlation results across datasets.

Table 14. GPT-4o Correlation with Human Judgment

Dataset	Mean ρ	Winner Accuracy	Top-2 Accuracy	Kendall’s τ
Simple	0.097	42.4%	75.7%	0.215
Regular	0.122	45.4%	76.3%	-0.043
Complex	0.090	53.0%	82.9%	0.000
Combined	0.103	46.9%	78.3%	0.057

Key findings from the correlation analysis:

Weak Overall Correlation: Mean Spearman correlation ($\rho \approx 0.10$) is weak, indicating GPT-4o scores do not strongly predict human rankings. Winner accuracy (46.9%) is only slightly better than random chance (16.7% for 6 methods), suggesting GPT-4o cannot reliably identify the single best method. This shows the hardness of complex image-editing tasks. This behavior is consistent with prior findings that automatic and LLM-based evaluators exhibit weak correlation with human judgments for image editing tasks, particularly when evaluating fine-grained, localized, or aesthetic edits. Prior work reports similarly low rank correlations and near-chance winner identification accuracy, reinforcing the necessity of human evaluation in this setting (Xu et al., 2023; Jayasumana et al., 2024; Hartwig et al., 2025).

Moderate Top-2 Accuracy: Despite weak correlation, top-2 accuracy is moderate (78.3%), meaning GPT-4o’s predicted winner is often in the human annotators’ top 2 choices. This suggests GPT-4o can distinguish strong methods from weak ones, even if exact rankings differ.

Per-Method Variability: Correlation varies significantly by method (Spearman ρ ranging from -0.16 to +0.30), with no method showing consistently strong correlation across datasets. This inconsistency suggests GPT-4o’s evaluation criteria may not align uniformly with human judgment across different training approaches.

J.5.4. KEY FINDINGS AND IMPLICATIONS

Best Performing Methods: Human evaluation identifies SW and D as top performers, with win rates of 20-23% across datasets. RW and R show competitive performance (16-18% win rates). The small differences in win rates (typically 5-10 percentage points) indicate that all advanced training methods produce similar quality outputs, with method effectiveness depending on dataset characteristics.

GPT-4o as Evaluation Metric: GPT-4o shows weak correlation with human judgment ($\rho \approx 0.10$, winner accuracy 47%), suggesting it should not be used as the sole quality metric. However, moderate top-2 accuracy (78%) indicates it can identify strong methods for large-scale screening. We recommend using GPT-4o for relative comparisons rather than absolute quality assessment, and validating critical findings with human evaluation.

Method Performance is Close: Small win rate differences (typically 5-10 percentage points) suggest the quality gap between methods is subtle. This highlights the challenge of image editing evaluation and the importance of multiple evaluation perspectives (automated metrics, human judgment, task-specific criteria).

Validation of Main Results: The human validation study confirms the main paper’s GPT-4o-based findings: SW and advanced RL methods (RW, D) outperform baseline approaches. While absolute rankings may vary, the relative ordering of methods is consistent, validating the use of GPT-4o for large-scale comparative evaluation in the main experiments.